Scuola Normale Superiore

Mathematical Models for Biaxial Nematic Liquid Crystals

Candidate

Giovanni De Matteis

Advisor

Prof. Epifanio G. Virga

Ph.D. Thesis

Pisa, May 2005

Acknowledgements

I wish to express my gratitude to my advisor Prof. Epifanio G. Virga for sharing his ideas on this exciting subject, giving me a solid guide towards the solutions of the problems.

I am also very grateful to Prof. Eugene C. Gartland, Jr. for discussions of crucial importance concerning some aspects of the numerical bifurcation analysis.

My sincere thanks also to Prof. Silvano Romano for many enlightening discussions, and to Fulvio Bisi and Riccardo Rosso for their constant helpfulness.

Finally, I am very grateful to the Dipartimento di Matematica "F. Casorati" of Pavia and to the Almo Collegio Borromeo for the kind hospitality during my PhD activity.

Contents

Plan

Biaxial nematic liquid crystals are fascinating objects on both experimental and theoretical points of view. Stable biaxial phases have been observed in lyotropic systems since 1980 [**1**]. Since 1986 there have been numerous reports of thermotropic biaxiality in low-molecular weight compounds ([**2**], [**3**], [**4**], [**5**]). Recently, the search for thermotropic biaxial liquid crystals has received a fresh impetus from new experimental evidence that appears to support their existence ([**6**], [**7**], [**8**], [**9**], [**10**]).

As remarked by Luckhurst, "The announcement has created considerable excitement, for it opens up new areas of both fundamental and applied research. It seems that a Holy Grail of liquid–crystal science has been found" [**11**].

Liquid crystals form the basis of several flat–screen displays technologies. The uniaxially ordered nematic phase can be achieved with low voltage. More recently, it has become evident that biaxiality plays an important role in the switching process of bistable display devices. Bistable devices are very appealing from a technical point of view, because the existence of two different stable states facilitates multiplexing in large displays. Also, since no energy is needed for maintaining the two states, bistable displays consume less power than monostable devices, which is particularly important in the huge commercial market for mobile displays.

The very existence of biaxial liquid crystal phases finds its primary justification in the intimate structure of liquid crystal molecules, which deviate from their rod–like structure and are indeed more similar to flat platelets. Thermal fluctuations prevent this microscopic symmetry from emerging at the macroscopic scale, if rotations of molecules about their long axis are efficient enough to create an effective rotationally symmetric molecule able to replace the actual flat molecule in its interactions with the neighbors. If no remains are left at the macroscopic scale of the intrinsic microscopic symmetry, no thermotropic biaxial phase can be expected to result from collective molecular cooperation. If molecular rotations are somewhat hampered by mutual interactions there is hope that a biaxial phase manifests itself.

On the theoretical side, over the last 30 years, the possible effects of molecular biaxiality on nematic order have been studied. The first theoretical prediction of biaxial phase is due to Freiser [**12, 13**]. Within a mean–field theory, he described a biaxial transition that follows at a lower temperature the

uniaxial one, first explained on a molecular basis by Maier and Saupe [**14**]. Molecular field models ([**12**] - [**22**]), and, later, simulations studies of lattice models ([**23**]-[**27**]), have shown that single–component models consisting of molecules possessing $D_{2h}-$symmetry (platelet symmetry), and interacting by appropriately chosen potentials, can produce biaxial phase. A similar scenario has emerged from the analytical study of systems of biaxial molecules interacting via hard–core potentials [**28**], supported by simulation results [**29**]. In all these works, a second–order uniaxial–to–biaxial phase transition is found and a mostly *singular* ("accidental" in Alben's terminology [**15**]) direct isotropic–to–biaxial is predicted as well.

In this Thesis we take a different avenue.

In Chapter 1, the main features of uniaxial nematic liquid crystals are described along with the main mathematical model for their description in the framework of continuum mechanics: from the classical vectorial description, to the introduction of the *degree of orientation*, to the use of the traditional order tensor of the Landau–deGennes theory.

In Chapter 2, after a brief derivation of the uniaxial nematic phase transition according to the molecular field model of Maier and Saupe [**14**], we review in a tensorial notation the classical Straley biaxial interaction potential [**16**] and find a special electrostatic model to justify the general expression of this potential. As a consequence, the free model parameters of the interaction energy turn out to be functions of physical quantities. A physical invariance property allows to find special duality transformations involving the microscopic molecular tensors and the model parameters. We then extend the stability analysis performed in [**30**] by Durand, Sonnet and Virga finding criteria that would restrict the choice of the model parameters. Finally, we propose a general mean–field model by employing two order tensors, closely related to that put forward by Straley [**16**], and discuss its connection to Freiser's molecular field model.

In Chapter 3, we study the tricriticality properties of a particular model from the general Straley potentials class proposed in [**30**]. First, we illustrate an analytical criterion to find tricritical points in a setting sufficiently general to encompass our biaxial model as a special case. Then, with the aid of the criterion, we predict the existence of a tricritical point for biaxial liquid crystals in a range of parameters not yet explored.

A complete bifurcation analysis is performed in Chapter 4 for the biaxial model proposed in [**30**]. The main result is the derivation of the complete phase diagram, supported by Monte Carlo simulations.

The last Chapter is devoted to some formal aspects of the Straley general quadrupolar potential, partially outlined in Chapter 2. By means of a systematic application of the conjugacy relations found in Chapter 2, it is shown how to derive another phase diagram starting from that found in Chapter 4.

Moreover, we analyze the meaning of self–duality for the conjugacy relations and its connection with the symmetry properties in the space of the order tensors.

The results presented here have been obtained in collaboration with prof. E. G. Virga and prof. S. Romano: the specific references are given througout the text.

CHAPTER 1

Introduction

In this first chapter we give a brief description of nematic liquid crystals, mostly based on the works by Capriz (1989)[**31**], Virga (1994)[**32**], Ericksen (1991)[**33**], and De Gennes (1993)[**34**].

In particular, the attention is focused on the nematic uniaxial phase. This theory constitutes only the starting point of the subsequent development, but it represents a solid base for the successive investigations and generalizations.

1.1. Nematic Liquid Crystals

Liquid crystals fall within the class of special materials. They are characterized by both the fluidity of a liquid and the anisotropy of a crystal; hence they are also called mesophases.

Most liquid crystals are standard organic compounds, but also exotic compounds such as colonies of viruses diluted in water can be liquid crystals.

In 1922 G. Friedel proposed to classify liquid crystals into three wide categories, which he called **nematic**, **cholesteric** and **smectic**. Hereafter we confine our attention to nematic liquid crystals. In general, the molecules of nematic liquid crystals closely resemble rods whose typical dimensions are 5Å by 20Å: they are elongated in one direction and symmetric around it. Actually, the word nematic, coming from the Greek $\nu\hat{\eta}\mu\alpha$, means thread.

These molecules enjoy a further symmetry: the *head–tail* symmetry, which means that they are symmetric with respect to a plane orthogonal to their axis. We call these molecules **uniaxial** and say that they enjoy a $D_{\infty h}-$symmetry (the invariance group of the cylinder). Mathematically, they can be represented by a uniaxial second-rank symmetric tensor

$$\mathbf{q} := \boldsymbol{m} \otimes \boldsymbol{m} - \frac{1}{3}\mathbf{I}, \tag{1.1.1}$$

where $\boldsymbol{m}$ is the axis of cylindrical symmetry. These properties should be regarded as pertaining to *ideal* molecules and apply to the *average* behaviour of real molecules: the asymmetries **seem** to cancel out. The material condenses in an orientationally ordered phase, the nematic phase, when the interaction between neighbouring molecules tends to make them parallel to one another. This orientational ordering effect is contrasted by the disordering thermal action. By increasing the temperature the orientational order is completely lost and the molecules are randomly oriented and the nematic phase

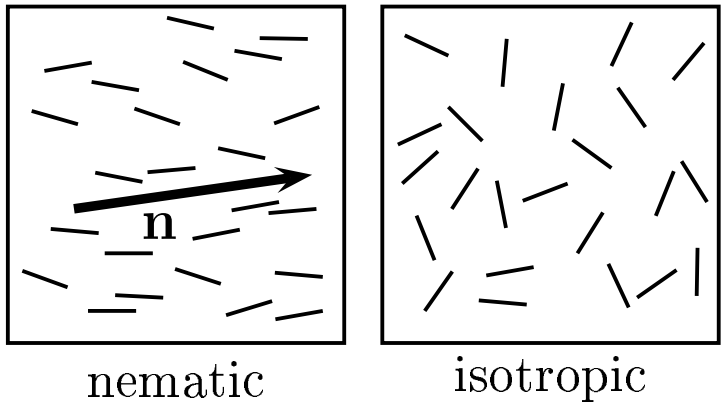

FIGURE 1.1.1. Nematic and isotropic phases in liquid crystals

is replaced by an isotropic phase. For thermotropic nematics this phase transition takes place at a specific temperature T_{NI}.

1.2. Order tensors

A continuum theory of liquid crystals needs a clear definition of the quantity that describes on a macroscopic scale the microscopic ordered structures outlined in Sec. 1.1.

For nematics such a spontaneous molecular assembling results in a degree of orientational order, whose signs survive on a macroscopic scale.

Liquid crystals constitute material bodies. In general, a continuous body can be identified with the collection of material points which constitute it. The region in space occupied by the continuous collection profiles the shape $\mathcal{B}$ of the material. The classical theory of continuous bodies regards each shape as such a set only. Liquid crystals cannot be studied within such a theory, since they are *bodies with microstructure*, for which further quantities are needed to take into account the macroscopic mechanical significance of the microscopic ordering. These quantities are called *order parameters*, which can be defined by means of simple considerations of statistical mechanics origin.

Each point in the set $\mathcal{B}$ corresponds to the place of a material element: following the lines put forward by Ericksen **[33]**, this latter can be conceived as a collection of elongated molecules, so large as to allow to take averages on it. Thus, given a point $p \in \mathcal{B}$, we consider N molecules contained in it: their centres of mass are randomly distributed, while their orientations are distributed on the unit sphere $\mathbb{S}^2$ according to a probability density function f

$$f : \mathbb{S}^2 \to \mathbb{R}^+. \tag{1.2.1}$$

Thus, if $U \subseteq \mathbb{S}^2$, the probability of finding a molecule oriented within $\mathbf{U}$ is

$$P(U) := \int_U f ds, \tag{1.2.2}$$

and $n(U) = NP(U)$ is the number of molecules which are expected to lie within U. By virtue of the head-tail symmetry, f is an even function of $\boldsymbol{m}$, or it depends on $\mathbf{q}$: $f(\boldsymbol{m}) = f(-\boldsymbol{m})$. As a consequence, the first moments of the probability density vanish, along with all the odd moments

$$\int_{\mathbb{S}^2} \boldsymbol{m} f(\boldsymbol{m})\, ds = \mathbf{0}. \tag{1.2.3}$$

The first non trivial moment is the second-order tensor

$$\mathbf{M} := \int_{\mathbb{S}^2} (\boldsymbol{m} \otimes \boldsymbol{m}) f(\boldsymbol{m})\, ds. \tag{1.2.4}$$

This tensor is symmetric

$$\mathbf{M}^T = \int_{\mathbb{S}^2} (\boldsymbol{m} \otimes \boldsymbol{m})^T f(\boldsymbol{m})\, ds = \mathbf{M}, \tag{1.2.5}$$

and

$$\mathrm{tr}\mathbf{M} = \int_{\mathbb{S}^2} \mathrm{tr}\,(\boldsymbol{m} \otimes \boldsymbol{m}) f(\boldsymbol{m})\, ds = \int_{\mathbb{S}^2} f(\boldsymbol{m})\, ds = 1. \tag{1.2.6}$$

Moreover, for a given unit vector $\boldsymbol{e} \in \mathbb{S}^2$

$$\boldsymbol{e} \cdot \mathbf{M}\boldsymbol{e} = \int_{\mathbb{S}^2} (\boldsymbol{m} \cdot \boldsymbol{e})^2 f(\boldsymbol{m})\, ds = \left\langle (\boldsymbol{m} \cdot \boldsymbol{e})^2 \right\rangle, \tag{1.2.7}$$

or, in other words,

$$\boldsymbol{e} \cdot \mathbf{M}\boldsymbol{e} = \left\langle \cos^2 \vartheta \right\rangle, \tag{1.2.8}$$

where ϑ denotes the angle between $\boldsymbol{e}$ and $\boldsymbol{m}$. As a consequence, the following inequality holds

$$0 \leq \boldsymbol{e} \cdot \mathbf{M}\boldsymbol{e} \leq 1, \tag{1.2.9}$$

where the lower and the upper bounds describe states in which the molecules are nearly all orthogonal to $\boldsymbol{e}$ or parallel to it. A special distribution function is that describing the microscopic arrangement in which the molecules are equally distributed in all directions

$$f = f_0 = \frac{1}{4\pi}. \tag{1.2.10}$$

This function describes the isotropic phase. In this phase the associated order tensor $\mathbf{M}_0$ commutes with all rotations $\mathbf{R}$

$$\mathbf{M}_0 = \int_{\mathbb{S}^2} \boldsymbol{m} \otimes \boldsymbol{m} f_0 ds = \int_{\mathbb{S}^2} \mathbf{R}\boldsymbol{m} \otimes \mathbf{R}\boldsymbol{m} f_0 ds = \mathbf{R}\mathbf{M}_0\mathbf{R}^T, \tag{1.2.11}$$

thus

$$\mathbf{M}_0 = \frac{1}{3}\mathbf{I}, \tag{1.2.12}$$

and

$$\left\langle \cos^2 \vartheta \right\rangle = \frac{1}{3}. \tag{1.2.13}$$

The second-order tensor

$$\mathbf{Q} := \mathbf{M} - \frac{1}{3}\mathbf{I} = \langle \mathbf{q} \rangle \tag{1.2.14}$$

is called the *order tensor* and it is the tensor employed in the Landau-deGennes theory (see Ref. [**34**]).

When f is uniform then $\mathbf{Q} = \mathbf{0}$. However, $\mathbf{Q} = \mathbf{0}$ can also be obtained for probability densities different from the isotropic one, so that to single out the isotropic distribution, the computation of higher moments is required. In general, in a continuum theory the degree of microscopic order is described only by $\mathbf{Q}$ and so, as an approximation, we say that when $\mathbf{M} = \mathbf{M}_0$, then f is isotropic.

As $\mathbf{M}$, $\mathbf{Q}$ is symmetric and from Eq. 1.2.14 and Eq. 1.2.6 it follows that

$$\mathrm{tr}\mathbf{Q} = 0, \tag{1.2.15}$$

and by the spectral theorem, there is a representation

$$\mathbf{Q} = \lambda_1 \boldsymbol{e}_1 \otimes \boldsymbol{e}_1 + \lambda_2 \boldsymbol{e}_2 \otimes \boldsymbol{e}_2 + \lambda_3 \boldsymbol{e}_3 \otimes \boldsymbol{e}_3, \tag{1.2.16}$$

where $\{\boldsymbol{e}_1, \boldsymbol{e}_2, \boldsymbol{e}_3\}$ are the eigenvectors relative to the eigenvalues $(\lambda_1, \lambda_2, \lambda_3)$, with the constraint

$$\lambda_3 = -\left(\lambda_1 + \lambda_2\right). \tag{1.2.17}$$

Thus, if $\lambda_1 = \lambda_2 = \lambda_3$, then they all vanish. If $\lambda_1 = \lambda_2$

$$\mathbf{Q} = s\left(\boldsymbol{n} \otimes \boldsymbol{n} - \frac{1}{3}\mathbf{I}\right), \tag{1.2.18}$$

where $s := -3\lambda_1, \boldsymbol{n} := \boldsymbol{e}_3$ and we say that the liquid crystal is **uniaxial**. In general, when $\lambda_1 \neq \lambda_2$, the order tensor takes the form

$$\mathbf{Q} = \frac{1}{2}\left(s_1 + s_2\right)\left(\boldsymbol{e}_3 \otimes \boldsymbol{e}_3 - \frac{1}{3}\mathbf{I}\right) + \frac{1}{2}\left(s_2 - s_1\right)\left(\boldsymbol{e}_1 \otimes \boldsymbol{e}_1 - \boldsymbol{e}_2 \otimes \boldsymbol{e}_2\right), \tag{1.2.19}$$

where $s_1 = -2\lambda_1 - \lambda_2$, $s_2 = -\lambda_1 - 2\lambda_2$. In this case we say that the liquid crystal is **biaxial**.

When the liquid crystal is uniaxial, then in Eq. (1.2.18), the unit vector $\boldsymbol{n}$ can be interpreted as a local average orientation of the molecules at the point $p \in \mathcal{B}$ that we are exploring and s as a **degree of orientation**. For this reason $\boldsymbol{n}$ is called the **director** of the liquid crystal.

1.3. Optical properties

The terms uniaxial and biaxial recall the language of optics and are indeed connected to some optical properties of the material. In an optically isotropic material, linearly polarized light can propagate in all directions without suffering any change in its polarization, while optically anisotropic materials behave differently. There is always at least one direction of propagation such that every polarization orthogonal to it travel undistorted. Usually, to describe the optical activity, the so–called Fresnel's ellipsoid is employed. Every optical medium is characterized by three mutually orthogonal directions and three scalars greater than 1. The three directions can be identified with three unit vectors of $\mathbb{S}^2$, $\boldsymbol{e}_1, \boldsymbol{e}_2, \boldsymbol{e}_3$; the scalar functions can be denoted by n_1, n_2, n_3. Then we can define the second-order tensor

$$\mathbf{F} := n_1 \boldsymbol{e}_1 \otimes \boldsymbol{e}_1 + n_2 \boldsymbol{e}_2 \otimes \boldsymbol{e}_2 + n_3 \boldsymbol{e}_3 \otimes \boldsymbol{e}_3, \tag{1.3.1}$$

the eigenvalues n_1, n_2, n_3 are called principal indices of refraction. Fresnel's ellipsoid is the surface in the three dimensional Euclidean space $\mathcal{E}$ given by

$$\mathcal{S} := \{x \in \mathcal{E} | \, (x - q) \cdot \mathbf{F} \, (x - q) = 1\}, \tag{1.3.2}$$

where $q \in \mathcal{E}$ is the point we are exploring. We study now the effects of the interaction of light with the liquid crystal. We suppose to consider linearly polarized light propagating in the direction of $\boldsymbol{e}_3$. As the wave travels, the polarization does not change only in two cases: when the wave is polarized in the direction of $\boldsymbol{e}_1$ and when it is polarized in the direction of $\boldsymbol{e}_2$; the speeds of propagation are c/n_1 and c/n_2, c denoting the speed of light in the vacuum.

When the polarization is in the plane orthogonal to $\boldsymbol{e}_3$, the optical vector (or the electric field) that represents it is the superposition of two vectors, one oscillating in the direction of $\boldsymbol{e}_1$ and the other in that of $\boldsymbol{e}_2$. If $n_1 \neq n_2$, these two polarizations propagate at different speeds, giving rise to a rotation of the optical vector around $\boldsymbol{e}_3$ as the wave travels inside the medium, thus generating an elliptic polarization. The same reasoning applies to waves propagating along $\boldsymbol{e}_1$ and $\boldsymbol{e}_2$.

We consider now the changes occurring in the linear polarization of light when it travels in a direction other than $\boldsymbol{e}_1, \boldsymbol{e}_2$ and $\boldsymbol{e}_3$. Firstly, we consider the case of a material optically uniaxial with $\boldsymbol{e}_3$ designating its optic axis, which means $n_1 = n_2 \neq n_3$. In this case Fresnel's ellipsoid is symmetric around $\boldsymbol{e}_3$. If we consider a generic unit vector $\boldsymbol{e}$ and the plane $\mathcal{P}_e$ passing for the center q and

orthogonal to $\boldsymbol{e}$, we call **principal section** of the ellipsoid the plane through q and generated by $\boldsymbol{e}_3$ and $\boldsymbol{e}$. The intersection between $\mathcal{S}$ and $\mathcal{P}_e$ is an ellipse with one axis orthogonal to the principal section. The corresponding semi–axis has length equal to $n = n_1 = n_2$; the other semi–axis has length n' with $n \leq n' \leq n_3$. Then, if the polarization is orthogonal to the principal section, it travels unchanged at the speed c/n. It propagates at the speed c/n' if it belongs to the principal section, but, in this case, the optical vector (the electric field) is no longer orthogonal to the direction of propagation. More precisely, in a uniaxial material, when the electric field is neither parallel nor orthogonal to the optic axis (*i.e.* $\boldsymbol{e}_3$), then the electric field and the electric displacement are not parallel. Moreover, a plane wave which propagates along a direction neither parallel nor orthogonal to the optic axis, the electric displacement oscillates orthogonally to the direction of propagation, while the electric field (*i.e.* the optical vector) does not.

As a conclusion, the wave polarized in the direction orthogonal to the principal section propagates at the same speed c/n for all directions of propagation $\boldsymbol{e}$ and it is called **ordinary wave**. The wave polarized on the principal section is called **extraordinary wave**, and its optical vector is no longer orthogonal to the direction of propagation, except for the optic axis and its orthogonal direction.

A wave polarized in a direction neither parallel nor orthogonal to the principal section is elliptically polarized in a plane no longer orthogonal to the direction of propagation.

A material is said to be **optically biaxial** if n_1, n_2, n_3 have distinct values. In this case Fresnels's ellipsoid is no longer symmetric and there are 2 planes which intersect the ellipsoid in a circle: they both pass through the axis of intermediate length. If the direction of propagation of a wave is orthogonal to one of these planes, the polarization travels undistorted. These directions of propagation are called **principal optic axes** and this explains why these materials are called biaxial.

Usually, one assumes the liquid crystal to be optically uniaxial when the order tensor $\mathbf{Q}$ has the uniaxial form (1.2.18), and $\boldsymbol{n}$ takes the role of the optic axis. At the same way, when $\mathbf{Q}$ is biaxial then the liquid crystal is optically biaxial. This assumption is valid for liquid crystals made up of molecules which allow a schematization like that in (1.1.1). In general, the liquid crystal can be made up of molecules which do not possess cylindrical symmetry, and a refined molecular model is needed to give the order tensors involved an optical interpretation.

CHAPTER 2

Preliminaries

In this Chapter, starting from the classical Maier–Saupe theory for the uniaxial nematic phase, we outline the general theory of biaxial nematic liquid crystals. This theory constitutes the framework where our further analysis develops. The methods and the results proposed in the following also open some prospects to further research in this field.

The attention is focused mainly on the general quadrupolar interaction energy put forward by Straley in [**16**], coupling molecules possessing a lower symmetry than those described in Chapter 1. This pairwise potential has been studied in the so–called dispersive approximation by several Authors ([**17, 20, 21, 23, 25, 26, 35**]). Here, we take a different avenue. We consider the general Straley interaction, referring to an electrostatic model to realize it.

2.1. Maier and Saupe's theory: uniaxial nematic phase transition

In this section, we present the Maier–Saupe molecular theory, now a classic, describing the isotropic-to-uniaxial phase transition in nematics, qualitatively described in Chapter 1. We consider two uniaxial molecules represented by the tensors $\mathbf{q}$ and $\mathbf{q}'$ in Eq. (1.1.1) and interacting via an orientational potential

$$V = -U_0 \mathbf{q} \cdot \mathbf{q}', \quad U_0 > 0, \tag{2.1.1}$$

which is the P_2-potential obtained by Maier and Saupe after appropriate averaging procedures [**14**]. Starting point is the interaction energy between two neutral molecules described by a system of point charges. They consider the dipolar part of the electrostatic interaction and treat it using quantum mechanics perturbation theory retaining a second–order approximation. Then they average isotropically over the intermolecular unit vectors and distances, arriving at the final expression (2.1.1).

At a macroscopic scale, the nematic order is described by the symmetric, traceless tensor $\mathbf{Q}$ introduced in Chapter 1. We can parameterize the order tensor $\mathbf{Q}$ as follows (see Section 1.2)

$$\mathbf{Q} = S\left(\boldsymbol{e}_z \otimes \boldsymbol{e}_z - \frac{1}{3}\mathbf{I}\right) + T\left(\boldsymbol{e}_x \otimes \boldsymbol{e}_x - \boldsymbol{e}_y \otimes \boldsymbol{e}_y\right), \tag{2.1.2}$$

where $\boldsymbol{e}_x, \boldsymbol{e}_y, \boldsymbol{e}_z$ are the eigenvectors of $\mathbf{Q}$ and constitute an orthonormal basis of $\mathbb{R}^3$ which is fixed in space. Choosing spherical coordinates (φ, ϑ) to represent the orientation of a molecule in the reference

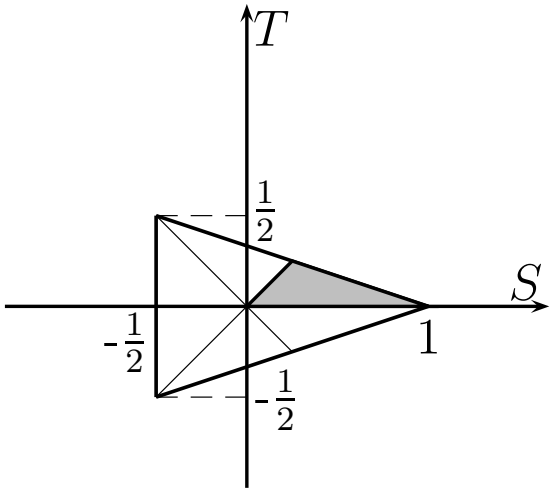

FIGURE 2.1.1. Representation of the states manifold.

frame $\boldsymbol{e}_x, \boldsymbol{e}_y, \boldsymbol{e}_z$

$$\boldsymbol{m} = \cos\varphi \sin\vartheta \boldsymbol{e}_x + \sin\varphi \sin\vartheta \boldsymbol{e}_y + \cos\vartheta \boldsymbol{e}_z, \tag{2.1.3}$$

then, for all the distribution functions f on the unit sphere $\mathbb{S}^2$, the following equations hold

$$\begin{aligned} S &= \frac{3}{2}\left\langle \boldsymbol{e}_z \cdot \mathbf{q}\boldsymbol{e}_z \right\rangle = \frac{3}{2}\left\langle \cos^2\vartheta - \frac{1}{3} \right\rangle, \\ T &= \frac{1}{2}\left\langle \boldsymbol{e}_x \cdot \mathbf{q}\boldsymbol{e}_x - \boldsymbol{e}_y \cdot \mathbf{q}\boldsymbol{e}_y \right\rangle = \frac{1}{2}\left\langle \cos 2\varphi \sin^2\vartheta \right\rangle, \end{aligned} \tag{2.1.4}$$

which lead to the following bounds for the order parameters

$$-\frac{1}{2} \leq S \leq 1, \quad -\frac{1}{3}(1-S) \leq T \leq \frac{1}{3}(1-S). \tag{2.1.5}$$

These bounds single out the order parameters manifold necessary to study the system (see Fig. (2.1.1)). The representation chosen for $\mathbf{Q}$ implies the following symmetry transformations for the parameters (S,T)

$$\begin{aligned} &(S,T) \mapsto (S,-T), \\ &(S,T) \mapsto \left(\tfrac{\pm 3T - S}{2}, \tfrac{T \pm S}{2}\right), \end{aligned} \tag{2.1.6}$$

which can be obtained by swapping the reference axes $\boldsymbol{e}_x, \boldsymbol{e}_y, \boldsymbol{e}_z$ and changing the order parameters in order to give rise to the same order tensor. The triangular region shaded in Fig. (2.1.1) is sufficient to analyze the system.

We now consider the molecular field approximation and compute the averages on the corresponding distribution function. The interaction energy V is replaced by the pseudo–potential

$$U = -U_0 \mathbf{q} \cdot \mathbf{Q}. \tag{2.1.7}$$

In this approximation, the probability density for a molecular orientation described by $\mathbf{q}$ is given by the Boltzmann distribution function

$$f(\boldsymbol{m}) = \frac{\exp(\beta \mathbf{q} \cdot \mathbf{Q})}{Z}, \tag{2.1.8}$$

where $Z = \int_{\mathbb{S}^2} \exp(\beta \mathbf{q} \cdot \mathbf{Q}) ds$ is the partition function and ds the area measure on the unit sphere $\mathbb{S}^2$. In all these expressions $\beta = \frac{U_0}{k_B t}$ where t is the absolute temperature and k_B the Boltzmann constant. Since f depends on $\mathbf{Q}$, a natural compatibility equation arises

$$\mathbf{Q} = \frac{1}{Z} \int_{\mathbb{S}^2} \mathbf{q} \exp(\beta \mathbf{q} \cdot \mathbf{Q}) ds, \tag{2.1.9}$$

which is the so–called *mean–field equation*. We are considering a homogeneous in space and mechanically isolated liquid crystal, thus, we have to consider the Helmholtz free–energy as appropriate thermodynamic potential since the volume is constant and it is thermally coupled with the ambient

$$\mathcal{F}_m = -k_B t \ln Z, \tag{2.1.10}$$

which represents the Helmholtz free–energy per molecule. In the mean-field approximation we have to add to $\mathcal{F}_m$, the mean field energy, which takes the form

$$\mathcal{F}_{field} = \frac{U_0}{2} \mathbf{Q} \cdot \mathbf{Q}, \tag{2.1.11}$$

since the generalized associated force is $\frac{\partial \mathcal{F}_{field}}{\partial \mathbf{Q}} = U_0 \mathbf{Q}$ and hence

$$U = -\frac{\partial \mathcal{F}_{field}}{\partial \mathbf{Q}} \cdot \mathbf{q} = -U_0 \mathbf{Q} \cdot \mathbf{q}. \tag{2.1.12}$$

Hence, we introduce the potential

$$\mathcal{F}(\mathbf{Q}) := U_0 \left\{ \frac{1}{2} \mathbf{Q} \cdot \mathbf{Q} - \frac{1}{\beta} \ln \left(\frac{Z}{4\pi} \right) \right\}, \tag{2.1.13}$$

which has the property of attaining its extrema precisely at that order tensor $\mathbf{Q}$ that complies with the compatibility condition (2.1.9). At equilibrium, $\mathcal{F}$ can be interpreted as the free–energy per molecule of the liquid crystal. As remarked in [**36**], arriving at the free-energy out of equilibrium $\mathcal{F}_{neq}$ requires more care; however both $\mathcal{F}$ and $\mathcal{F}_{neq}$ possess the same stationary points.

The compatibility equation (2.1.9) is a non–linear system for the order parameters S, T

$$S = \frac{3}{2}\int_0^{2\pi}\int_0^{\pi}\left(\cos^2\vartheta - \frac{1}{3}\right) f(\varphi,\vartheta)\sin\vartheta d\vartheta d\varphi, \tag{2.1.14}$$

$$T = \frac{1}{2}\int_0^{2\pi}\int_0^{\pi}\sin^2\vartheta\cos 2\varphi f(\varphi,\vartheta)\sin\vartheta d\vartheta d\varphi, \tag{2.1.15}$$

where

$$f(\varphi,\vartheta) = \frac{\exp\left\{\beta\left[S\left(\cos^2\vartheta - \frac{1}{3}\right) + T\sin^2\vartheta\cos 2\varphi\right]\right\}}{Z}, \tag{2.1.16}$$

$$Z = \int_0^{2\pi}\int_0^{\pi}\exp\left\{\beta\left[S\left(\cos^2\vartheta - \frac{1}{3}\right) + T\sin^2\vartheta\cos 2\varphi\right]\right\}\sin\vartheta d\vartheta d\varphi. \tag{2.1.17}$$

Now, we want to show that the only admissible solutions are of the form $(S, 0)$. Firstly, we show that it is true in the asymptotic case $\beta \to \infty$ and for small β, and then we make it plausible for all β. The equation (2.1.15) can be put in the form

$$\int_0^{\pi}\exp\left[\beta S\left(\cos^2\vartheta - \frac{1}{3}\right)\right]\left[2TI_0\left(\beta T\sin^2\vartheta\right) - I_1\left(\beta T\sin^2\vartheta\right)\sin^2\vartheta\right]\sin\vartheta d\vartheta = 0, \tag{2.1.18}$$

where

$$I_\nu(x) = \sum_{k=0}^{\infty}\frac{1}{\Gamma(k+\nu+1)\,k!}\left(\frac{x}{2}\right)^{2k+\nu}, \tag{2.1.19}$$

is the modified Bessel function of the first kind. In the asymptotic case $\beta \to \infty$, taking into account that

$$I_\nu(x) \simeq \frac{\exp(x)}{\sqrt{2\pi x}}\left(1 + o\left(\frac{1}{x}\right)\right) \quad x \to \infty \tag{2.1.20}$$

and under the hypothesis that $T \neq 0$, we arrive at the following integral equation

$$\int_0^{\pi}\left(2T - \sin^2\vartheta\right)\exp\left\{\beta\left[S\left(\cos^2\vartheta - \frac{1}{3}\right) + T\sin^2\vartheta\right]\right\}d\vartheta = 0, \tag{2.1.21}$$

which can be put in the form

$$(4T-1)\,I_0\left(\frac{\beta}{2}(S-T)\right) + I_1\left(\frac{\beta}{2}(S-T)\right) = 0. \tag{2.1.22}$$

From the last equation we deduce that if $S \neq T$, then the only solution is attained for $T = 0$, while if $S = T$ for $S = T = \frac{1}{4}$, which can be mapped to the state $(-\frac{1}{2}, 0)$ by using (2.1.6). Thus, both these asymptotic solutions represent uniaxial states.

It is possible to give the equation (2.1.18) a series representation

$$\sum_{k=0}^{\infty} \frac{1}{(k!)^2} \left(\frac{\beta T}{2}\right)^{2k} J_k(\beta, S) = 0, \tag{2.1.23}$$

where

$$J_k(\beta, S) := \int_0^{\pi} \exp\left[\beta S \cos^2\vartheta\right] \left(2 - \frac{\beta \sin^4\vartheta}{2(k+1)}\right) \sin^{4k+1}\vartheta d\vartheta, \tag{2.1.24}$$

this representation allows us to state that for $\beta < 4$ then $J_k(\beta, S) > 0$ for all S and k. As a consequence, the only admissible solution for $\beta < 4$ is $T = 0$.

Thus, the solutions of the nonlinear system of coupled equations (2.1.14, 2.1.15), in the limit of low temperature ($\beta \to \infty$) and high temperature ($\beta < 4$) represent uniaxial states $(S, 0)$, which are the only admissible. To the best of our knowledge, a mathematical proof of this fact for all β has not been given until now.

Now we explore this type of solutions and the behaviour of the nonlinear system in their vicinity. The second equation (2.1.15) is identically satisfied for $T = 0$, while the first one (2.1.14) becomes

$$S = -\frac{1}{2} - \frac{3}{4S\beta} + \frac{3}{4\sqrt{S\beta}\, d\left(\sqrt{S\beta}\right)}, \tag{2.1.25}$$

where

$$d(x) := e^{-x^2} \int_0^x e^{t^2} dt = -\frac{i}{2}\sqrt{\pi} Erf(ix)\, e^{-x^2} \quad \text{for all } x \in \mathbb{R}, \tag{2.1.26}$$

is the Dawson's function and Erf the error function. The equation (2.1.25) is the same nonlinear equation of the Maier–Saupe model [**14**]. The solution to this equation is represented in Fig. 2.1.2. At the critical value $\beta_* = \frac{15}{2}$, two branches bifurcate from the isotropic solution $S = 0$: S_+ corresponds to the positive solution of (2.1.25), while S_- to the negative one. At $\beta = \beta^* \approx 6.73$, the positive branch becomes stable and at $\beta_c \approx 6.81$ it attains the least free-energy $\mathcal{F}$, thus a first-order phase transition takes place with a corresponding order parameter $S_+(\beta_c) \approx 0.44$. It corresponds to the oriented nematic phase (solid heavy line in Fig. 2.1.2), a configuration in the liquid crystal where the molecules are nearly aligned around the director $\boldsymbol{e}_z$. It was also confirmed experimentally [**34**].

To explore the behaviour of the system in the vicinity of this solution, we consider T as a small perturbation and expand the free–energy around $T = 0$

$$\frac{\mathcal{F}}{U_0} = \frac{1}{3}S^2 - \frac{2}{3}S - \frac{1}{\beta}\ln\left(\frac{d\left(\sqrt{S\beta}\right)}{\sqrt{S\beta}}\right) + T^2\left(1 + \beta g\left(\sqrt{S\beta}\right)\right) + O\left(T^4\right), \tag{2.1.27}$$

where

$$g(x) := -\frac{1}{4} - \frac{1}{4x} - \frac{3}{16x^2} + \frac{1}{8\sqrt{x}d(\sqrt{x})} + \frac{3}{16x\sqrt{x}d(\sqrt{x})}, \tag{2.1.28}$$

which is an increasing negative function

$$\lim_{x\to 0^+} g(x) = -\frac{2}{15}, \quad g' > 0, \quad \lim_{x\to\infty} g(x) = 0. \tag{2.1.29}$$

The free-energy is even with respect to T, thus the Hessian form associated with it at $(S,0)$ is diagonal and the eigenvalues on the stationary solutions given by Eq. (2.1.25) are

$$\frac{\partial^2 \mathcal{F}}{\partial S^2}(S,0) = \frac{1}{9}\left[15 + \beta\left(4S^2 - 2S - 2\right)\right], \tag{2.1.30}$$

$$\frac{\partial^2 \mathcal{F}}{\partial T^2}(S,0) = \frac{1}{6}\left(15 - 2\beta + 2S\beta\right), \tag{2.1.31}$$

then, by requiring that $\frac{\partial^2 \mathcal{F}}{\partial S^2}(S,0) > 0$, the following bounds are obtained for the stable portions of the positive and negative branches

$$S_+ \geq S_+^0 := \frac{1}{4}\left(1 + 3\sqrt{1 - \frac{20}{3\beta}}\right), \quad \text{for all } \beta \geq \beta^* \tag{2.1.32}$$

$$S_- \leq S_-^0 := \frac{1}{4}\left(1 - 3\sqrt{1 - \frac{20}{3\beta}}\right), \quad \text{for all } \beta > \beta_*, \tag{2.1.33}$$

while the unstable portion of S_+ is bounded by

$$S_-^0 \leq S_+ \leq S_+^0, \quad \text{for all } \beta^* \leq \beta \leq \beta_* \tag{2.1.34}$$

The first bound, in particular, allows to state that the stable portion of S_+ is stable against all perturbations in T, actually, since $g' > 0$ then

$$1 + \beta g\left(\sqrt{\beta S_+}\right) > 1 + \beta g\left(\sqrt{\beta S_+^0}\right) := \tilde{g}(\beta), \tag{2.1.35}$$

and the r.h.s term in the inequality can be computed by means of (2.1.32), and it turns out to be strictly positive for $\beta \geq \frac{20}{3}$

$$\tilde{g}(\beta) = \frac{1}{12}\left[15 - 2\beta + 2\beta\left(\frac{1}{4} + \frac{3}{4}\sqrt{1 - \frac{20}{3\beta}}\right)\right]. \tag{2.1.36}$$

On the other hand, all the positive branch is characterized by a positive value of $\frac{\partial^2 \mathcal{F}}{\partial T^2}(S_+,0) > 0$ since

$$\frac{\partial^2 \mathcal{F}}{\partial T^2}(S_+,0) = \frac{1}{6}\left(15 - 2\beta + 2S_+\beta\right) > \frac{1}{6}\left(15 - 2\beta + 2S_-^0\beta\right) > 0 \quad \text{for all } \beta^* \leq \beta \leq \beta_*, \tag{2.1.37}$$

The negative branch S_- is stable against all perturbations in S, but is unstable against those in T

$$\frac{\partial^2 \mathcal{F}}{\partial T^2}(S_-, 0) = \frac{1}{6}(15 - 2\beta + 2S_-\beta) < \frac{1}{6}\left(15 - 2\beta + 2S_-^0\beta\right) < 0 \quad \text{for all } \beta \geq \beta_*, \tag{2.1.38}$$

It can be checked also numerically that

$$\begin{aligned} &\frac{\partial^2 \mathcal{F}}{\partial T^2}(S_+, 0) > 0, \\ &\frac{\partial^2 \mathcal{F}}{\partial T^2}(0, 0) = 0, \quad \text{when } \beta = \frac{15}{2}, \\ &\frac{\partial^2 \mathcal{F}}{\partial T^2}(S_-, 0) < 0, \end{aligned}$$

which means that there are no bifurcations from the solution $(S, 0)$, except for that leading to the isotropic state $S = T = 0$. In particular this means that no second–order uniaxial-to-biaxial phase transitions can occur.

As a consequence, the first coefficient of the series representation (2.1.23) turns out to be strictly positive on the branch S_+

$$J_0(\beta, S_+) = e^{\beta S_+} \frac{15 + 2\beta S_+ - 2\beta}{3 + 2\beta S_+ + 2\beta S_+^2} > 0. \tag{2.1.39}$$

A further analysis can be done to improve the result: up to the 16^{th} order it was shown that in the series (2.1.23)

$$J_k(\beta, S_+) > 0,$$

which reinforces the conjecture that the only admissible solutions are uniaxial, thus they can be represented by the pair $(S, 0)$ for all β.

2.2. Biaxial molecules

In order to have an intrinsically (so in the absence of any external electric field) biaxially–ordered liquid crystal, it must made up of molecules with lower symmetry than the cylindrically symmetric ones considered in the previous section. Thus, we pass from $D_{\infty h}$ (the invariance group of the cylinder) to D_{2h} symmetric molecules, represented in Fig. 2.2.1, where D_{2h} is the invariance group of the parallelepiped.

In Fig. 2.2.1 a biaxial molecule is represented schematically as a platelet. In this platelet, it is possible to distinguish 3 molecular axes $\{\boldsymbol{e}, \boldsymbol{e}_\perp, \boldsymbol{m}\}$. They constitute the eigenframe of any molecular polarizability tensor. The anisotropic part of every molecular biaxial tensor has two traceless, symmetric, second-rank orthogonal components $(\mathbf{q}, \mathbf{b})$, where

$$\mathbf{q} := \boldsymbol{m} \otimes \boldsymbol{m} - \frac{1}{3}\mathbf{I}, \tag{2.2.1}$$

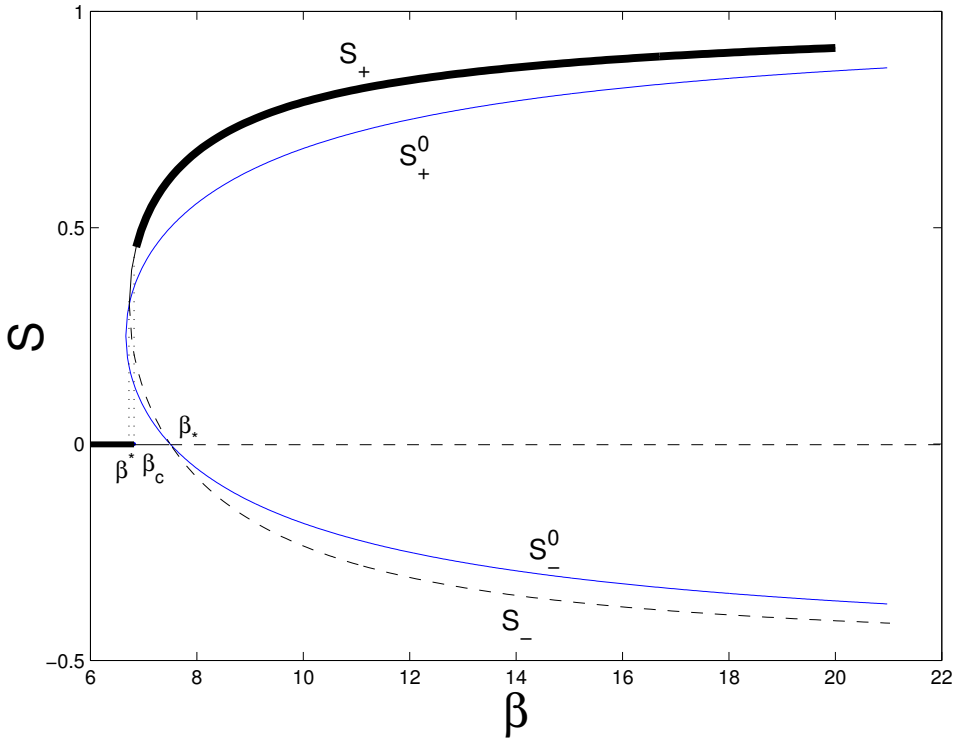

FIGURE 2.1.2. Maier–Saupe model solution: S_+ is the positive branch bifurcating from the $S = 0$ at $\beta_* = \frac{15}{2}$, S_- is the negative one. The isotropic state becomes unstable at β_*. The solid heavy portion of S_+ represents the order parameter in the condensed uniaxial nematic phase, while the full solid line is the stable portion against all perturbations in S and T. The blue line represent the curve given by S^0_+ and S^0_-.

is purely uniaxial around the long molecular axis $\boldsymbol{m}$, and

$$\mathbf{b} := \boldsymbol{e} \otimes \boldsymbol{e} - \boldsymbol{e}_\perp \otimes \boldsymbol{e}_\perp, \tag{2.2.2}$$

is fully biaxial and orthogonal to $\mathbf{q}$. Their matrix representation in the eigenframe is

$$[\mathbf{q}] = \begin{pmatrix} -\frac{1}{3} & 0 & 0 \\ 0 & -\frac{1}{3} & 0 \\ 0 & 0 & \frac{2}{3} \end{pmatrix}, \quad [\mathbf{b}] = \begin{pmatrix} 1 & 0 & 0 \\ 0 & -1 & 0 \\ 0 & 0 & 0 \end{pmatrix}. \tag{2.2.3}$$

2.3. Straley's general interaction

Letting $(\mathbf{q}, \mathbf{b})$ and $(\mathbf{q}', \mathbf{b}')$ represent two interacting molecules, the most general quadrupolar orientational interaction energy V coupling them and symmetric under their interchange, takes the form

$$V = -U_0 \left\{ \xi \mathbf{q} \cdot \mathbf{q}' + \gamma \left(\mathbf{q} \cdot \mathbf{b}' + \mathbf{b} \cdot \mathbf{q}' \right) + \lambda \mathbf{b} \cdot \mathbf{b}' \right\}. \tag{2.3.1}$$

where $U_0 > 0$ is a typical interaction energy, and ξ, λ and γ are model parameters. When $\lambda = \gamma = 0$, the potential (2.3.1) reduces to the Maier–Saupe model (see Ref. [**14**]) if $\xi > 0$, while it represents

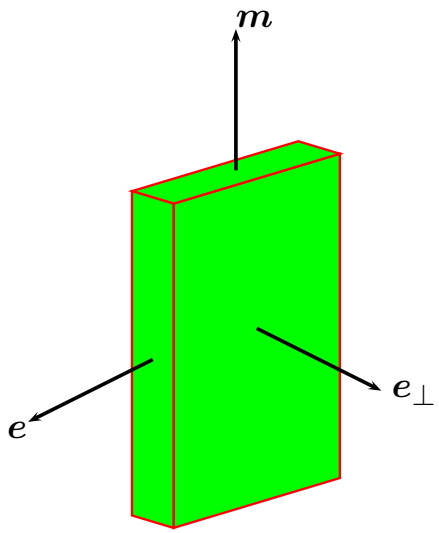

FIGURE 2.2.1. Schematic representation of a biaxial molecule

an antinematic interaction when $\xi < 0$ (see Refs. [**37**], [**38**], [**39**]), which couples only the uniaxial molecular tensors $\mathbf{q}$ and $\mathbf{q}'$. When the interaction involves the contributions in λ and γ, then the biaxial and uniaxial molecular tensors are coupled. A special case of this general potential consists of setting $\lambda\xi = \gamma^2$ for which it simplifies to

$$V = -U_0\xi\left(\mathbf{q} + \frac{\gamma}{\xi}\mathbf{b}\right)\cdot\left(\mathbf{q} + \frac{\gamma}{\xi}\mathbf{b}\right), \tag{2.3.2}$$

which can be interpreted within London's dispersion forces approximation as we will show in the next section, by referring to an electrostatic model.

2.3.1. London-van der Waals forces. Let ρ_i $(i = 1, 2, 3)$ be the molecular polarizabilities along the three principal molecular axes. We take this polarizability to be due to three orthogonal harmonic oscillators with characteristic frequencies ω_k. The London-van der Waals force between the two molecules is of the form (Bergersen *et al.* [**20**], Buckingham [**40**], Gray and Gubbins [**41**])

$$V_w = -\frac{h}{r^6}\sum_{j,k=1}^{3}\left(\omega_k + \omega_j\right)\rho_j\rho_k C_{jk}^2, \tag{2.3.3}$$

where the components C_{jk} of the coupling tensor $\mathbf{C}$ are given by

$$\begin{aligned}
C_{11} &= 3\left(\boldsymbol{e}\otimes\boldsymbol{e}'\right)\cdot\left(\boldsymbol{n}\otimes\boldsymbol{n}-\frac{1}{3}\mathbf{I}\right),\\
C_{12} &= 3\left(\boldsymbol{e}\otimes\boldsymbol{e}'_{\perp}\right)\cdot\left(\boldsymbol{n}\otimes\boldsymbol{n}-\frac{1}{3}\mathbf{I}\right),\\
C_{13} &= 3\left(\boldsymbol{e}\otimes\boldsymbol{m}'\right)\cdot\left(\boldsymbol{n}\otimes\boldsymbol{n}-\frac{1}{3}\mathbf{I}\right),\\
C_{22} &= 3\left(\boldsymbol{e}_{\perp}\otimes\boldsymbol{e}'_{\perp}\right)\cdot\left(\boldsymbol{n}\otimes\boldsymbol{n}-\frac{1}{3}\mathbf{I}\right),\\
C_{23} &= 3\left(\boldsymbol{e}_{\perp}\otimes\boldsymbol{m}'\right)\cdot\left(\boldsymbol{n}\otimes\boldsymbol{n}-\frac{1}{3}\mathbf{I}\right),\\
C_{33} &= 3\left(\boldsymbol{m}\otimes\boldsymbol{m}'\right)\cdot\left(\boldsymbol{n}\otimes\boldsymbol{n}-\frac{1}{3}\mathbf{I}\right),
\end{aligned}$$

where $\boldsymbol{n}$ is the intermolecular unit vector. The remaining coefficients are obtained by exchanging the primed and the unprimed molecule, the potential being invariant. Moreover, r is the intermolecular distance between the two centers of mass and h is Planck's constant. It turns out convenient to rewrite the potential in (2.3.3) in the following way

$$V_w = -\frac{\epsilon_0}{r^6}\sum_{j,k=1}^{3}\left(\omega_k+\omega_j\right)\rho_j\rho_k C_{jk}^2. \tag{2.3.4}$$

In the spirit of Maier–Saupe's theory, we average isotropically over the intermolecular vector $\boldsymbol{n}$, thus getting

$$\begin{aligned}
\tilde{V} &= -\frac{\epsilon_0}{5}\bar{\rho}\sum_{jk}^{3}\left(\omega_j+\omega_k\right)\rho_j\rho_k\left[\left(\boldsymbol{u}_k\cdot\boldsymbol{u}'_j\right)^2+3\right]=\\
&= -\frac{2}{15}\epsilon_0\bar{\rho}\sum_{jk}^{3}\left(\omega_j+\omega_k\right)\rho_j\rho_k P_2\left(\boldsymbol{u}_k\cdot\boldsymbol{u}'_j\right)-\frac{2}{3}\bar{\rho}\epsilon_0\sum_{jk}^{3}\left(\omega_j+\omega_k\right)\rho_j\rho_k, \qquad (2.3.5)
\end{aligned}$$

where, for notational convenience, we denote the molecular unit vectors $\{\boldsymbol{e},\boldsymbol{e}_{\perp},\boldsymbol{m}\}$ with $\{\boldsymbol{u}_1,\boldsymbol{u}_2,\boldsymbol{u}_3\}$, and $\bar{\rho}$ is a number density, stemming from the average of intermolecular distances. The function $P_2(x)$ denotes the second Legendre polynomial $\frac{1}{2}\left(3x^2-1\right)$. Dropping the last additive term, the interaction can be rewritten in the form

$$V = -\epsilon_1\sum_{jk}^{3}\left(\omega_j+\omega_k\right)\rho_j\rho_k P_2\left(\boldsymbol{u}_k\cdot\boldsymbol{u}'_j\right), \tag{2.3.6}$$

which can be diagonalized as follows. We introduce the symmetric tensor $\mathbf{K}$, whose matrix representation is

$$\left[\mathbf{K}\right]_{jk} := -\epsilon_1\left(\omega_j+\omega_k\right)\rho_j\rho_k, \tag{2.3.7}$$

and the tensor $\mathbf{P}$ defined by

$$[\mathbf{P}]_{jk} := P_2\left(\boldsymbol{u}_k \cdot \boldsymbol{u}'_j\right). \tag{2.3.8}$$

As a consequence the potential takes the form

$$V = \mathrm{tr}\left(\mathbf{KP}\right) = \mathbf{K} \cdot \mathbf{P}. \tag{2.3.9}$$

The nine matrix coefficients $[\mathbf{P}]_{jk}$ are not linearly independent, owing to the six constraints

$$\sum_{j=1}^{3} [\mathbf{P}]_{jp} = \sum_{k=1}^{3} [\mathbf{P}]_{qk} = 0 \quad p, q = 1, 2, 3. \tag{2.3.10}$$

Starting from Eq. (2.3.10), it can be shown (see also Ref. [**42**]) that Eq. (2.3.9) can be written in the form

(2.3.11)

$$V = aP_2\left(\boldsymbol{m} \cdot \boldsymbol{m}'\right) + b\left[P_2\left(\boldsymbol{e}_\perp \cdot \boldsymbol{e}'_\perp\right) - P_2\left(\boldsymbol{e} \cdot \boldsymbol{e}'\right)\right] + c\left[2\left(P_2\left(\boldsymbol{e}_\perp \cdot \boldsymbol{e}'_\perp\right) + P_2\left(\boldsymbol{e} \cdot \boldsymbol{e}'\right)\right) - P_2\left(\boldsymbol{m} \cdot \boldsymbol{m}'\right)\right],$$

or, in terms of the molecular tensors $(\mathbf{q}, \mathbf{b})$, in the form

$$V = \frac{3a}{2}\mathbf{q} \cdot \mathbf{q}' + \frac{3b}{4}\left(\mathbf{q} \cdot \mathbf{b}' + \mathbf{q}' \cdot \mathbf{b}\right) + \frac{3c}{2}\mathbf{b} \cdot \mathbf{b}'. \tag{2.3.12}$$

The origin of the six constraints lies in the fact that the potential is a function of the scalar products of the molecular vectors of the unprimed and primed interacting molecules, so it is a function of the rotation $\mathbf{R}$ that takes the first into the second

$$\mathbf{q}' = \mathbf{RqR}^T \qquad \mathbf{b}' = \mathbf{RbR}^T, \tag{2.3.13}$$

$$V : SO(3) \to \mathbb{R}$$

$$V = \frac{3a}{2}\mathrm{tr}\left(\mathbf{qRqR}^T\right) + \frac{3b}{4}\left(\mathrm{tr}\left(\mathbf{qRbR}^T\right) + \mathrm{tr}\left(\mathbf{bRqR}^T\right)\right) + \frac{3c}{2}\mathrm{tr}\left(\mathbf{bRbR}^T\right), \tag{2.3.14}$$

where $SO(3)$ is the special orthogonal group which is characterized by three free parameters, *i.e.* the number of free coefficients of $\mathbf{P}$.

Upon rescaling, Eq. (2.3.12) can be rewritten as follows

$$V = -U_0\left\{\xi\mathbf{q} \cdot \mathbf{q}' + \gamma\left(\mathbf{q} \cdot \mathbf{b}' + \mathbf{q}' \cdot \mathbf{b}\right) + \lambda\mathbf{b} \cdot \mathbf{b}'\right\}, \tag{2.3.15}$$

where U_0 is a positive constant setting energy scale, and the parameters (ξ, γ, λ) are linked to (a, b, c) in the following way

$$\xi = -\frac{3a}{2U_0}, \quad \gamma = -\frac{3b}{4U_0}, \quad \lambda = -\frac{3c}{2U_0}. \tag{2.3.16}$$

The coefficients (a, b, c) have the following general expressions

$$\begin{aligned} a &= -\frac{\epsilon_1}{2}\left\{\omega_1\rho_1^2 + (\omega_1+\omega_2)\,\rho_1\rho_2 + \omega_2\rho_2^2 - 2\,(\omega_1+\omega_3)\,\rho_1\rho_3 - 2\,(\omega_2+\omega_3)\,\rho_2\rho_3 + 4\omega_3\rho_3^2\right\}, \\ b &= -\epsilon_1\left\{\omega_2\rho_2^2 + (\omega_1+\omega_3)\,\rho_1\rho_3 - (\omega_2+\omega_3)\,\rho_2\rho_3 - \omega_1\rho_1^2\right\}, \\ c &= -\frac{\epsilon_1}{2}\left\{\omega_1\rho_1^2 - (\omega_1+\omega_2)\,\rho_1\rho_2 + \omega_2\rho_2^2\right\}. \end{aligned} \tag{2.3.17}$$

Now, a first approximation consists of studying the dispersive case corresponding to three equal frequencies $\omega_1 = \omega_2 = \omega_3 = \bar{\omega}$. In this case the model parameters become

$$\begin{aligned} a &= -\frac{\epsilon_1}{2}\bar{\omega}\,(2\rho_3 - \rho_1 - \rho_2)^2, \\ b &= -\epsilon_1\bar{\omega}\,(2\rho_3 - \rho_1 - \rho_2)\,(\rho_1 - \rho_2), \\ c &= -\frac{\epsilon_1}{2}\bar{\omega}\,(\rho_1 - \rho_2)^2. \end{aligned} \tag{2.3.18}$$

As a consequence, the potential takes the classical dispersive form

$$\begin{aligned} V_{\bar{\omega}} \;=\; & -\frac{\epsilon_1\bar{\omega}}{2}\Delta^2\left\{P_2\left(\boldsymbol{m}\cdot\boldsymbol{m}'\right) - 2\frac{\rho_2-\rho_1}{\Delta}\left[P_2\left(\boldsymbol{e}_\perp\cdot\boldsymbol{e}'_\perp\right) - P_2\left(\boldsymbol{e}\cdot\boldsymbol{e}'\right)\right]\right. \\ & \left. + \left(\frac{\rho_2-\rho_1}{\Delta}\right)^2\left[2\left(P_2\left(\boldsymbol{e}_\perp\cdot\boldsymbol{e}'_\perp\right) + P_2\left(\boldsymbol{e}\cdot\boldsymbol{e}'\right)\right) - P_2\left(\boldsymbol{m}\cdot\boldsymbol{m}'\right)\right]\right\}, \end{aligned} \tag{2.3.19}$$

where $\Delta = 2\rho_3 - (\rho_1 + \rho_2)$. In tensorial notation

$$V_{\bar{\omega}} = -\frac{3}{4}\epsilon_1\bar{\omega}\Delta^2\left\{\mathbf{q}\cdot\mathbf{q}' + \frac{\rho_2-\rho_1}{\Delta}\left(\mathbf{q}\cdot\mathbf{b}' + \mathbf{q}\cdot\mathbf{b}'\right) + \left(\frac{\rho_2-\rho_1}{\Delta}\right)^2\mathbf{b}\cdot\mathbf{b}'\right\}, \tag{2.3.20}$$

which can be rewritten in the usual form

$$V_{\bar{\omega}} = -U_0\left\{\mathbf{q}\cdot\mathbf{q}' + \gamma\left(\mathbf{q}\cdot\mathbf{b}' + \mathbf{q}\cdot\mathbf{b}'\right) + \gamma^2\mathbf{b}\cdot\mathbf{b}'\right\} = -U_0\left(\mathbf{q} + \gamma\mathbf{b}\right)\cdot\left(\mathbf{q}' + \gamma\mathbf{b}'\right). \tag{2.3.21}$$

As regards as the general case with distinct frequencies, the potential enjoys a special symmetry property. It is invariant under simultaneous transformations of the model parameters (ξ, γ, λ) or (a, b, c) and the molecular tensors $(\mathbf{q}, \mathbf{b})$. We imagine to exchange the three independent harmonic oscillators or, equivalently, the three orthogonal axes. Therefore we consider a class of linear transformations acting simultaneously on the pairs of interacting molecules and leaving unchanged the potential. We

consider the set of orthogonal involution operators

$$\tau \in O(3), \quad \tau^2 = \mathbf{I}, \tag{2.3.22}$$

and three particular operators τ_1, τ_2, τ_3, represented by

$$[\tau_1] = \begin{pmatrix} 1 & 0 & 0 \\ 0 & 0 & 1 \\ 0 & 1 & 0 \end{pmatrix}, \qquad [\tau_2] = \begin{pmatrix} 0 & 1 & 0 \\ 1 & 0 & 0 \\ 0 & 0 & 1 \end{pmatrix}, \qquad [\tau_3] = \begin{pmatrix} 0 & 0 & 1 \\ 0 & 1 & 0 \\ 1 & 0 & 0 \end{pmatrix}. \tag{2.3.23}$$

The three operators τ_1, τ_2, τ_3 realize an exchange of the molecular arms $\{\boldsymbol{e}, \boldsymbol{e}_\perp, \boldsymbol{m}\}$. More precisely

$$\tau_1 \boldsymbol{m} = \boldsymbol{e}_\perp, \quad \tau_1 \boldsymbol{e}_\perp = \boldsymbol{m}, \quad \tau_1 \boldsymbol{e} = \boldsymbol{e} \Leftrightarrow \mathbf{q} \mapsto \tau_1 \mathbf{q} \tau_1^t = -\frac{1}{2}(\mathbf{q} + \mathbf{b}), \quad \mathbf{b} \mapsto \tau_1 \mathbf{b} \tau_1^t = \frac{1}{2}(\mathbf{b} - 3\mathbf{q}), \tag{2.3.24}$$

while the action of τ_2 is

$$\tau_2 \boldsymbol{m} = \boldsymbol{m}, \quad \tau_2 \boldsymbol{e}_\perp = \boldsymbol{e}, \quad \tau_2 \boldsymbol{e} = \boldsymbol{e}_\perp \Leftrightarrow \mathbf{q} \mapsto \tau_2 \mathbf{q} \tau_2^t = \mathbf{q}, \quad \mathbf{b} \mapsto \tau_2 \mathbf{b} \tau_2^t = -\mathbf{b}. \tag{2.3.25}$$

The third symmetry operator leads to the transformations

$$\tau_3 \boldsymbol{m} = \boldsymbol{e}, \quad \tau_3 \boldsymbol{e}_\perp = \boldsymbol{e}_\perp, \quad \tau_3 \boldsymbol{e} = \boldsymbol{m} \Leftrightarrow \mathbf{q} \mapsto \tau_3 \mathbf{q} \tau_3^t = \frac{1}{2}(\mathbf{b} - \mathbf{q}), \quad \mathbf{b} \mapsto \tau_3 \mathbf{b} \tau_3^t = \frac{1}{2}(3\mathbf{q} + \mathbf{b}). \tag{2.3.26}$$

These transformations change the set of parameters (a, b, c) as follows:

for the operator τ_1 the action yields

$$\begin{aligned} a &\mapsto \frac{1}{4}(a + 3b + 9c), \\ b &\mapsto \frac{1}{2}(b - 3c + a), \\ c &\mapsto \frac{1}{4}(a - b + c), \end{aligned}$$

while for τ_2

$$\begin{aligned} a &\mapsto a, \\ b &\mapsto -b, \\ c &\mapsto c, \end{aligned}$$

and for τ_3

$$\begin{aligned} a &\mapsto \frac{1}{4}(a-3b+9c), \\ b &\mapsto -\frac{1}{2}(a-3c-b), \\ c &\mapsto \frac{1}{4}(a+b+c). \end{aligned}$$

The simultaneous action over the tensor and the parameters leaves unchanged the potential V in Eq. (2.3.12).

2.3.2. Special models. Now, we consider the special model $\gamma = 0$ and find a condition for realizing it. Suppose that the absorption frequencies ω_1 and ω_2 have the common value $\tilde{\omega}$. Consequently, the model parameters reduce to

$$\begin{aligned} a &= -\frac{\epsilon_1}{2}(\rho_1+\rho_2-2\rho_3)\left[\tilde{\omega}(\rho_1+\rho_2)-2\omega_3\rho_3\right], \\ b &= -\epsilon_1(\rho_1-\rho_2)\left[(\tilde{\omega}+\omega_3)\rho_3-\tilde{\omega}(\rho_1+\rho_2)\right], \\ c &= -\frac{\epsilon_1}{2}\tilde{\omega}(\rho_1-\rho_2)^2. \end{aligned} \tag{2.3.27}$$

We consider the case in which it is possible to neglect the cross term $(\mathbf{q}\cdot\mathbf{b}'+\mathbf{b}\cdot\mathbf{q}')$ in the potential. For a biaxial molecule the anisotropic part of the dielectric polarizability tensor is given by

$$\boldsymbol{\epsilon} = \epsilon_u \mathbf{q} + \epsilon_b \mathbf{b}, \tag{2.3.28}$$

where ϵ_u and ϵ_b are the uniaxial and biaxial polarizabilities of the molecule which depend on the frequency ω of the polarizing field. In terms of the polarizabilities along the three molecular axes

$$\begin{aligned} \epsilon_u &= \frac{1}{3}(2\rho_3-\rho_1-\rho_2), \\ \epsilon_b &= \frac{3}{4}(\rho_1-\rho_2), \end{aligned} \tag{2.3.29}$$

and $\boldsymbol{\epsilon}$ can be rewritten as

$$\boldsymbol{\epsilon} = \boldsymbol{e}\otimes\boldsymbol{e}\left(\epsilon_b-\frac{1}{3}\epsilon_u\right)+\boldsymbol{e}_\perp\otimes\boldsymbol{e}_\perp\left(-\epsilon_b-\frac{1}{3}\epsilon_u\right)+\frac{2}{3}\epsilon_u\boldsymbol{m}\otimes\boldsymbol{m}. \tag{2.3.30}$$

We consider the ratios

$$\frac{b}{c} = 2\frac{\Delta_\alpha}{\rho_2-\rho_1} = \frac{3}{2}\left(3\frac{\epsilon_u}{\epsilon_b}+g\frac{\rho_3}{\epsilon_b}\right), \quad \Delta_\alpha = \alpha\rho_3-(\rho_1+\rho_2), \tag{2.3.31}$$

where $\alpha := \frac{\omega_3}{\tilde{\omega}} + 1$, $g = \alpha - 2$ and

$$\frac{b}{a} = \frac{8}{9} \frac{\Delta_\alpha}{\Delta_\alpha + (\alpha - 1)\,\rho_3} \left(\frac{\epsilon_b}{\epsilon_u} \right). \tag{2.3.32}$$

As a consequence,

$$\frac{c}{a} = \frac{16}{27} \left(\frac{\epsilon_b}{\epsilon_u} \right) \frac{\epsilon_b}{\Delta_\alpha + (\alpha - 1)\,\rho_3}. \tag{2.3.33}$$

The dispersive model is recovered for $\alpha = 2$, since this would mean that $\omega_3 = \tilde{\omega}$, but this is a singular case. If $\alpha \neq 2$, we can have various cases. It is interesting to observe from Eq. (2.3.20), that the case $\alpha = 2$ and $\epsilon_u = 0$ represents the extremum biaxiality point in the dispersive model phase diagram, that is a purely biaxial potential of the form

$$V = -u_0 \mathbf{b} \cdot \mathbf{b}'. \tag{2.3.34}$$

But, if $\alpha \neq 2$ and both $\rho_3, \epsilon_u \ll \epsilon_b$, then we are out of the dispersive model. But, in principle it is possible to distinguish the case $0 < \alpha < 2$ and the case $\alpha > 2$.

If $1 < \alpha < 2$ then $\omega_3 < \tilde{\omega}$ and we consider a particular dispersion of the dielectric shape susceptibility. At low frequencies, $\epsilon_b \ll \epsilon_u$, then $c \ll a$ and $b \ll a$, thus the effective interaction just creates a uniaxial nematic phase. In the regime of high frequencies $\epsilon_u \ll \epsilon_b$, then $a \ll c$ and, moreover, since

$$\left(\frac{\rho_3}{\epsilon_b} \right) \ll \frac{\rho_{1,2}}{\epsilon_b} \tag{2.3.35}$$

it is plausible to retain also $b \ll c$. As a conclusion, the interaction is reduced to the pure biaxial term, thus promoting a nematic biaxial phase. In the intermediate range of frequencies, $\epsilon_u \sim \epsilon_b$ all the model parameters (a, b, c) are of the same order and, in principle, the dispersion forces interaction between real molecules should be described by the general Straley interaction. The *parabola* model $\lambda = \gamma^2$ corresponds to the particular choice $\epsilon_b = \gamma \epsilon_u$ and $\alpha = 2$, i.e. $\omega_3 = \tilde{\omega}$. But since $1 < \alpha < 2$, then we could make the plausible assumption that

$$\left(3\epsilon_u - g^+ \rho_3 \right) \ll \epsilon_b, \quad 0 < g^+ < 1, \tag{2.3.36}$$

where $g^+ = -g$, i.e. the difference between the polarizabilities ρ_1 and ρ_2 is much greater than that between the uniaxial polarizability ϵ_u and the polarizability ρ_3. With this choice $b \ll c$ and $b \ll a$ and the interaction between molecules is modeled by the effective potential

$$V = -U_0 \left\{ \mathbf{q} \cdot \mathbf{q}' + \lambda \mathbf{b} \cdot \mathbf{b}' \right\}. \tag{2.3.37}$$

In the case $\alpha > 2$, the interaction is purely uniaxial in the frequencies range $\epsilon_b \ll \epsilon_u$ and purely biaxial when $\epsilon_u \ll \epsilon_b$. But in the range $\epsilon_u \sim \epsilon_b$ the interaction should be represented by the general expression of V.

We close this section devoted to a precise electrostatic model by considering another special model deserving notice: Freiser's potential ([**12, 13**]). It can be written in the form

$$V_F = -V_0 \boldsymbol{\epsilon} \cdot \boldsymbol{\epsilon}', \tag{2.3.38}$$

assuming that the anisotropic part of the molecular polarizability $\boldsymbol{\epsilon}$ be represented by Eq. (2.3.28). Mathematically, it can be recovered in our framework by setting $\gamma = \frac{\epsilon_b}{\epsilon_u}$ and $\xi = 1$ and it becomes equivalent to the dispersive model (2.3.21), even though Freiser put forward a mean field theory employing only one order tensor. It was completely solved by Boccara *et al.* in Ref. [**18**], where they found a phase diagram very similar to that computed by Straley [**16**] for a special relation between the parameters ξ, γ, λ.

2.3.3. Stability Analysis. It was remarked in Ref. [**23**] that setting $\lambda = 0$ would never allow the molecules to reach a stable equilibrium when they all lie parallel to one another. More generally, consider two molecules represented by the pairs $(\mathbf{q}, \mathbf{b})$ and $(\mathbf{q}', \mathbf{b}')$, so nearly parallel to one another that the rotation $\mathbf{R}$ that takes the first into the second, for which Eqs. (2.3.13) hold, can be represented as

$$\mathbf{R} = \mathbf{I} + \alpha \mathbf{W} + \frac{1}{2}\alpha^2 \mathbf{W}^2 + o\left(\alpha^2\right), \tag{2.3.39}$$

where α is the rotation angle and $\mathbf{W}$ is the skew–symmetric tensor associated with the unit vector $\boldsymbol{w}$ along the axis of rotation (Eq. (2.46), p. 66 of [**32**]). By use of Eqs. (2.3.13) and (2.3.39) in Eq. (2.3.15), we arrive at the following expression for the incremental energy δV relative to the state of complete alignment of the two molecules (where $\alpha = 0$) (see also Ref. [**30**])

$$\begin{aligned} \delta V \;=\; & -\frac{1}{2} U_0 \alpha^2 \left\{ \xi \left(\mathrm{tr}\left(\mathbf{W}^2\mathbf{q}^2\right) - \mathrm{tr}\left(\mathbf{W}\mathbf{q}\right)^2 \right) + 2\gamma \left[\mathrm{tr}\left(\mathbf{q}\mathbf{b}\mathbf{W}^2\right) \right. \right. \\ & \left. \left. - \mathrm{tr}\left(\mathbf{q}\mathbf{W}\mathbf{b}\mathbf{W}\right) \right] + \lambda \left[\mathrm{tr}\left(\mathbf{W}^2\mathbf{q}^2\right) - \mathrm{tr}\left(\mathbf{W}\mathbf{b}\right)^2 \right] \right\} + o\left(\alpha^2\right). \end{aligned} \tag{2.3.40}$$

Since $\mathbf{W}\boldsymbol{v} = \boldsymbol{w} \times \boldsymbol{v}$ for all vectors $\boldsymbol{v}$, we can give an explicit form to Eq. (2.3.40) in terms of the components (w_1, w_2, w_3) of $\boldsymbol{w}$ in the eigenframe $\{\boldsymbol{e}, \boldsymbol{e}_\perp, \boldsymbol{m}\}$ of both $\mathbf{q}$ and $\mathbf{b}$:

$$\delta V = \frac{1}{2} U_0 \alpha^2 \left\{ \left(\xi + 2\gamma + \lambda\right) w_1^2 + \left(\xi - 2\gamma + \lambda\right) w_2^2 + 4\lambda w_3^2 \right\} + o\left(\alpha^2\right). \tag{2.3.41}$$

It is apparent from Eq. (2.3.41) that δV is positive–definite whenever $\lambda > 0$ and $2\left|\gamma\right| < \xi + \lambda$.

When $\xi = 1$ the range of positive definiteness of δV is given by the fan-shaped region $\lambda > 0$ and $|2\gamma| < 1 + \lambda$ depicted in Fig. 2.3.1. While in the antinematic case $\xi < 0$, the region of positive definiteness is given by a V–shaped domain and in Fig. 2.3.2 the case $\xi = -1$ is represented.

Moreover, it is possible to restrict the interesting area by requiring that the ground state is *calamitic*, that is with the long molecular axis $\boldsymbol{m}$ harder to be disoriented than the other two. In order to assure this physical property, we have to require the least eigenvalue of the quadratic form δV in Eq. (2.3.41) be associated with the eigenvector $\boldsymbol{w} = \boldsymbol{m}$. Thus, for a given α, the torque tending to restore the complete alignment between two interacting molecules is larger when the two long axes are misaligned. Thus, requiring that

$$4\lambda < \xi - 2\gamma + \lambda \quad \text{and} \quad 4\lambda < \xi + 2\gamma + \lambda,$$

the following inequality arises

$$2\,|\gamma| < \xi - 3\lambda. \tag{2.3.42}$$

When $\xi > 0$, this requirement singles out the shaded triangle in Fig. 2.3.1, represented for $\xi = 1$ by the inequality

$$2\,|\gamma| < 1 - 3\lambda. \tag{2.3.43}$$

It is apparent from (2.3.42) that, in the antinematic case $\xi < 0$ such a configuration is not admissible. Nevertheless, we could ask whether the ground state is still calamitic, but around the other two molecular axes $\boldsymbol{e}$ or $\boldsymbol{e}_\perp$. Thus, we consider the case $\xi = -1$ and require the ground state of complete alignment to be calamitic around $\boldsymbol{e}$, then we have to submit the V–shaped region to the following restrictions

$$-1 + 2\gamma + \lambda < 4\lambda \quad \text{and} \quad -1 + 2\gamma + \lambda < -1 - 2\gamma + \lambda, \tag{2.3.44}$$

which means $\gamma < 0$ and $\lambda > \frac{2\gamma - 1}{3}$, that is inside the $\gamma-$negative sector of the V–shaped region in Fig.2.3.2. Reasoning in a similar way for $\boldsymbol{e}_\perp$, we arrive at the conclusion that the ground state is $\boldsymbol{e}_\perp-$calamitic if $\gamma > 0$ and $\lambda > -\frac{2\gamma + 1}{3}$ which single out the $\gamma-$positive sector.

2.3.4. Another representation. In this section we present another useful representation of the quadrupolar interaction V in Eq. (2.3.15). It is closely connected to the biaxial molecules which possess the so-called $D_{2h}-$symmetry: three mutually orthogonal mirror planes with inversion symmetry

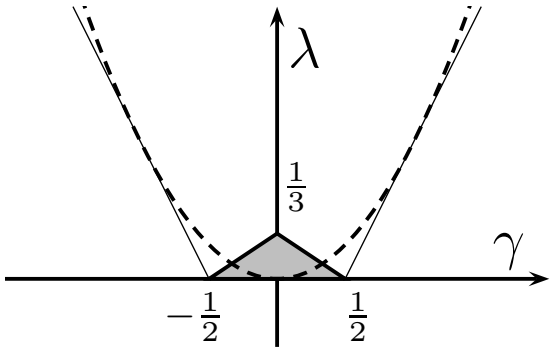

FIGURE 2.3.1. Model parameters space for $\xi = 1$. The fan–shaped region singles out the subset of positive definiteness of V. Within this domain, the shaded triangle represents the $\boldsymbol{m}-$calamitic ground states. The dashed line is the parabola $\lambda = \gamma^2$ corresponding to the dispersion forces approximation; it is tangent to the fan–shaped region for $\lambda = 1$.

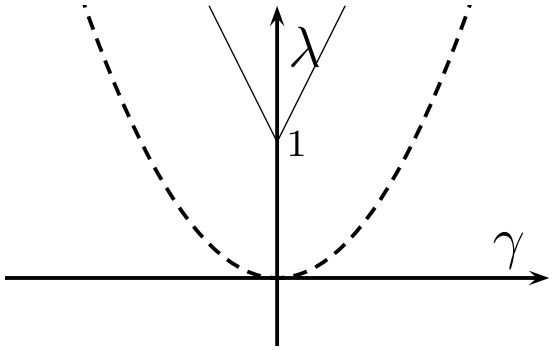

FIGURE 2.3.2. Model parameters space for $\xi = -1$. The V–shaped region with $\lambda > 1$ represents the region of positive definiteness of V. There are no $\boldsymbol{m}-$calamitic ground states inside it.

through their intersection. Thus it is not surprising that V can be put in the $D_{2h}-$invariant form

$$V = -U_0 \left\{ -\left(\lambda + \frac{\xi}{3}\right) + (\xi - \lambda)\left(\boldsymbol{m}\cdot\boldsymbol{m}'\right)^2 + 2\left(\lambda + \gamma\right)\left(\boldsymbol{e}'_\perp \cdot \boldsymbol{e}_\perp\right)^2 + 2\left(\lambda - \gamma\right)\left(\boldsymbol{e}'\cdot\boldsymbol{e}\right)^2 \right\}. \tag{2.3.45}$$

Equivalently, V can be written as a linear combination of symmetry-adapted basis functions $\{s_k(\hat{\omega})\}_{k=1,\ldots 4}$ (see, e.g. Refs. **[25, 26, 28, 42]**), where $\hat{\omega} = \left(\hat{\varphi}, \hat{\vartheta}, \hat{\psi}\right)$ denotes the triplet of Euler angles ([**43, 44, 45**]) defining the relative orientation of the pair of interacting molecules

(2.3.46)

$$\begin{aligned}
\boldsymbol{e}' &= \left(\cos\hat{\psi}\cos\hat{\varphi}\cos\hat{\vartheta} - \sin\hat{\psi}\sin\hat{\varphi}\right)\boldsymbol{e} + \left(\cos\hat{\psi}\sin\hat{\varphi}\cos\hat{\vartheta} + \sin\hat{\psi}\cos\hat{\varphi}\right)\boldsymbol{e}_\perp - \cos\hat{\psi}\sin\hat{\vartheta}\boldsymbol{m}, \\
\boldsymbol{e}'_\perp &= -\left(\sin\hat{\psi}\cos\hat{\varphi}\cos\hat{\vartheta} + \cos\hat{\psi}\sin\hat{\varphi}\right)\boldsymbol{e} - \left(\sin\hat{\psi}\sin\hat{\varphi}\cos\hat{\vartheta} - \cos\hat{\psi}\cos\hat{\varphi}\right)\boldsymbol{e}_\perp + \sin\hat{\psi}\sin\hat{\vartheta}\boldsymbol{m}, \\
\boldsymbol{m}' &= \cos\hat{\varphi}\sin\hat{\vartheta}\boldsymbol{e} + \sin\hat{\varphi}\sin\hat{\vartheta}\boldsymbol{e}_\perp + \cos\hat{\vartheta}\boldsymbol{m},
\end{aligned}$$

and the invariant functions are given by the following expressions

$$
\begin{aligned}
s_1(\hat{\omega}) &= P_2\left(\cos\hat{\vartheta}\right), \\
s_2(\hat{\omega}) &= \tfrac{\sqrt{6}}{4}\sin^2\hat{\vartheta}\cos 2\hat{\varphi}, \\
s_3(\hat{\omega}) &= \tfrac{\sqrt{6}}{4}\sin^2\hat{\vartheta}\cos 2\hat{\psi}, \\
s_4(\hat{\omega}) &= \tfrac{1}{4}\left(1+\cos^2\hat{\vartheta}\right)\cos 2\hat{\varphi}\cos 2\hat{\psi} - \tfrac{1}{2}\cos\hat{\vartheta}\sin 2\hat{\varphi}\sin 2\hat{\psi}.
\end{aligned}
\tag{2.3.47}
$$

The potential takes the form

$$
V(\hat{\omega}) = -\epsilon\left\{\xi s_1(\hat{\omega}) + \sqrt{6}\gamma\left[s_2(\hat{\omega}) + s_3(\hat{\omega})\right] + 6\lambda s_4(\hat{\omega})\right\},
\tag{2.3.48}
$$

which is useful in view of a mean–field approximation.

2.4. Mean Field Model

In this section, we present a mean field model for the biaxial potential. We start by considering a homogeneous nematic liquid crystal in the absence of any external field and made up of biaxial molecules. Macroscopically the liquid crystal is described by two order tensors, both defined as ensemble averages

$$
\mathbf{Q} := \langle \mathbf{q} \rangle,
\tag{2.4.1}
$$

and

$$
\mathbf{B} := \langle \mathbf{b} \rangle.
\tag{2.4.2}
$$

Moreover, we introduce the second-rank tensor as we have done for uniaxially symmetric molecules in Chapter 1

$$
\mathbf{M} := \langle \boldsymbol{m} \otimes \boldsymbol{m} \rangle = \mathbf{Q} + \frac{1}{3}\mathbf{I}.
\tag{2.4.3}
$$

In all these definitions the symbol $\langle . \rangle$ denotes the average over an appropriate biaxial distribution function f.

2.4.1. Biaxial distributions. The most general distribution function for biaxial molecules represented by the molecular tensors $\mathbf{q}$ and $\mathbf{b}$ and interacting throughout the biaxial potential in Eq. (2.3.15) is a function of the tensor $\mathbf{b}$ alone, since the tensor $\mathbf{q}$ is determined by the direction of the eigenvector relative to the eigenvalue zero of $\mathbf{b}$, so

$$
f : \mathcal{N} \to \mathbb{R}_0^+, \quad \int_{\mathcal{N}} f(\mathbf{b}) = 1,
\tag{2.4.4}
$$

where

$$\mathcal{N} = \left\{ (\mathbf{q}, \mathbf{b}) \in Sym_0 : \det \mathbf{b} = 0, \mathrm{tr}\left(\mathbf{b}^2\right) = 2, \mathbf{q} \cdot \mathbf{b} = 0, \mathrm{tr}\left(\mathbf{q}^2\right) = \frac{2}{3}, [\mathbf{q}, \mathbf{b}] = \mathbf{0} \right\}, \tag{2.4.5}$$

where $[\mathbf{q}, \mathbf{b}] = \mathbf{qb} - \mathbf{bq}$ indicates the commutator. We can derive now the main properties of the macroscopic tensors $\mathbf{Q}$, $\mathbf{B}$ and $\mathbf{M}$. They are all symmetric, $\mathbf{Q}$ and $\mathbf{B}$ are traceless while

$$\mathrm{tr}\mathbf{M} = \int_{\mathcal{N}} \mathrm{tr}\left(\boldsymbol{m} \otimes \boldsymbol{m}\right) f\left(\mathbf{b}\right) = \int_{\mathcal{N}} f\left(\mathbf{b}\right) = 1. \tag{2.4.6}$$

Let $\boldsymbol{u} \in \mathbb{R}^3$, $\mathbf{M}$ is a linear mapping which maps $\boldsymbol{u}$ in $\mathbf{M}\boldsymbol{u}$. From (2.4.3) it follows that

$$\boldsymbol{u} \cdot \mathbf{M}\boldsymbol{u} = \int_{\mathcal{N}} \left(\boldsymbol{u} \cdot \boldsymbol{m}\right)^2 f\left(\mathbf{b}\right) > 0, \quad \forall \boldsymbol{u} \in \mathbb{R}^3, \tag{2.4.7}$$

this means that $\mathbf{M}$ is positive definite, and since it is symmetric, it induces an inner product

$$(\boldsymbol{u}, \boldsymbol{v}) := \boldsymbol{u} \cdot \mathbf{M}\boldsymbol{v}, \quad \forall \boldsymbol{u}, \boldsymbol{v} \in \mathbb{R}^3. \tag{2.4.8}$$

Now, since $\mathbf{M}$ is symmetric and positive definite and $\mathbf{B}$ is symmetric, then there exists a basis $\{\boldsymbol{v}_1, \boldsymbol{v}_2, \boldsymbol{v}_3\}$ in $\mathbb{R}^3$ of common eigenvectors or, in other words, they can be diagonalized simultaneously. Moreover, since $\mathbf{Q}$ differs from $\mathbf{M}$ by the identity tensor, the simultaneous diagonalization holds for the pair $(\mathbf{Q}, \mathbf{B})$ as well, and they share the same basis $\{\boldsymbol{v}_1, \boldsymbol{v}_2, \boldsymbol{v}_3\}$. In this basis $\boldsymbol{v}_i \cdot \mathbf{M}\boldsymbol{v}_j = \delta_{ij}$, i.e. it is orthonormal in the inner product induced by $\mathbf{M}$. The basis is orthonormal in the standard Euclidean inner product if and only if the tensors $\mathbf{Q}$ and $\mathbf{B}$ commute

$$[\mathbf{M}, \mathbf{B}] = [\mathbf{Q}, \mathbf{B}] = 0, \tag{2.4.9}$$

but the occurrence of this special property depends on the distribution function modeling the liquid crystal.

We assume that f possesses a symmetry property, that is, assume that there exist two orthogonal elements $\boldsymbol{e}_x$ and $\boldsymbol{e}_z$ ($\boldsymbol{e}_x \cdot \boldsymbol{e}_z$=0) of the unit sphere $\mathbb{S}^2$, such that, letting $\mathbf{R}_x$ and $\mathbf{R}_z$ denote the rotations by an angle π about $\boldsymbol{e}_x$ and $\boldsymbol{e}_z$ respectively

$$\begin{aligned} \mathbf{R}_x &:= 2\boldsymbol{e}_x \otimes \boldsymbol{e}_x - \mathbf{I}, \\ \mathbf{R}_z &:= 2\boldsymbol{e}_z \otimes \boldsymbol{e}_z - \mathbf{I}, \end{aligned} \tag{2.4.10}$$

f satisfies the invariance condition

$$f\left(\mathbf{R}_x \mathbf{b} \mathbf{R}_x^T\right) = f\left(\mathbf{R}_z \mathbf{b} \mathbf{R}_z^T\right) = f\left(\mathbf{b}\right) \qquad \text{for all } \mathbf{b} \in \mathcal{N}. \tag{2.4.11}$$

This symmetry property, which is plausible in the absence of any external distorting anisotropic causes, has some consequences on the order tensors $\mathbf{Q}$ and $\mathbf{B}$ in definitions (2.4.1) and (2.4.2). Such definitions are equivalent to

$$\mathbf{Q} = \int_{\mathbf{R}_x\mathcal{N}} \mathbf{R}_x \mathbf{q} \mathbf{R}_x^T f\left(\mathbf{R}_x \mathbf{b} \mathbf{R}_x^T\right), \qquad \mathbf{B} = \int_{\mathbf{R}_x\mathcal{N}} \mathbf{R}_x \mathbf{b} \mathbf{R}_x^T f\left(\mathbf{R}_x \mathbf{b} \mathbf{R}_x^T\right), \tag{2.4.12}$$

or

$$\mathbf{Q} = \int_{\mathbf{R}_z\mathcal{N}} \mathbf{R}_z \mathbf{q} \mathbf{R}_z^T f\left(\mathbf{R}_z \mathbf{b} \mathbf{R}_z^T\right), \qquad \mathbf{B} = \int_{\mathbf{R}_z\mathcal{N}} \mathbf{R}_z \mathbf{b} \mathbf{R}_z^T f\left(\mathbf{R}_z \mathbf{b} \mathbf{R}_z^T\right). \tag{2.4.13}$$

Since both f and $\mathcal{N}$ are invariant under $\mathbf{R}_x$ and $\mathbf{R}_z$, the equations (2.4.12) and (2.4.13) give rise to the following conditions

$$\mathbf{Q} = \int_{\mathcal{N}} \mathbf{R}_x \mathbf{q} \mathbf{R}_x^T f\left(\mathbf{b}\right), \qquad \mathbf{B} = \int_{\mathcal{N}} \mathbf{R}_x \mathbf{b} \mathbf{R}_x^T f\left(\mathbf{b}\right), \tag{2.4.14}$$

and

$$\mathbf{Q} = \int_{\mathcal{N}} \mathbf{R}_z \mathbf{q} \mathbf{R}_z^T f\left(\mathbf{b}\right), \qquad \mathbf{B} = \int_{\mathcal{N}} \mathbf{R}_z \mathbf{b} \mathbf{R}_z^T f\left(\mathbf{b}\right). \tag{2.4.15}$$

Thus, the following commutation relations hold

$$\mathbf{R}_x \mathbf{Q} = \mathbf{Q} \mathbf{R}_x, \qquad \mathbf{R}_x \mathbf{B} = \mathbf{B} \mathbf{R}_x, \tag{2.4.16}$$

and similar relations involve the rotation $\mathbf{R}_z$. As a consequence, the two tensors $\mathbf{Q}$ and $\mathbf{B}$ commute with

$$\mathbf{R}_y := 2\boldsymbol{e}_y \otimes \boldsymbol{e}_y - \mathbf{I}, \tag{2.4.17}$$

where $\boldsymbol{e}_y \in \mathbb{S}^2$ and it is orthogonal to both $\boldsymbol{e}_x$ and $\boldsymbol{e}_z$. Applying either operator in equation (2.4.16) to the unit vector $\boldsymbol{e}_x$, we see that $\mathbf{Q}\boldsymbol{e}_x$ is a proper vector of $\mathbf{R}_x$ with proper value 1; hence, necessarily,

$$\mathbf{Q}\boldsymbol{e}_x = q\boldsymbol{e}_x, \qquad \mathbf{B}\boldsymbol{e}_x = b\boldsymbol{e}_x, \tag{2.4.18}$$

where q and b are appropriate real number. Similar reasoning applied to the vectors $\boldsymbol{e}_y$ and $\boldsymbol{e}_z$, leads us to conclude that

PROPOSITION 2.4.1. *If the distribution function f satisfies the invariance property (2.4.11), then $\{\boldsymbol{e}_x, \boldsymbol{e}_y, \boldsymbol{e}_z\}$ is an orthonormal basis of eigenvectors of $\mathbf{Q}$ and $\mathbf{B}$. Equivalently the following commutation relation holds*

$$\mathbf{Q}\mathbf{B} = \mathbf{B}\mathbf{Q}. \tag{2.4.19}$$

Vice versa, if the two tensors $\mathbf{Q}$ and $\mathbf{B}$ commute, they have an orthonormal basis of common eigenvectors. As a consequence, both the tensors commute with the rotations $\mathbf{R}_x$ and $\mathbf{R}_z$. But, in general, we cannot infer from these properties, regarding the second-moments tensors, that the distribution function satisfies the invariance property (2.4.11).

As a conclusion, under the symmetry assumption (2.4.11), we can represent the tensor $\mathbf{Q}$ and $\mathbf{B}$ in the following way

$$\mathbf{Q} := S\left(\boldsymbol{e}_z \otimes \boldsymbol{e}_z - \frac{1}{3}\mathbf{I}\right) + T\left(\boldsymbol{e}_x \otimes \boldsymbol{e}_x - \boldsymbol{e}_y \otimes \boldsymbol{e}_y\right), \tag{2.4.20}$$

$$\mathbf{B} := S'\left(\boldsymbol{e}_z \otimes \boldsymbol{e}_z - \frac{1}{3}\mathbf{I}\right) + T'\left(\boldsymbol{e}_x \otimes \boldsymbol{e}_x - \boldsymbol{e}_y \otimes \boldsymbol{e}_y\right), \tag{2.4.21}$$

where S, T, S', T' are the *order parameters* of the system. They are essentially the same order parameters employed in **[16]** by Straley. Choosing standard Euler angles $(\varphi, \vartheta, \psi)$ to specify the molecular tensors $\mathbf{q}$ and $\mathbf{b}$ in the basis $\{\boldsymbol{e}_x, \boldsymbol{e}_y, \boldsymbol{e}_z\}$

(2.4.22)

$$\begin{aligned}
\boldsymbol{e} &= \left(\cos\psi\cos\varphi\cos\vartheta - \sin\psi\sin\varphi\right)\boldsymbol{e}_x + \left(\cos\psi\sin\varphi\cos\vartheta + \sin\psi\cos\varphi\right)\boldsymbol{e}_y - \cos\psi\sin\vartheta\boldsymbol{e}_z,\\
\boldsymbol{e}_\perp &= -\left(\sin\psi\cos\varphi\cos\vartheta + \cos\psi\sin\varphi\right)\boldsymbol{e}_x - \left(\sin\psi\sin\varphi\cos\vartheta - \cos\psi\cos\varphi\right)\boldsymbol{e}_y + \sin\psi\sin\vartheta\boldsymbol{e}_z,\\
\boldsymbol{m} &= \cos\varphi\sin\vartheta\boldsymbol{e}_x + \sin\varphi\sin\vartheta\boldsymbol{e}_y + \cos\vartheta\boldsymbol{e}_z.
\end{aligned}$$

and to parameterize the manifold $\mathcal{N}$, the components (S, T, S', T') are defined by

$$S := \frac{3}{2}\int_{\mathbb{T}}\left(\cos^2\vartheta - \frac{1}{3}\right) f(\varphi, \vartheta, \psi)\, d\omega, \tag{2.4.23}$$

$$T := \frac{1}{2}\int_{\mathbb{T}}\sin^2\vartheta\cos 2\varphi f(\varphi, \vartheta, \psi)\, d\omega, \tag{2.4.24}$$

$$S' := \frac{3}{2}\int_{\mathbb{T}}\sin^2\vartheta\cos 2\psi f(\varphi, \vartheta, \psi)\, d\omega, \tag{2.4.25}$$

$$T' := \frac{1}{2}\int_{\mathbb{T}}\left[\left(1 + \cos^2\vartheta\right)\cos 2\varphi\cos 2\psi - 2\cos\vartheta\sin 2\varphi\sin 2\psi\right] f(\varphi, \vartheta, \psi)\, d\omega, \tag{2.4.26}$$

where $\mathbb{T}$ is the toroidal manifold $\mathbb{S}^2 \times \mathbb{S}^1$ parameterized by the Euler angles, with $\mathbb{S}^n$ the unit sphere in the $n-$dimensional Euclidean space. The area measure $d\omega$ on $\mathbb{T}$ is $\sin\vartheta d\vartheta d\varphi d\psi$.

There are two ways for the system to become biaxial. If f is isotropic in ψ, but anisotropic in φ, then $T' = 0$, whereas $T \neq 0$: this is the *phase* biaxiality produced, for instance, by an anisotropic distribution of rod-like molecules under an external field, but which is unlikely to occur spontaneously. On the other hand, a function f isotropic in φ, but anisotropic in ψ, would give $T = 0$, but $T' \neq 0$: this is the macroscopic sign of the *intrinsic*, molecular biaxiality, that would correspond to the natural tendency of biaxial molecules to orient parallel to one another. Whatever may be the choice of the

distribution function f used for the computation of these ensemble averages, the following bounds hold, due to the admissible ranges of the Euler angles

$$
\begin{aligned}
&-\tfrac{1}{2} \leq S \leq 1, \quad -\tfrac{1}{3}(1-S) \leq T \leq \tfrac{1}{3}(1-S), \\
&-(1-S) \leq S' \leq (1-S), \quad -1 \leq T' \leq 1,
\end{aligned}
\tag{2.4.27}
$$

which represents a compact subset $\mathcal{M}$ of $\mathbb{R}^4$. A rather telling geometric interpretation can be given for these bounds: the state manifold $\mathcal{M}$ can be represented as the product $\mathcal{W} \times [-1,1]$, where $\mathcal{W}$ is the wedge in the (S,T,S')-space defined by the inequalities (2.4.27). Fig. 2.4.1 shows the triangular base of this wedge on the (S,T)-plane. The vertices of this triangle represent the fully ordered uniaxial states along the axis of the reference frame; the medians correspond to the partially ordered uniaxial states, with the isotropic state in their common intersection; any other point in the triangle represents a state of phase biaxiality as explained in **[30]**. Of course, each vertex represents the same uniaxial state, oriented along one of the three reference axes. This equivalence property is indeed more general, as it applies to all inner points of the triangle: all points conjugated relative to one and the same median represent the same state with a different orientation. As a consequence, the states represented by the shaded region in Fig. 2.4.1 cover all possible (S,T)-states of the system. Clearly, the symmetry transformations thus illustrated in the (S,T)-plane act accordingly on the (S',T')-plane; formally, they are described by the mappings

$$
\begin{aligned}
&(S,T,S',T') \mapsto (S,-T,S',-T'), \\
&(S,T,S',T') \mapsto \left(\tfrac{\pm 3T-S}{2}, \tfrac{T\pm S}{2}, \tfrac{\pm 3T'-S'}{2}, \tfrac{T'\pm S'}{2}\right),
\end{aligned}
\tag{2.4.28}
$$

These transformations, together with their analogs for S and T, must leave invariant any macroscopic potential expressed in terms of the order parameters (S,T,S',T').

2.4.2. Molecular–field approximation. We now build a distribution function f by using a **mean-field** approximation for the potential in equation (2.3.15). In this approximation the two-bodies interaction potential is replaced by a single-particle pseudo-potential

$$
\Omega(\mathbf{q},\mathbf{b}) = -U_0 \Psi(\mathbf{q},\mathbf{b}), \tag{2.4.29}
$$

where

$$
\Psi(\mathbf{q},\mathbf{b}) := \xi \mathbf{q}\cdot\mathbf{Q} + \gamma(\mathbf{q}\cdot\mathbf{B} + \mathbf{b}\cdot\mathbf{Q}) + \lambda \mathbf{b}\cdot\mathbf{B}. \tag{2.4.30}
$$

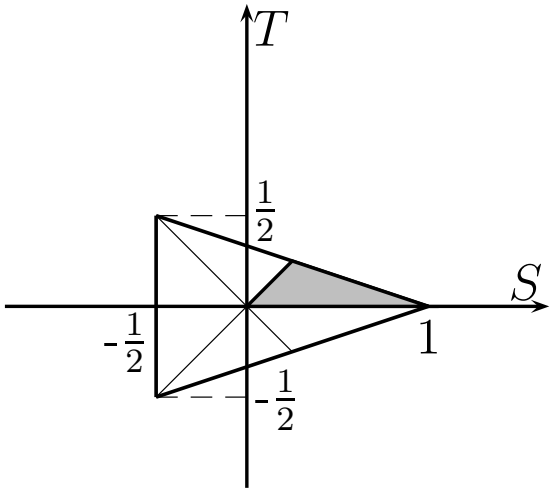

FIGURE 2.4.1. (S,T)-plane projection of the state manifold $\mathcal{M}$.

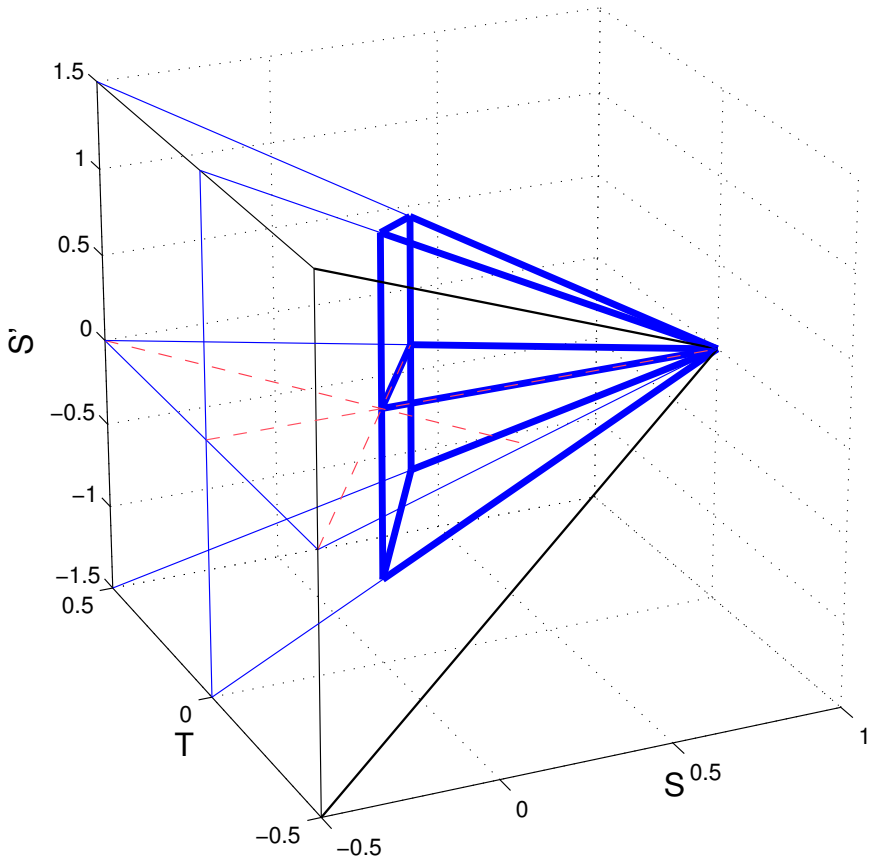

FIGURE 2.4.2. (S,T,S')-space $(\mathcal{W})$ visualization of the state manifold $\mathcal{M}$.

The Boltzmann distribution function in this approximation is

$$f = \frac{\exp\left(\beta\left(\xi \mathbf{q}\cdot\mathbf{Q} + \lambda \mathbf{b}\cdot\mathbf{B} + \gamma\left(\mathbf{q}\cdot\mathbf{B} + \mathbf{Q}\cdot\mathbf{b}\right)\right)\right)}{Z\left(\mathbf{Q},\mathbf{B},\beta,\xi,\lambda,\gamma\right)} \tag{2.4.31}$$

where $\beta = \frac{U_0}{k_B t}$, k_B is the Boltzmann constant and t the absolute temperature. Z is the partition function

$$Z(\mathbf{Q}, \mathbf{B}, \beta, \xi, \lambda, \gamma) = \int_{\mathbb{T}} \exp\left(\beta\left(\xi \mathbf{q}\cdot\mathbf{Q} + \lambda \mathbf{b}\cdot\mathbf{B} + \gamma\left(\mathbf{q}\cdot\mathbf{B} + \mathbf{Q}\cdot\mathbf{b}\right)\right)\right) d\omega. \tag{2.4.32}$$

Within the class of mean-field distribution functions (2.4.31), the inverse implication of Proposition (2.4.1) holds. Actually, if the two tensors commute then there exists an orthonormal basis of eigenvector $\boldsymbol{e}_x, \boldsymbol{e}_y, \boldsymbol{e}_z$ and they commute with the rotations

$$\mathbf{R}_x = 2\boldsymbol{e}_x \otimes \boldsymbol{e}_x - \mathbf{I}, \quad \mathbf{R}_z = 2\boldsymbol{e}_z \otimes \boldsymbol{e}_z - \mathbf{I}. \tag{2.4.33}$$

Hence, if we consider the distribution function (2.4.31), the partition function Z does not depend on $(\mathbf{q}, \mathbf{b})$ and

$$\mathbf{R}_x \mathbf{q} \mathbf{R}_x^T \cdot \mathbf{Q} = \mathrm{tr}\left(\mathbf{R}_x \mathbf{q} \mathbf{R}_x^T \mathbf{Q}\right) = \mathrm{tr}\left(\mathbf{R}_x \mathbf{q} \mathbf{Q} \mathbf{R}_x^T\right) = \mathrm{tr}\left(\mathbf{R}_x^T \mathbf{R}_x \mathbf{q} \mathbf{Q}\right) = \mathrm{tr}\left(\mathbf{q}\mathbf{Q}\right), \tag{2.4.34}$$

similar equalities holding for the other scalar products in the exponential function in (2.4.31). Thus we conclude that f is invariant under $\mathbf{R}_x$ and $\mathbf{R}_z$.

In the molecular field approximation, the free-energy takes the form

$$\mathcal{F}(\mathbf{Q}, \mathbf{B}, \beta, \xi, \lambda, \gamma) = U_0 \left\{ \frac{1}{2}\left(\xi \mathbf{Q}\cdot\mathbf{Q} + \lambda \mathbf{B}\cdot\mathbf{B} + 2\gamma \mathbf{Q}\cdot\mathbf{B}\right) - \frac{1}{\beta} \ln\left(\frac{Z(\mathbf{Q}, \mathbf{B}, \beta, \xi, \lambda, \gamma)}{8\pi^2}\right)\right\}. \tag{2.4.35}$$

Thus, since f in Eq. (2.4.31) depends on the averages $\mathbf{Q}$ and $\mathbf{B}$, it must obey the following compatibility conditions

$$\mathbf{Q} = \int_{\mathbb{T}} f \mathbf{q} d\omega, \qquad \mathbf{B} = \int_{\mathbb{T}} f \mathbf{b} d\omega, \tag{2.4.36}$$

which entail the extremum conditions of free-energy (2.4.35) and they are called *mean–field equations.*

We now consider again Freiser's model in Eq. (2.3.38) (Refs. **[12, 13]**) to show how it can be recovered as a special mean–field of ours. In particular, we choose the model $\xi = 1$ and $\gamma = 0$, *i.e.* the microscopic potential in Eq. (2.3.37), and write down the corresponding pseudo–potential

$$\Omega(\mathbf{q}, \mathbf{b}) = -U_0\left(\mathbf{q}\cdot\mathbf{Q} + \lambda \mathbf{b}\cdot\mathbf{B}\right). \tag{2.4.37}$$

In this equation, setting $\lambda = \frac{\epsilon_b}{\epsilon_u}$ and introducing the constraint $\mathbf{Q} = \mathbf{B}$ we get

$$\Omega = -\frac{U_0}{\epsilon_u} \boldsymbol{\epsilon}\cdot\mathbf{Q}, \tag{2.4.38}$$

and taking into account that

$$\langle \boldsymbol{\epsilon} \rangle = \langle \epsilon_u \mathbf{q} + \epsilon_b \mathbf{b} \rangle = \mathbf{Q} \left(\epsilon_u + \epsilon_b \right) = \epsilon_u \mathbf{Q} \left(1 + \lambda \right) = \epsilon_u \left(\mathbf{Q} + \lambda \mathbf{B} \right), \tag{2.4.39}$$

we arrive at

$$\Omega = -V_0 \boldsymbol{\epsilon} \cdot \langle \boldsymbol{\epsilon} \rangle, \quad V_0 := \frac{U_0}{\epsilon_u \left(\epsilon_u + \epsilon_b \right)} \tag{2.4.40}$$

which is equivalent to Freiser's molecular field model, since he takes $\langle \boldsymbol{\epsilon} \rangle$ as macroscopic order tensor instead of $\langle \mathbf{q} \rangle$. Thus, the two models, which differ from a microscopic point of view, reconcile mathematically on a macroscopic scale, with a precise distinction: the constraint $\mathbf{Q} = \mathbf{B}$ forces T and T' to be the same order parameter and merges S and T' in the same tensor, while the original model has two distinct tensors with different physical meanings.

Another equivalent manner to build a molecular field theory consists of starting from the parameterization in terms of Euler angles and the symmetry-adapted functions (2.3.47). We consider two molecules interacting via V in Eq. (2.3.45). Their orientations can be specified via two orthonormal triplets of $3-$components vectors $\left\{ \boldsymbol{e}^1, \boldsymbol{e}^1_\perp, \boldsymbol{m}^1 \right\}$ and $\left\{ \boldsymbol{e}^2, \boldsymbol{e}^2_\perp, \boldsymbol{m}^2 \right\}$ with respect to a common Cartesian frame (we can choose $\{\boldsymbol{e}_x, \boldsymbol{e}_y, \boldsymbol{e}_z\}$) by a triplet of Euler angles $\omega_\alpha = (\varphi_\alpha, \vartheta_\alpha, \psi_\alpha)$, with $\alpha = 1, 2$ and V is a function of ω_1 and ω_2. The mean–field theory consists of implementing the D_{2h} molecular symmetry in the mean field itself, realizing a symmetry–conserving mean–field. We can achieve this purpose by projecting the potential V on the basis

$$b_{jk} \left(\omega_1, \omega_2 \right) := s_j \left(\omega_1 \right) s_k \left(\omega_2 \right), \tag{2.4.41}$$

and replacing the pair potential with the field

$$\tilde{V} \left(\omega_1, \omega_2 \right) = \sum_{j,k=1}^{4} d_{jk} b_{jk} \left(\omega_1, \omega_2 \right), \tag{2.4.42}$$

where

$$d_{jk} = \frac{\int_{\mathbb{T}_1} \int_{\mathbb{T}_2} V \left(\omega_1, \omega_2 \right) b_{jk} \left(\omega_1, \omega_2 \right) d\omega_1 d\omega_2}{\int_{\mathbb{T}_1} \int_{\mathbb{T}_2} \left(b_{jk} \left(\omega_1, \omega_2 \right) \right)^2 d\omega_1 d\omega_2}. \tag{2.4.43}$$

This strategy is equivalent to that adopted by other Authors (see [**17**] and [**46**]). The coupling matrix **d** is given by

$$[\mathbf{d}] = -U_0 \begin{pmatrix} \frac{2}{3}\xi & 0 & \sqrt{\frac{8}{3}}\gamma & 0 \\ 0 & \frac{4}{3}\xi & 0 & 2\sqrt{\frac{8}{3}}\gamma \\ \sqrt{\frac{8}{3}}\gamma & 0 & 4\lambda & 0 \\ 0 & 2\sqrt{\frac{8}{3}}\gamma & 0 & 8\lambda \end{pmatrix}, \tag{2.4.44}$$

and the potential is replaced by the pseudo-potential

$$\Omega = \sum_{j,k=1}^{4} d_{jk} \langle s_j \rangle s_k(\omega) \tag{2.4.45}$$

which is the same of the equation (2.4.29) with the identification

$$S = \langle s_1 \rangle, \quad T = \sqrt{\frac{2}{3}} \langle s_2 \rangle, \quad S' = \sqrt{6} \langle s_3 \rangle, \quad T' = 2 \langle s_4 \rangle. \tag{2.4.46}$$

and $\omega = (\varphi, \vartheta, \psi)$ the Euler angles representing the orientation of a molecule in the frame $\{\boldsymbol{e}_x, \boldsymbol{e}_y, \boldsymbol{e}_z\}$. As a consequence, the free–energy $\mathcal{F}$ takes the form

$$\mathcal{F} = -\frac{1}{2} \sum_{j,k=1}^{4} d_{jk} \langle s_j \rangle \langle s_k \rangle - k_B t \ln(\frac{Z}{8\pi^2}), \tag{2.4.47}$$

and the consistency equations take the form

$$\frac{\partial \mathcal{F}}{\partial \langle s_k \rangle} = 0, \quad k = 1, 2, 3, 4. \tag{2.4.48}$$

which are equivalent to (2.4.36).

In general, in a mean–field framework, a set of self–consistency equations has to be satisfied in order to make the theory reliable. As a consequence, the Helmholtz free–energy attains the true minimum on the subset of the order parameters space which consists of the solutions of the consistency relationships. Hence, the free–energy (2.4.35) has to be minimized on the subset of $\mathcal{M}$ fulfilling the equations (2.4.36). In solving these equations, when several stable solutions can exist at a certain temperature, the stable phase is that with the lowest Helmholtz free–energy. Moreover, in our case the *mean–field equations* turn out to be the stationarity conditions for $\mathcal{F}$, but this is not the general case.

In Chapter 4 we will perform a bifurcation analysis of the model $\xi = 1$ and $\gamma = 0$, in order to compute the phase diagram of the liquid crystal.

CHAPTER 3

Tricriticality

In Ref. [**30**], the case where $\xi = 1$, $\gamma = 0$ and λ ranges in the interval $\left[0, \frac{1}{3}\right]$ was extensively considered and a tricritical point was discovered in the phase diagram. More precisely, it was shown that for small enough values of λ the classical Maier-Saupe first-order transition from the isotropic phase is followed, at a large enough value of β, by a second-order transition to a biaxial phase characterized by $T' \neq 0$ and by both T and S' almost vanishing. This *scenario* changes qualitatively when λ grows: the transition to the biaxial phase becomes first-order, as shown by solving numerically the equilibrium equations, thus disclosing a tricritical point. In this Chapter we firstly introduce a criterion to find tricritical points and then apply it to this model predicting biaxial phases.

The Chapter is organized as follows. In Sec. 3.1, we recall the main definitions of the tricritical points. In Sec. 3.2, we derive a criterion to identify these points. In Sec. 3.3, we contrast the criterion worked out here with the one already known from the literature. In Sec. 3.4 we show how this criterion is able to identify correctly the tricritical points already known to be exhibited by the phase diagrams for smectic and biaxial liquid crystals. Moreover, we predict the existence of a new tricritical point for biaxial liquid crystals in a range of parameters not yet explored (see also Ref. [**47**]).

3.1. Symmetric tricritical points

In general, tricritical points occur whenever *three* coexisting fluid phases become simultaneously identical [**48**]. A tricritical point is thus different from both a critical point, where only two coexisting phases become identical, and a critical end point, where two phases become identical, in the presence of a third dissimilar phase. Ordered soft matter systems other than fluid mixtures can also exhibit tricritical points: there, three ordered phases become identical. Often two such phases are conjugated by a symmetry transformation: when this is the case, the tricritical points are referred to as being symmetric [**48**]. Symmetric tricritical points are the object of this Chapter, especially in liquid crystals, where the underling molecular symmetry is more likely to induce them [**49, 50, 51, 52**]. In Griffiths's terminology [**53**], a tricritical point is also a point on a phase diagram where a first-order transition becomes second-order (the equivalence between these two definitions of a tricritical point is well explained, for example, on pp. 29-30 of Ref. [**54**]; Ref. [**55**] is another relevant general reference).

Within a simplified model describing the ordered phase of a system in terms of a single order parameter ψ, the free energy $\mathcal{F}$ can be given the following Landau expansion:

$$\mathcal{F} = a_2\psi^2 + a_4\psi^4 + \psi^6 + o(\psi^6), \tag{3.1.1}$$

where only even powers of ψ are retained since ψ and $-\psi$ are thought of as corresponding to one and the same state. The coefficients a_2 and a_4 in Eq. (3.1.1) depend on a set of physical field variables, generally including the temperature. The coefficient of ψ^6, which must be positive for thermodynamic stability, is set equal to unity, as its specific value is inessential [**56**]. In this simplified setting, the criterion for the existence of a tricritical point is given by the equations [**48, 56**]:

$$a_2 = a_4 = 0. \tag{3.1.2}$$

These equations have been extended to multi-component fluid mixtures [**57, 58**], though the reasoning was essentially left unchanged. In liquid crystals, however, the occurrence of tricritical points is more likely related to ordered phases that need to be described by more than a single order parameter [**49, 50, 30**]. The existing criterion for tricritical points in the liquid crystal literature [**59, 60, 61**] appears as an extension of the classical criterion (3.1.2) based on the assumption that all order parameters can be seen as functions of a leading one, still conventionally denoted by ψ, which is different from zero only in the ordered phase and which then makes all other order parameters differ from zero as well. Under this assumption, $\mathcal{F}$ can again be given an effective form like in Eq. (3.1.1), but with both a_2 and a_4 expressed in terms of the coefficients of the Landau expansion of $\mathcal{F}$ thought of as a function of all independent order parameters. Accordingly, the criterion for tricriticality is still derived from Eqs. (3.1.2) [**59, 60**].

In this Chapter we take a different avenue. We consider a general ordered system with two independent order parameters, symmetric in one of them. Our motivation comes from the study of the molecular model for biaxial phases in nematic liquid crystals with $\xi = 1$ and $\gamma = 0$ [**30**], which represents a special case of the model envisaged by Straley [**16**] and presented in Chapter 2. Straley's model introduces four independent order parameters to describe a fully developed biaxial phase, while essentially two of them suffice in the simpler model studied in Ref. [**30**]. The occurrence of a tricritical point in the phase diagram predicted by this model called for a more general criterion fit to identify both such points and the portion of the critical manifold that indeed corresponds to second-order phase transitions.

3.2. Criterion

We study a model system with ordered phases described by two order parameters, X and Y, for which we confine attention to states homogeneous in space. We assume that the free energy $\mathcal{F}$ is a smooth function of X, Y, and several physical parameters $\{\beta, \lambda_1, ..., \lambda_n\}$, among which is $\beta := \frac{U_0}{\kappa_B t}$, where κ_B is the Boltzmann constant, t is the absolute temperature and U_0 a typical energy of the system. In the following, we denote by $\lambda := (\lambda_1, ..., \lambda_n)$ the vector of $\mathbb{R}^n$ comprising all parameters independent of the temperature. In general, the admissible parameters λ range in a subset of $\mathbb{R}^n$, which we denote by $\mathbb{A}$. For simplicity, we further assume that $\mathcal{F}$ enjoys the symmetry property

$$\mathcal{F}(X, Y, \beta, \lambda) = \mathcal{F}(X, -Y, \beta, \lambda), \tag{3.2.1}$$

which makes equilibria with $Y = 0$ the natural candidates for states whence a second-order phase transition could develop. Though these assumptions might appear to be quite restrictive at first glance, they are valid for disparate mean-field models of liquid crystals, as shown in Sec. 3.4 below.

At equilibrium, for given β and λ, the order parameters of the system solve the equations

$$\frac{\partial \mathcal{F}}{\partial X}(X, Y, \beta, \lambda) = 0, \tag{3.2.2}$$

$$\frac{\partial \mathcal{F}}{\partial Y}(X, Y, \beta, \lambda) = 0. \tag{3.2.3}$$

These equations may possess more than a single root (X, Y), each of which represents an equilibrium phase. We call *locally stable* a phase where $\mathcal{F}$ attains a relative minimum and *globally stable* a phase where $\mathcal{F}$ attains its absolute minimum. We assume that the system always admits a globally stable phase in $\mathbb{A}$. Let first λ_0 be given in $\mathbb{A}$. Suppose that for all β in an appropriate range I there is an equilibrium phase described by $X = X_0(\beta, \lambda_0)$ and $Y = 0$. Conventionally, we say that $(X_0, 0)$ represents a *reference state* for the system. It may represent a stable phase of the system and it may not: it could be any equilibrium state of the system whose vicinity is worth exploring. We denote by $[H_0]$ the Hessian matrix of $\mathcal{F}$ at the point $(X_0, 0)$. By the symmetry requirement (3.2.1), $[H_0]$ is diagonal, and its two eigenvalues are given by

$$\Sigma_X(\beta, \lambda_0) := \frac{\partial^2 \mathcal{F}}{\partial X^2}(X_0(\beta, \lambda_0), 0, \beta, \lambda_0), \tag{3.2.4}$$

$$\Sigma_Y(\beta, \lambda_0) := \frac{\partial^2 \mathcal{F}}{\partial Y^2}(X_0(\beta, \lambda_0), 0, \beta, \lambda_0). \tag{3.2.5}$$

Our strategy will be to look for other equilibrium phases near a given reference state and, if there is any, to see which is likely to be locally stable. The success of this strategy will clearly depend on the

choice of the reference state. We expand the free energy $\mathcal{F}$ in power series about $(X_0, 0)$:

$$\begin{aligned} \mathcal{F}(X_0 + \delta X, Y) &= \mathcal{F}(X_0, 0) + F_1 Y^2 + F_2 Y^4 + F_3 Y^2 \delta X \\ &+ F_4 (\delta X)^2 + F_5 (\delta X)^4 + F_6 Y^2 (\delta X)^2 + F_7 (\delta X)^3 + O(5), \end{aligned} \tag{3.2.6}$$

where use has been made again of the symmetry requirement (3.2.1). The coefficients $\{F_j\}_{j=1...7}$ are related to the partial derivatives of $\mathcal{F}$ with respect to X and Y at the reference state: they are all functions of (β, λ_0). In particular, also by Eqs. (3.2.4) and (3.2.5),

$$F_1 := \frac{1}{2} \Sigma_Y (\beta, \lambda_0), \tag{3.2.7}$$

$$F_2 := \frac{1}{24} \left(\frac{\partial^4 \mathcal{F}}{\partial Y^4} \right)_{(X_0, 0)}, \tag{3.2.8}$$

$$F_3 := \frac{1}{2} \left(\frac{\partial^3 \mathcal{F}}{\partial Y^2 \partial X} \right)_{(X_0, 0)}, \tag{3.2.9}$$

$$F_4 := \frac{1}{2} \Sigma_X (\beta, \lambda_0). \tag{3.2.10}$$

If there exist equilibrium phases near the reference state, they can be found by requiring the function in Eq. (3.2.6) to be stationary, that is, by solving the equations

$$F_3 Y^2 + 2F_4 \delta X + 4F_5 (\delta X)^3 + 2F_6 Y^2 \delta X + 3F_7 (\delta X)^2 = 0, \tag{3.2.11}$$

$$F_1 Y + 2F_2 Y^3 + F_3 Y \delta X + F_6 Y (\delta X)^2 = 0. \tag{3.2.12}$$

Under the assumption that $Y \neq 0$, to the lowest approximation, these equations reduce to the following linear system

$$\begin{pmatrix} 2F_4 & F_3 \\ F_3 & 2F_2 \end{pmatrix} \begin{pmatrix} \delta X \\ Y^2 \end{pmatrix} = \begin{pmatrix} 0 \\ -F_1 \end{pmatrix}. \tag{3.2.13}$$

It is apparent from (3.2.13) that a new single equilibrium phase fails to exist whenever

$$\Delta F := 4F_2 F_4 - F_3^2 = 0. \tag{3.2.14}$$

This condition actually identifies a set in the space $I \times \mathbb{A}$, which we call the *singular manifold*. More properly, we should momentarily think of λ as being freed from the assigned value λ_0 and of $(X_0(\beta, \lambda), 0)$ as the continuation in λ of the equilibrium solution $(X_0(\beta, \lambda_0), 0)$. Thus, Eq. (3.2.14)

explicitly becomes

(3.2.15)
$$\Delta F(\beta,\lambda) := \frac{\partial^4 \mathcal{F}}{\partial Y^4}\left(X_0(\beta,\lambda),0,\beta,\lambda\right)\frac{\partial^2 \mathcal{F}}{\partial X^2}\left(X_0(\beta,\lambda),0,\beta,\lambda\right) - 3\left(\frac{\partial^3 \mathcal{F}}{\partial Y^2 \partial X}\left(X_0(\beta,\lambda),0,\beta,\lambda\right)\right)^2 = 0.$$

When (β,λ_0) does not belong to the singular manifold, the solution to Eq. (3.2.13) is *admissible*, that is, it delivers $Y^2 > 0$, only if

$$F_1 F_4 \Delta F < 0. \tag{3.2.16}$$

Moreover, the new equilibrium phase is close to the reference state $(X_0, 0)$, if F_1 is infinitesimal. For this reason we choose the reference state $(X_0, 0)$ such that (β,λ_0) is near the *critical manifold* in the space $I \times \mathbb{A}$, which is defined by the conditions

$$\Sigma_Y(\beta,\lambda) := \frac{\partial^2 \mathcal{F}}{\partial Y^2}\left(X_0(\beta,\lambda),0,\beta,\lambda\right) = 0, \tag{3.2.17}$$

$$\Sigma_X(\beta,\lambda) := \frac{\partial^2 \mathcal{F}}{\partial X^2}\left(X_0(\beta,\lambda),0,\beta,\lambda\right) > 0, \tag{3.2.18}$$

where the latter ensures that the equilibrium phase $(X_0(\beta,\lambda),0)$ is locally stable against all perturbations in the X order parameter. When (β,λ_0) lies precisely on the critical manifold, F_1 vanishes in Eq. (3.2.13) and the new equilibrium phases reduce to the reference state: all equilibrium solutions corresponding to the critical manifold can be thought of as states whence new equilibria are to bifurcate. Choosing (β,λ_0) near the critical manifold captures the bifurcation onset, and so makes it successful the strategy of finding new equilibrium phases near the reference state.

As a consequence of inequality (3.2.18), F_4 is positive in Eq. (3.2.11) and this reduces the admissibility condition (3.2.16) to

$$F_1 \Delta F < 0. \tag{3.2.19}$$

This inequality is central in the following stability analysis. At the lowest approximation, the Hessian matrix of $\mathcal{F}$ computed at $(X_0 + \delta X, Y)$, where $(\delta X, Y)$ solves Eq. (3.2.13), is

$$[H] = \begin{pmatrix} 2F_4 & 2F_3 Y \\ 2F_3 Y & 2F_1 + 12F_2 Y^2 + 2F_3 \delta X \end{pmatrix}. \tag{3.2.20}$$

Since $F_4 > 0$, the sign of $\det[H]$ suffices to characterize the local stability of $(X_0 + \delta X, Y)$:

$$\det[H] = 4F_1F_4 + 6Y^2\left(4F_2F_4 - F_3^2\right) = -8F_1F_4. \tag{3.2.21}$$

Moreover, within the same approximation, the energy difference reads as

$$\Delta\mathcal{F} := \mathcal{F}(X_0 + \delta X, Y) - \mathcal{F}(X_0, 0) = -\frac{F_1^2 F_4}{\Delta F}. \tag{3.2.22}$$

Our general assertion is that the intersection between the critical and the singular manifolds, if not empty, is constituted by tricritical points, which represent states where the character of a phase transition changes from first- to second-order. Here we prove our assert in a special case. In Fig. 3.2.1, only for illustration purposes, we describe the case where λ is a single parameter model. The following analysis can be easily extended to the general case where $\lambda \in \mathbb{R}^n$, though it becomes more cumbersome to illustrate it. Both the critical and the singular manifolds now become curves, which in Fig. 3.2.1 are represented in the $(\lambda, 1/\beta)$-plane. We assume that these curves cross at the point C. In Fig. 3.2.1, ΔF vanishes along the singular curve $\mathcal{S}$, and Σ_Y vanishes along the critical curve $\mathcal{C}$. Near C, a tubular neighborhood of the critical curve is divided into four parts by $\mathcal{S}$ and $\mathcal{C}$, which we call $\mathcal{A}_1$, $\mathcal{A}_2$, $\mathcal{A}_3$, and $\mathcal{A}_4$. For definiteness, we assume that $\Sigma_Y > 0$ in $\mathcal{A}_2 \cup \mathcal{A}_3$ and $\Sigma_Y < 0$ in $\mathcal{A}_1 \cup \mathcal{A}_4$, while $\Delta F > 0$ in $\mathcal{A}_1 \cup \mathcal{A}_3$ and $\Delta F < 0$ in $\mathcal{A}_2 \cup \mathcal{A}_4$. By inequality (3.2.19), $\mathcal{A}_1 \cup \mathcal{A}_2$ is the *admissible set*, that is, the set where there are equilibrium phases near the reference state. By Eqs. (3.2.21) and (3.2.22), in $\mathcal{A}_1$ the new equilibrium phase is locally stable since $\det[H] > 0$ and it possesses less energy than the reference state since $\Delta\mathcal{F} < 0$. Moreover, since there $\Sigma_Y < 0$, the reference state has become unstable. Clearly, in $\mathcal{A}_1$ a new stable phase bifurcates from the reference state. Similarly, in $\mathcal{A}_2$ $\det[H] < 0$ and $\Delta\mathcal{F} > 0$, while $\Sigma_Y > 0$. This means that the new equilibrium phase represents an unstable equilibrium with more energy than the reference state, while the reference state is still stable. Here no bifurcation occurs. Away from the admissible set, the reference state is not accompanied by any other equilibrium phase in its vicinity. The reference state itself is locally stable in $\mathcal{A}_3$ and unstable in $\mathcal{A}_4$. Since here we assume that a globally stable phase always exists for the system, when the parameters are chosen in $\mathcal{A}_4$, this phase must lie away from the reference state. On the other hand, in $\mathcal{A}_2$ the reference state could be either locally or globally stable.

Taking now the reference state in $\mathcal{A}_3$ as globally stable, we conclude from the foregoing discussion that it migrates slightly upon crossing the critical curve $\mathcal{C}$ from $\mathcal{A}_3$ into $\mathcal{A}_1$, whereas it jumps abruptly upon crossing the point C from $\mathcal{A}_3$ in $\mathcal{A}_4$. Such a behavior is only compatible with the presence of a first-order transition line emanating from C within $\mathcal{A}_2$ and with the interpretation of the portion of the curve $\mathcal{C}$ that separates $\mathcal{A}_1$ and $\mathcal{A}_3$ as a second-order transition line.

Thus, C is a *tricritical* point, because there two different transition lines meet: one is first-order, the other is second-order. In Fig. 3.2.1, according to Griffiths's notation **[53]**, first-order transitions are represented by a solid line, while second-order transitions are represented by a broken line.

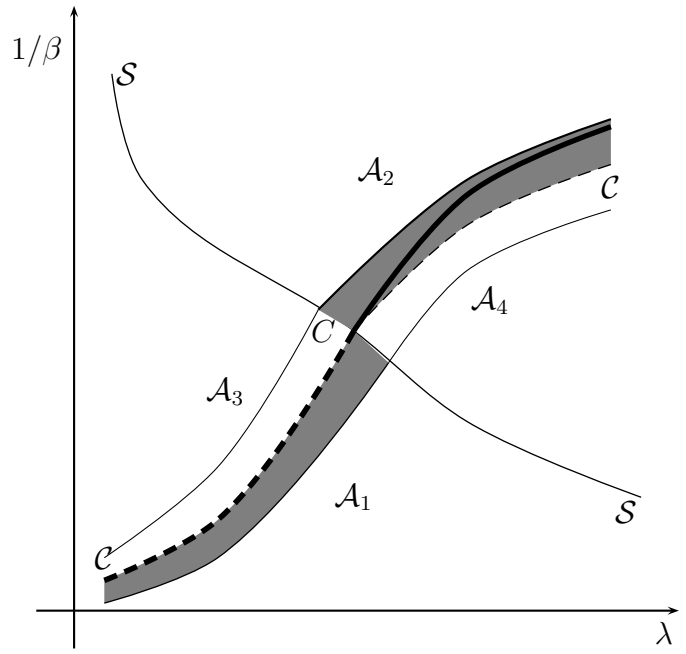

FIGURE 3.2.1. The tricritical point C is identified as the intersection between the critical curve $\mathcal{C}$ and the singular curve $\mathcal{S}$ in the plane $(\lambda, 1/\beta)$. $\mathcal{A}_1 \cup \mathcal{A}_2$ is the admissible set, where there is an equilibrium phase near the reference state. The heavy dashed line is a second-order transition line, while the heavy solid line is a first-order transition line, whose existence is predicted by the arguments developed in the text.

The situation envisaged in Fig. 3.2.1 can easily be extended. As shown in Fig. 3.2.2, the critical curve $\mathcal{C}$ and the singular curve $\mathcal{S}$ can have multiple intersections. Here the admissible set $\mathcal{A}_1 \cup \mathcal{A}_2$ has more than two adjacent components, but it is still connected; a first-order transition line joins two tricritical points, whence two distinct second-order transition lines emerge.

In conclusion, returning to the general formulation employed above, we may hold that the *tricritical manifold* is defined by Eqs. (3.2.15) and (3.2.17) and that the conditions

$$\frac{\partial^2 \mathcal{F}}{\partial Y^2}\left(X_0\left(\beta,\lambda\right),0,\beta,\lambda\right)=0 \tag{3.2.23a}$$

$$\frac{\partial^4 \mathcal{F}}{\partial Y^4}\left(X_0\left(\beta,\lambda\right),0,\beta,\lambda\right)\frac{\partial^2 \mathcal{F}}{\partial X^2}\left(X_0\left(\beta,\lambda\right),0,\beta,\lambda\right)-3\left(\frac{\partial^3 \mathcal{F}}{\partial Y^2 \partial X}\left(X_0\left(\beta,\lambda\right),0,\beta,\lambda\right)\right)^2>0, \tag{3.2.23b}$$

determine the submanifold of the critical manifold consisting of second-order transition points.

Finally, we note for later use that a better approximation for the equilibrium phase near the reference state can be obtained in the admissible set from Eqs. (3.2.11) and (3.2.12):

$$\delta X=\frac{F_1 F_3}{4F_2F_4-F_3^2-2F_1F_6}, \tag{3.2.24}$$

$$Y^2=\frac{\left(F_1F_6-2F_2F_4\right)}{4F_2F_4-F_3^2-2F_1F_6}\frac{F_1}{F_2}. \tag{3.2.25}$$

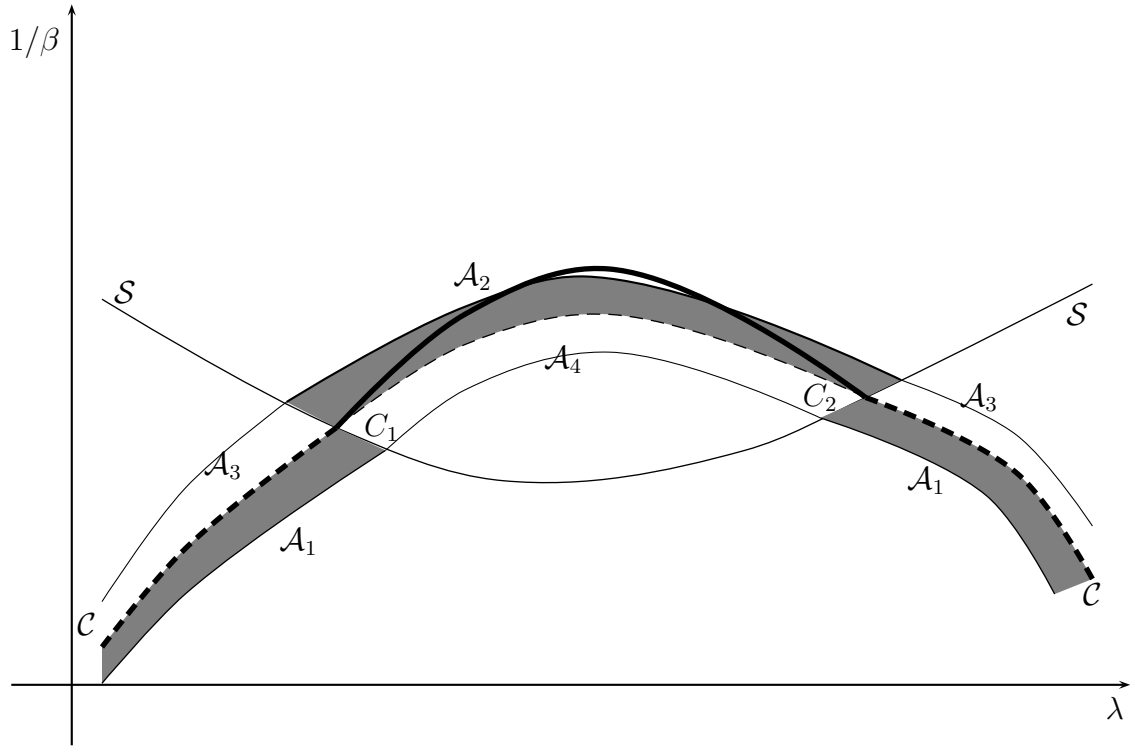

FIGURE 3.2.2. The critical curve $\mathcal{C}$ and the singular curve $\mathcal{S}$ cross in two tricritical points, C_1 and C_2, connected by a first-order transition line (heavy solid line). The second-order transition line has two distinct components (heavy dashed lines).

These formulae are useful in sketching the bifurcating solution branches and to continue them numerically. A similar improvement of the lowest approximation employed above can be obtained for both the determinant of the Hessian matrix and the energy difference along the bifurcating branches.

3.3. Comparison

We derived a criterion to identify the symmetric tricritical points in the phase diagram for a general ordered system described by two order parameters, X and Y, knowing only the free energy $\mathcal{F} = \mathcal{F}(X, Y)$. Our criterion is embodied by Eqs. (3.2.15) and (3.2.17). Moreover, since our reasoning rests essentially on a local stability analysis, we were also able to characterize the subset of the critical manifold bordered by the tricritical manifold where the transition is genuinely second-order (see inequality (3.2.23b) above). In general, the criterion proposed here is valid if the free energy is however given in terms of the order parameters; this is always the case for a molecular field theory, as was for the applications shown in Sec. 3.4.

We already mentioned in the Sec. 3.1 another criterion to find tricritical points separating liquid crystal phases **[59, 60]**. It stems from extending Griffiths's criterion to a system with more than one order parameter, under the assumption that there is always a single leading order parameter, on which all others depend in the ordered phase. Taking in our setting Y as the leading order parameter and denoting by f the function linking $\delta X := X - X_0$ to Y, so that $\delta X = f(Y)$, we easily see that the path

of equilibrium states in the vicinity of the reference state $(X_0, 0)$, where $\delta X = Y = 0$, is described by the equations

$$\frac{\partial(\Delta\mathcal{F})}{\partial Y}(f(Y), Y) = 0, \qquad \frac{\partial(\Delta\mathcal{F})}{\partial(\delta X)}(f(Y), Y) = 0, \tag{3.3.1}$$

where $\Delta\mathcal{F}$ is defined as in Eq. (3.2.22). It follows from the second of Eqs. (3.3.1) that

$$\frac{\partial^2(\Delta\mathcal{F})}{\partial(\delta X)\partial Y} + \frac{\partial^2(\Delta\mathcal{F})}{\partial(\delta X)^2} f' = 0, \tag{3.3.2}$$

where a prime denotes differentiation with respect to Y. Since $\Delta\mathcal{F}$ is symmetric in Y, also by Eq. (3.2.18), Eq. (3.3.2) implies that f' vanishes at the reference state $(X_0, 0)$, whenever this lies on the critical manifold. Thus, evaluating both $(\Delta\mathcal{F})''$ and $(\Delta\mathcal{F})''''$ at the reference state, we find that there

$$(\Delta\mathcal{F})'' = \left(\frac{\partial^2\mathcal{F}}{\partial Y^2}\right)_{(X_0,0)}, \qquad (\Delta\mathcal{F})'''' = \left(\frac{\partial^4\mathcal{F}}{\partial Y^4}\right)_{(X_0,0)} - \frac{3}{\left(\frac{\partial^2\mathcal{F}}{\partial X^2}\right)_{(X_0,0)}} \left(\frac{\partial^3\mathcal{F}}{\partial Y^2 \partial X}\right)^2_{(X_0,0)}.$$

Requiring both $(\Delta\mathcal{F})''$ and $(\Delta\mathcal{F})''''$ to vanish, as prescribed by Griffiths's criterion, reproduces our Eqs. (3.2.15) and (3.2.17). This shows that the existing criterion **[59, 60]**, which assumes the existence of a leading order parameter, reduces to ours, which does not require that assumption. An assumption which appears not to apply to the general molecular model for biaxial liquid crystals, where one or another of the four Straley's order parameters can remain virtually zero after an ordering transition **[42, 62]**.

3.4. Applications

In this section we apply the criterion presented above to two different molecular models. These are mean-field models for smectic and biaxial phases in liquid crystals. In both cases, the reference state is one of the equilibrium phases predicted by Maier-Saupe's molecular model for nematic liquid crystals **[14]**.

3.4.1. McMillan's model for smectics. McMillan's mean-field theory for smectics is a two-order-parameter theory **[49]**. This theory extends Maier-Saupe's by accounting for the possibility that the slender liquid crystal molecules be also subject to a positional ordering superimposed to the orientational ordering. At variance with Maier-Saupe's pair potential, McMillan's pair potential V_{12} also includes a part depending on the intermolecular distance r_{12}:

$$V_{12}(r_{12}, \cos\vartheta_{12}) = -\left(\frac{V_0}{N r_0^3 \pi^{\frac{3}{2}}}\right) \exp\left[-\left(\frac{r_{12}}{r_0}\right)^2\right] \left(\frac{3}{2}\cos^2\vartheta_{12} - \frac{1}{2}\right), \tag{3.4.1}$$

where ϑ_{12} is the angle between the orientations of the interacting molecules, V_0 is a typical interaction energy, N is the number density of particles, r_0 is a typical molecular length. In this equation, V_{12} decays exponentially with r_{12}, thus reflecting the short range character of the interaction. Within the mean-field theory, one assumes that each molecule feels a mean potential V_1 which can be viewed as an average of the pair potential V_{12}. Under the further assumption that all molecules are preferentially aligned along the z-axis and that their centers of mass tend to lie on planes parallel to the (x, y)-plane, at the distance d from one another, McMillan arrived at the following expression for V_1

$$V_1(z, \cos\vartheta) = -V_0\left[S + \sigma\alpha\cos\left(\frac{2\pi z}{d}\right)\right]\left(\frac{3}{2}\cos^2\vartheta - \frac{1}{2}\right), \tag{3.4.2}$$

where ϑ is the angle that the individual molecule makes with the z-axis, S and σ are order parameters, and $\alpha := 2\exp\left[-(\pi r_0/d)^2\right]$ is a model parameter ranging in the interval $[0, 2]$. S is the classical Maier-Saupe order parameter **[14]**, which expresses the orientational order within the molecules, while σ is a smectic order parameter, which expresses the degree of positional order within the layer structure of the molecular centers of mass. S ranges in the interval $\left[-\frac{1}{2}, 1\right]$, while σ ranges in the interval $[-1, 1]$. Within the mean-field approximation, the partition function and the free energy per molecule of this system are, respectively,

$$Z(S, \sigma, \beta, \alpha) = \int_0^{2\pi} d\varphi \int_0^1 du \exp\left[\beta(S + \alpha\sigma\cos\varphi)\left(u^2 - \frac{1}{3}\right)\right] \tag{3.4.3}$$

and

$$\mathcal{F}(S, \sigma, \beta, \alpha) = \frac{1}{2}V_0\left\{\left(S^2 + \alpha\sigma^2\right) - \frac{3}{\beta}\ln\frac{Z(S, \sigma, \beta, \alpha)}{2\pi}\right\}, \tag{3.4.4}$$

where $\beta := \frac{3}{2}\frac{V_0}{\kappa_B t}$ and κ_B is the Boltzmann constant **[49]**. It should be noted that $\mathcal{F}$ is even in σ:

$$\mathcal{F}(S, \sigma, \beta, \alpha) = \mathcal{F}(S, -\sigma, \beta, \alpha),$$

and so it falls within the class of free energies to which the criterion presented in the preceding section can be directly applied, with the identifications $X = S$ and $Y = \sigma$. When α is sufficiently small, McMillan's model appears to be a perturbation of Maier-Saupe's. As is well-known, this latter predicts that the isotropic phase corresponding to $S = 0$ is accompanied by another locally stable equilibrium phase as soon as $\beta > \beta^* \approx 6.73$ (see Fig. 2.1.2). This is the oriented nematic phase, which is characterized by the largest positive root $S_+(\beta)$ of the equilibrium equation

$$\frac{\partial\mathcal{F}}{\partial S} = 0,$$

which for $\alpha = 0$ becomes

$$\frac{2}{3}S + \frac{1}{3} + \frac{1}{2S\beta} - \frac{\exp(S\beta)}{\sqrt{\pi S\beta}Erfi\left(\sqrt{S\beta}\right)} = 0, \tag{3.4.5}$$

where

$$Erfi(x) := \frac{2}{\sqrt{\pi}}\int_0^x e^{t^2}dt \quad \text{for all } x \in \mathbb{R}. \tag{3.4.6}$$

For $\beta > \beta_c \approx 6.81$, the nematic phase has indeed lower free energy than the isotropic phase, which is still locally stable, and so the system undergoes a first-order phase transition. For $\beta > \beta_* = \frac{15}{2}$, the isotropic phase becomes locally unstable and another equilibrium ordered phase with a negative order parameter $S_-(\beta)$ arises; in the absence of any external field, this phase never attains the least energy, and so it fails to be globally stable. When $\alpha = 0$, the only phase transition undergone by the system occurs at $\beta = \beta_c$, where S condenses in S_+, but when $\alpha > 0$, this is followed by a smectic transition which establishes an equilibrium value of $\sigma \neq 0$ for $\beta > \beta_c' > \beta_c$. This secondary transition can be either first- or second-order [**49**]: we show now how our criterion is able to locate correctly the tricritical point where the change of type in the secondary phase transition occurs. Specifically, for $\alpha > 0$ and $\beta > \beta^*$, we take the state with $S = S_+(\beta)$ and $\sigma = 0$ as reference state. The eigenvalues Σ_σ and Σ_S defined in (3.2.17) and (3.2.18) here become

$$\Sigma_S(\beta,\alpha) := \frac{\partial^2 \mathcal{F}}{\partial S^2}(S_+(\beta),0) = \frac{5}{2} + \frac{\beta}{3}\left(2S_+^2(\beta) - S_+(\beta) - 1\right), \tag{3.4.7}$$

$$\Sigma_\sigma(\beta,\alpha) := \frac{\partial^2 \mathcal{F}}{\partial \sigma^2}(S_+(\beta),0) = \alpha\left[1 - \alpha\left(\frac{\beta}{6}(S_+(\beta)+1) - \frac{3}{4}\right)\right], \tag{3.4.8}$$

whence it follows that Σ_S is actually independent of α and it is positive for $\beta > \beta^*$.

The critical line defined in Sec. 3.2 by Eq. (3.2.17) is here represented by the equation

$$\Sigma_\sigma(\beta,\alpha) = 0, \tag{3.4.9}$$

while the singular line defined by Eq. (3.2.15) is here (see also the Appendix)

$$\begin{aligned} &\frac{3\alpha^4}{128S_+^2}\left[75 + 20\beta\left(S_+^2 + S_+ - 1\right) + \frac{16}{27}\beta^3 S_+\left(3 + 19S_+ + 15S_+^2 - 17S_+^3\right)\right. \\ &\left. + \frac{4}{3}\beta^2\left(1 - 12S_+ - 36S_+^2 + 6S_+^3\right) + \frac{16}{81}\beta^4 S_+^2\left(10S_+^3 + S_+^2 - 8S_+ - 3\right)\right] = 0. \end{aligned} \tag{3.4.10}$$

Thus, the tricritical points are identified as the common roots of Eqs. (3.4.9) and (3.4.10), where $S_+ = S_+(\beta)$ is the largest root of Eq. (3.4.5). Figure 3.4.1 shows both critical and singular lines described by Eqs. (3.4.9) and (3.4.10) on the plane $(\alpha, 1/\beta)$. In particular, since the critical line is

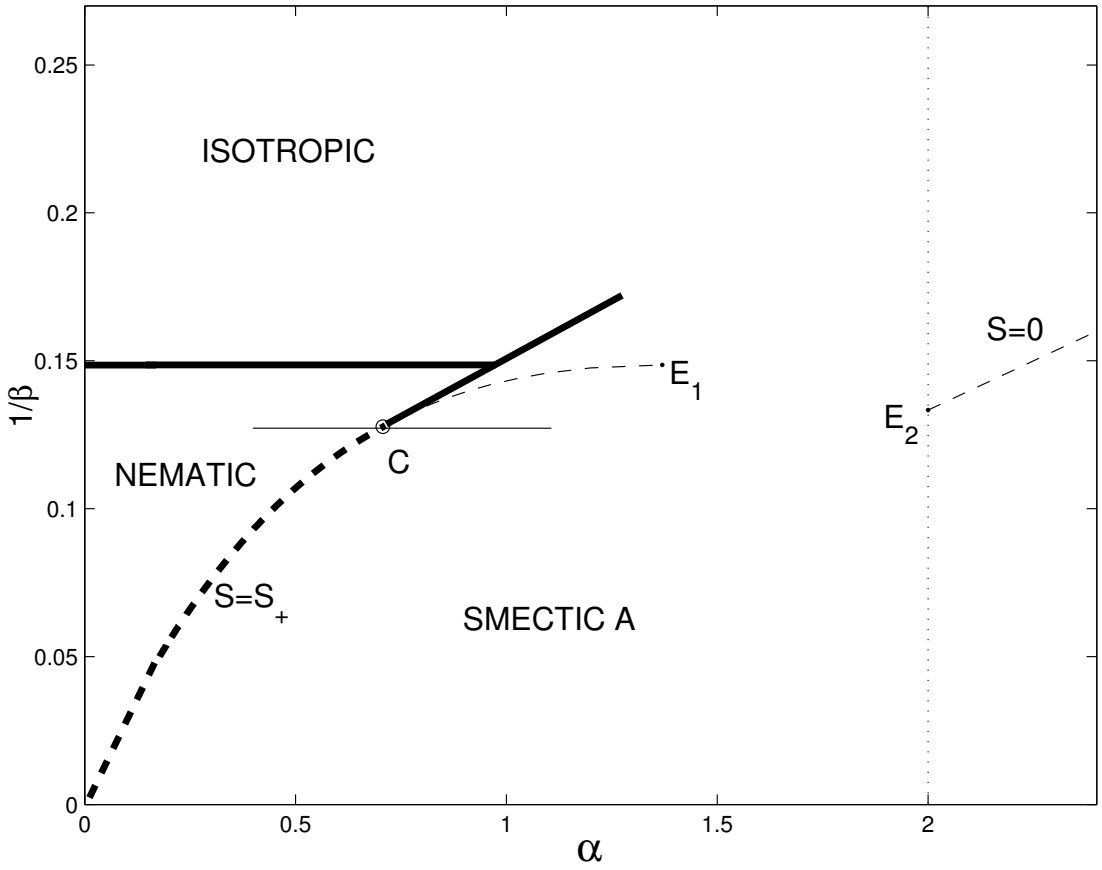

FIGURE 3.4.1. Phase diagram in the plane $(\alpha, 1/\beta)$ associated with McMillan's model for smectics A. The critical line relative to the nematic state $S = S_+$ and $\sigma = 0$ starts from the origin and ends in E_1: it is confined to the stable manifold $\beta > \beta^*$. The heavily dashed portion of this line, bounded by the line $\beta = \beta_t$, marks the second-order transition between nematic and smectic phases. C is the tricritical point. The critical line relative to the isotropic phase $S = \sigma = 0$ is confined to the stable manifold $\beta < \frac{15}{2}$: it starts from the point E_2 where $\alpha = 2$ and falls entirely outside the range of validity of the model. The heavy solid line represents first-order transitions: between isotropic and nematic phases, and between isotropic and smectic phases.

meaningful only when $\Sigma_S > 0$, the curve corresponding to Eq. (3.4.9) is restricted to the region where $\beta > \beta^*$, and so it ends at the point E_1, where $\beta = \beta^*$. Moreover, since for all $\alpha > 0$ the roots of Eq. (3.4.10) are independent of α, the singular line has indeed the equation $\beta = \beta_t$, where β_t is the root of the function of β between brackets in Eq. (3.4.10). It can be shown numerically that there is only one such root. The tricritical point C in Fig. 3.4.1 has the following co-ordinates:

$$(\beta_t, \alpha_t) \approx (7.831, 0.707) \tag{3.4.11}$$

with $S_t := S_+(\beta_t) \approx 0.657$. This tricritical point coincides with the one found by McMillan [**49**] by solving directly the equilibrium equations of the model: it is the same found by Kloczkowski and Stecki [**59**] by another method (see the discussion in the following section). By applying Eq. (3.2.23b), we finally conclude that the portion of critical line that marks a second-order transition between

nematic and smectic phases is the one heavily dashed in Fig. 3.4.1. Fig. 3.4.1 also depicts the line $\beta = \beta_c$ where the first-order transition between isotropic and nematic phases takes place and a sketch of the first-order line originated in C; when this line meets the line $\beta = \beta_c$, a first-order direct transition between isotropic and smectic phases takes place.

In principle, along this line there could be another tricritical point, where the isotropic-to-smectic transition becomes second-order, in the same spirit of the ideal situation illustrated in Fig. 3.2.2. To see whether this putative tricritical point does actually exist, we now apply our criterion taking the isotropic phase as reference state. Thus we compute both Σ_S and Σ_σ for $S = \sigma = 0$:

$$\Sigma_S(\beta, \alpha) := \frac{\partial^2 \mathcal{F}}{\partial S^2}(0,0) = 1 - \frac{2\beta}{15}, \tag{3.4.12}$$

$$\Sigma_\sigma(\beta, \alpha) := \frac{\partial^2 \mathcal{F}}{\partial \sigma^2}(0,0) = \alpha - \frac{\alpha^2 \beta}{15}. \tag{3.4.13}$$

It follows from Eq. (3.4.12) that $\Sigma_S > 0$ for $\beta < \frac{15}{2}$ and that the critical line is represented by the equation

$$\frac{1}{\beta} = \frac{\alpha}{15}. \tag{3.4.14}$$

The singular line is now represented by (see also the Appendix)

$$\alpha^4 \beta^3 (35 + 22\beta) = 0, \tag{3.4.15}$$

It is clear that Eqs. (3.4.14) and (3.4.15) have no common root for $\alpha > 0$. Moreover, by Eq. (3.4.14), Σ_S would be positive on the critical line only for $\alpha > 2$, that is, away from the range of validity of the model. Thus, the only tricritical point compatible with McMillan's model is the one in Eq. (3.4.11): the direct phase transition isotropic-to-smectic predicted by this model is first-order for all admissible values of α.

3.4.2. Model for biaxial nematics. In the mean–field approximation adopted in Chapter 2, the liquid crystal is modeled by the free–energy in Eq. (2.4.35). In Ref. **[30]** the case $\xi = 1$, $\gamma = 0$ and $\lambda \in \left[0, \frac{1}{3}\right]$ has been considered. In this case the free–energy takes the form

$$\mathcal{F}(\mathbf{Q}, \mathbf{B}, \beta, \lambda) = U_0 \left\{ \frac{1}{2}\mathbf{Q} \cdot \mathbf{Q} + \frac{\lambda}{2}\mathbf{B} \cdot \mathbf{B} - \frac{1}{\beta} \ln \left(\frac{Z(\mathbf{Q}, \mathbf{B}, \beta, \lambda)}{8\pi^2} \right) \right\}, \tag{3.4.16}$$

$$Z(\mathbf{Q}, \mathbf{B}, \beta, \lambda) = \int_{\mathbb{T}} \exp\left(\beta \left(\mathbf{Q} \cdot \mathbf{q} + \lambda \mathbf{B} \cdot \mathbf{b}\right)\right) d\omega,$$

and the equilibrium equations are given formally by

$$\frac{\partial \mathcal{F}}{\partial \mathbf{Q}} = 0, \quad \frac{\partial \mathcal{F}}{\partial \mathbf{B}} = 0, \tag{3.4.17}$$

which are the consistency mean–field equations.

Here we apply the criterion presented in Sec. 3.2 to this model. Though all admissible states are described by four scalar order parameters, instead of two, our criterion is still directly applicable since T and S' can be set equal to zero at all equilibrium phases **[30]** and the free energy $\mathcal{F}$ in Eq. (3.4.16) turns out to be even in T'. Thus, we identify X with S and Y with T' in our formal development above. Taking again as reference state Maier-Saupe's uniaxial phase described by the pair $(S_+(\beta), 0)$, with S_+ as above, we compute the following eigenvalues of the Hessian matrix $[H_0]$:

$$\Sigma_S(\beta) = \frac{2}{3}\left[\frac{5}{2} + \frac{\beta}{3}(2S_+^2 - 2S_+ - 1)\right], \tag{3.4.18}$$

$$\Sigma_{T'}(\beta, \lambda) = \frac{1}{12}\lambda\left[24 + (3 - 10\beta - 14S_+\beta)\lambda\right], \tag{3.4.19}$$

where the expression for Σ_S is proportional to the one in Eq. (3.4.7), and so again $\Sigma_S > 0$ for $\beta > \beta^* \approx 6.73$. The critical and the singular lines are represented by the equations

$$\Sigma_{T'} = 0 \tag{3.4.20}$$

and

$$\begin{aligned} &\frac{\lambda^4}{27648S_+^2}\left[2025 + 180(-3 + 17S_+ + 3S_+^2)\beta + 12(3 - 184S_+ - 652S_+^2 + 74S_+^3)\beta^2\right. \\ &\left. + \quad 80S_+(3 + 97S_+ + 181S_+^2 + 7S_+^3)\beta^3 + 16S_+^2(-65 - 192S_+ + 3S_+^2 + 254S_+^3)\beta^4\right] = 0, \end{aligned} \tag{3.4.21}$$

respectively (see also the Appendix). Thus, the tricritical points are identified as the common roots of Eqs. (3.4.20) and (3.4.21), where $S_+ = S_+(\beta)$ is defined precisely as above.

In complete analogy with our development in the above subsection, Fig. 3.4.2 shows both critical and singular lines described by Eqs. (3.4.20) and (3.4.21) on the plane $(\lambda, 1/\beta)$. In particular, since the critical line is meaningful only when $\Sigma_S > 0$, the curve corresponding to Eq. (3.4.20) is restricted to the region where $\beta > \beta^*$, and so it ends at the point E_1, where $\beta = \beta^*$. Moreover, since for $\lambda > 0$ the roots of Eq. (3.4.21) are independent of λ, the singular line has the equation $\beta = \beta_t$, where β_t is the root of the function of β within brackets in Eq. (3.4.21). By use of the asymptotic behavior of S_+ for $\beta \to \infty$,

$$S_+(\beta) \simeq \frac{1}{2}\left(1 + \sqrt{1 - \frac{6}{\beta}}\right), \tag{3.4.22}$$

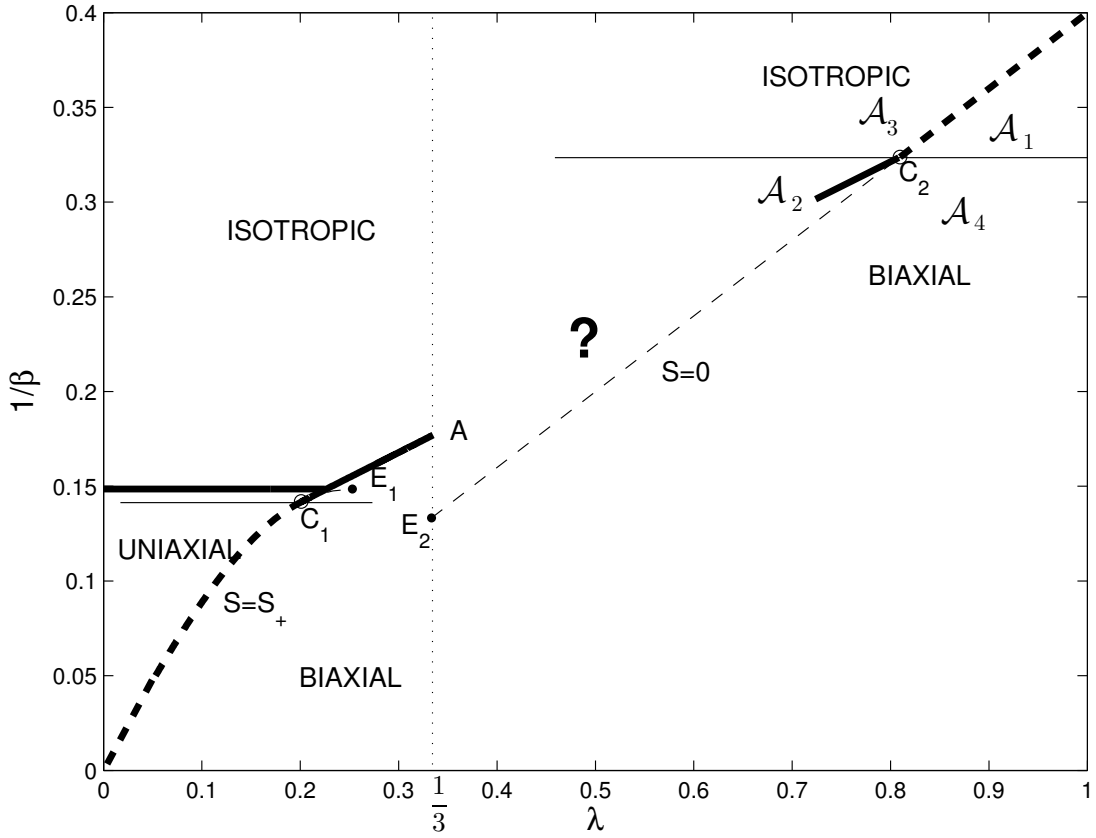

FIGURE 3.4.2. Phase diagram in the plane $(\lambda, 1/\beta)$ associated with a model for biaxials [**30**]. The critical line relative to the uniaxial state $S = S_+$ and $T' = 0$ starts from the origin and ends in E_1: it is confined to the stable manifold $\beta > \beta^*$. The heavily dashed portion of this line, bounded by the line $\beta = \beta_t^{(1)}$, marks the second-order transition between uniaxial and biaxial phases. C_1 is the first tricritical point. The critical line relative to the isotropic phase $S = T' = 0$ is confined to the stable manifold $\beta < \frac{15}{2}$: it starts from the point E_2 and goes to infinity. It hosts the second tricritical point C_2 at $\beta = \beta_t^{(2)}$; the regions $\mathcal{A}_1$, $\mathcal{A}_2$, $\mathcal{A}_3$, and $\mathcal{A}_4$ have the same meaning as in Sec. 3.2. The heavy dashed line starting from C_2 is a sketch representing second-order transitions between isotropic and biaxial phases. The heavy line represents first-order phase transitions computed for $0 < \lambda < \frac{1}{3}$ [**30**]: a bifurcation analysis is needed to know how the points A and C_2 are to be joined.

it is easily shown that there exists a single root $\beta_t^{(1)}$. The tricritical point C_1 in Fig. 3.4.2 has the following co-ordinates:

$$\left(\beta_t^{(1)}, \lambda_t^{(1)}\right) \approx (7.07, 0.20)\,, \tag{3.4.23}$$

with $S_t = S_+(\beta_t^{(1)}) \approx 0.53$. It coincides with the point found in Ref. [**30**] by inspecting the numerical solutions of the equilibrium equations. By applying Eq. (3.2.23b), we conclude that the portion of critical line that marks a second-order transition between uniaxial and biaxial phases is the one heavily dashed in Fig. 3.4.2. This figure also depicts the lines of first-order transitions computed for $0 < \lambda < \frac{1}{3}$ in Ref. [**30**].

It could also be asked for this model the same question asked for McMillan's model: as to whether the transition between isotropic and biaxial phases can possibly become second-order. To answer this question, we also study this model for $\lambda > \frac{1}{3}$ and we take the isotropic phase as reference state in our criterion. We compute both Σ_S and $\Sigma_{T'}$, for $S = T' = 0$:

$$\Sigma_S(\beta, \lambda) := \frac{\partial^2 \mathcal{F}}{\partial S^2}(0,0) = \frac{1}{3} - \frac{2\beta}{45}, \tag{3.4.24}$$

$$\Sigma_{T'}(\beta, \lambda) := \frac{\partial^2 \mathcal{F}}{\partial T'^2}(0,0) = \lambda - \frac{2\lambda^2\beta}{5}. \tag{3.4.25}$$

It follows from Eq. (3.4.24) that $\Sigma_S > 0$ for $\beta < \frac{15}{2}$ and that the critical line is represented by the equation

$$\frac{1}{\beta} = \frac{2\lambda}{5}. \tag{3.4.26}$$

The singular line is now (see also the Appendix)

$$\beta^3\lambda^4(34\beta - 105) = 0. \tag{3.4.27}$$

It is clear that Eqs. (3.4.26) and (3.4.27) have only the following root

$$\left(\beta_t^{(2)}, \lambda_t^{(2)}\right) = \left(\frac{105}{34}, \frac{17}{21}\right), \tag{3.4.28}$$

which identifies a second tricritical point C_2. By Eq. (3.2.23b), the heavy dashed line emanating in Fig. 3.4.2 from C_2 represents the locus of second-order transitions between isotropic and biaxial phases.

The criterion presented here can only predict the existence of this second tricritical point, where the phase transition between isotropic and biaxial phases becomes second-order. It says nothing on how to complete the phase diagram in the plane $(\lambda, 1/\beta)$ for $\frac{1}{3} < \lambda < \lambda_t^{(2)}$: this requires a bifurcation analysis of the equilibrium phases. Our present conjecture is that the points A and C_2 in Fig. 3.4.2 are joined by a first-order transition line. It was remarked in Ref. **[30]** that the model proposed there for biaxial nematics has a striking resemblance to McMillan's model for smectics A, in that it predicts a similar phase diagram with a tricritical point.

The main outcome of our study, surprisingly enough, was to predict the existence of another tricritical point in the phase diagram for biaxial nematics according to the model employed in Ref. **[30]**, which should occur in a range of parameter not yet explored. As explained also in **[47]**, this makes this model and McMillan's qualitatively very different, as our criterion confirmed for the latter the existence of a single tricritical point.

A bifurcation analysis of the whole class of equilibrium phases predicted by the biaxials model in Ref. [**30**] is still needed to complete the phase diagram. This study will be the subject of the subsequent Chapters.

Appendix

In this appendix we list the coefficients of the expansion in Eq. (3.2.6) for the free energy $\mathcal{F}$ that enter the definitions of both the critical and singular lines for the specific models studied above. For each model we distinguish explicitly two cases: the one where $S = S_0 \neq 0$ and the one where $S = 0$. In the former case, repeated use of Eq. (3.4.5) is made.

3.4.3. McMillan's model.

3.4.3.1. $S = S_0$.

$$F_1(S_0, \beta, \alpha) = \frac{1}{2}\Sigma_\sigma(\beta, \alpha) = -\frac{1}{8}\alpha\left[-4 + \frac{2}{3}\alpha\left(\beta S_0 + \beta - \frac{9}{2}\right)\right],$$

$$F_2(S_0, \beta, \alpha) = \\ = \frac{\alpha^4\left[105 + \frac{8}{27}\beta^3 S_0^2\left(1 + 3S_0 + 4S_0^2\right) - \frac{4}{3}\beta^2 S_0\left(-2 + S_0 + 8S_0^2\right) + 2\beta\left(-7 - 15S_0 + 12S_0^2\right)\right]}{512 S_0^2},$$

$$F_3(S_0, \beta, \alpha) = \frac{\alpha^2\left[-15 + 2\beta\left(1 + 2S_0 - 2S_0^2\right) + \frac{4}{9}\beta^2 S_0\left(-1 - S_0 + 2S_0^2\right)\right]}{16 S_0},$$

$$F_4(S_0, \beta) = \frac{1}{2}\Sigma_S(\beta) = \frac{1}{4}\left[5 + \frac{2}{3}\beta\left(-1 - S_0 + 2S_0^2\right)\right].$$

3.4.3.2. $S = 0$.

$$F_1(\beta, \alpha) = \frac{1}{2}\Sigma_\sigma(\beta, \alpha) = \frac{\alpha}{2}\left(1 - \frac{\alpha\beta}{15}\right),$$

$$F_2(\beta, \alpha) = -\frac{\alpha^4\beta^3}{37800},$$

$$F_3(\beta, \alpha) = -\frac{2\alpha^2\beta^2}{315},$$

$$F_4(\beta) = \frac{1}{2}\Sigma_S(\beta) = \frac{1}{2}\left(1 - \frac{2\beta}{15}\right).$$

3.4.4. Biaxials model.

3.4.4.1. $S = S_0$.

$$F_1(S_0, \beta, \lambda) = \frac{1}{2}\Sigma_{T'}(\beta, \lambda) = \frac{1}{24}\lambda\left[24 + (3 - 10\beta - 14 S_0\beta)\lambda\right],$$

$$F_2(S_0, \beta, \lambda) = \\ = \frac{\left[945 + 18\beta(8S_0^2 - 135S_0 - 7) + 12S_0\beta^2(26 + 287S_0 - 112S_0^2) + 8S_0^2\beta^3(392S_0^2 + 185S_0 - 1)\right]\lambda^4}{18432 S_0^2},$$

$$F_3(S_0,\beta,\lambda)=\frac{\left[-45+\beta(6+132S_0-12S_0^2)+28S_0\beta^2(2S_0^2-S_0-1)\right]\lambda^2}{144S_0},$$

$$F_4(S_0,\beta)=\frac{1}{2}\Sigma_S\left(\beta\right)=\frac{1}{18}\left[15+(-2-2S_0+4S_0^2)\beta\right].$$

3.4.4.2. $S=0$.

$$F_1\left(\beta,\lambda\right)=\frac{1}{2}\Sigma_{T'}\left(\beta,\lambda\right)=\lambda\left(1-\frac{2\beta\lambda}{5}\right),$$

$$F_2\left(\beta,\lambda\right)=\frac{4\beta^3\lambda^4}{175},$$

$$F_3\left(\beta,\lambda\right)=-\frac{8\beta^2\lambda^2}{105},$$

$$F_4\left(\beta\right)=\frac{1}{2}\Sigma_S\left(\beta\right)=\frac{1}{3}-\frac{2\beta}{45}.$$

CHAPTER 4

Bifurcations

4.1. Introduction

This Chapter is devoted to the bifurcation analysis of a special model falling within the general Straley's class of intermolecular potentials. The main result is the construction of the complete phase diagram for this model. Moreover, this phase diagram is qualitatively confirmed by another independent analysis based on a Monte Carlo simulation study (see also Refs. [**42, 62**]).

On the experimental side, more recently, Merkel *et al.* [**10**] have observed experimental evidence of biaxiality in two liquid crystalline tetrapodes with two different mesogenic systems. The tetrapodes exhibit biaxiality close to the ambient temperature and it is the first quantitative observation for this class of liquid crystals. In the individual tetrapode the mesogenic molecules are connected to a siloxane (that is a chemical compound of silicon, oxygen, and carbon and hydrogen) core through four siloxane spacers, leading to a macromolecule having a quasi flat platelet shape. This structure hampers the rotation of each rod-like mesogen within the platelet around its long axis, thus promoting biaxiality. These experimental results have been interpreted within the theoretical predictions of the special model we are going to study, and in particular the tricritical region has been explored, confirming it.

4.2. A simplified model

The special model we are considering consists of setting $\gamma = 0$ and $\xi = 1$ in the general expression of the quadrupolar potential. Thus, the starting point of our analysis is the expression

$$V = -U_0 \left\{ \mathbf{q} \cdot \mathbf{q}' + \lambda \mathbf{b} \cdot \mathbf{b}' \right\} \tag{4.2.1}$$

of the orientational interaction energy between two biaxial molecules represented by the pair of tensors $(\mathbf{q}, \mathbf{b})$ and $(\mathbf{q}', \mathbf{b}')$. In terms of the molecular axes $\{\boldsymbol{e}, \boldsymbol{e}_\perp, \boldsymbol{m}\}$ the potential in (4.2.1) can be written:

$$V = -U_0 \left\{ -\left(\lambda + \frac{1}{3}\right) + (1-\lambda)\left(\boldsymbol{m} \cdot \boldsymbol{m}'\right)^2 + 2\lambda \left(\boldsymbol{e}'_\perp \cdot \boldsymbol{e}_\perp\right)^2 + 2\lambda \left(\boldsymbol{e}' \cdot \boldsymbol{e}\right)^2 \right\}, \tag{4.2.2}$$

or, equivalently, in the form

$$V = \epsilon \left\{ -P_2\left(\boldsymbol{m} \cdot \boldsymbol{m}'\right) - \lambda \left[2P_2\left(\boldsymbol{e}'_\perp \cdot \boldsymbol{e}_\perp\right) + 2P_2\left(\boldsymbol{e}' \cdot \boldsymbol{e}\right) - P_2\left(\boldsymbol{m} \cdot \boldsymbol{m}'\right) \right] \right\}, \tag{4.2.3}$$

where $\epsilon = \frac{2}{3} U_0$ and $P_2(...)$ denotes the second Legendre polynomial (see Sec. 2.3.1).

The notation in Eq. (4.2.3) has the advantage of easing comparison with the well known and extensively studied Lebwohl–Lasher model, to which it reduces when $\lambda = 0$ as well.

In the following we will deal with the potential in the form (4.2.1) or (4.2.3).

In Chapter 2, we have investigated existence and mechanical stability of a biaxial ground state of complete alignment between the two interacting molecules. This stability analysis has been performed for the general case by considering the variation δV of V for nearly parallel molecules

$$\delta V = \frac{U_0}{2}\alpha^2 \left\{4\lambda w_m^2 + (\xi - 2\gamma + \lambda)\, w_e^2 + (\xi + 2\gamma + \lambda)\, w_\perp^2\right\} + o\left(\alpha^2\right), \tag{4.2.4}$$

where α is the angle of rotation which changes the relative orientation of two interacting molecules and $\boldsymbol{w} \in \mathbb{S}^2$ is the axis of rotation

$$\boldsymbol{w} = w_e \boldsymbol{e} + w_\perp \boldsymbol{e}_\perp + w_m \boldsymbol{m}. \tag{4.2.5}$$

The stability requirement $\delta V > 0$ implies $\lambda > 0$ and $2\,|\gamma| < \xi + \lambda$, moreover the condition of a calamitic state, which means that the $\boldsymbol{m}$ axis is harder to be disoriented than the other two, is $2\,|\gamma| < \xi - 3\lambda$. If we consider the model with $\gamma = 0$ and $\xi = 1$, this condition leads to the bound $0 < \lambda < \frac{1}{3}$. When $\gamma = 0$ the quadratic form (4.2.4) has two degenerate eigenvalues whose eigenspace is the plane π spanned by $\{\boldsymbol{e}, \boldsymbol{e}_\perp\}$, and for $\lambda > \frac{1}{3}$ the degenerate eigenvalue has a lower value than the eigenvalue associated with the eigenvector $\boldsymbol{m}$. Thus, we conclude that the ground state is still calamitic since for $\lambda > \frac{1}{3}$ the plane π is harder to be disoriented and this implies a stronger alignment of the axes $\boldsymbol{m}$ and $\boldsymbol{m'}$. Moreover, it is apparent from (4.2.2), that the configuration with $\boldsymbol{e}$ aligned with $\boldsymbol{e}'$ and $\boldsymbol{e}_\perp$ aligned with $\boldsymbol{e}'_\perp$ is an absolute minimum for the potential (4.2.2) and so we conclude that the configuration with all the molecular axes aligned is favorable. Another equivalent way to say the same thing is to interpret δV as fluctuation energy and for $0 < \lambda < \frac{1}{3}$, it is symmetric about $\boldsymbol{m}$ and attains its minimum at the poles of $\mathbb{S}^2$ ($\boldsymbol{w} = \boldsymbol{m}$). Going beyond this range, δV attains its minimum on the equator of $\mathbb{S}^2$, *i.e.* $\boldsymbol{w} \perp \boldsymbol{m}$.

Moreover, this model with $\gamma = 0, \xi = 1$ reveals a special symmetry property: the potential is invariant under a $\frac{\pi}{2}$-rotation about the $\boldsymbol{m}$-axis and $\boldsymbol{m}'$-axis in the individual molecular frames. More properly, we consider the rotation (Th. 2.10, p. 66 of [**32**])

$$\mathbf{R} = \mathbf{I} + \mathbf{W} + \mathbf{W}^2, \tag{4.2.6}$$

where $\mathbf{W}$ is the skew-symmetric tensor associated with $\boldsymbol{m}$

$$\mathbf{W} = \boldsymbol{e} \otimes \boldsymbol{e}_\perp - \boldsymbol{e}_\perp \otimes \boldsymbol{e}. \tag{4.2.7}$$

We imagine a simultaneous rotation acting on the primed molecule and expressed in the intrinsic frame of the molecule

$$\mathbf{R}' = \mathbf{I}' + \mathbf{W}' + \mathbf{W}'^2, \tag{4.2.8}$$

where

$$\mathbf{W}' = \boldsymbol{e}' \otimes \boldsymbol{e}'_\perp - \boldsymbol{e}'_\perp \otimes \boldsymbol{e}'. \tag{4.2.9}$$

The transformed molecular tensors are

$$\mathbf{q}^* = \mathbf{R}\mathbf{q}\mathbf{R}^T = \mathbf{q}, \quad \mathbf{b}^* = \mathbf{R}\mathbf{b}\mathbf{R}^T = -\mathbf{b}, \tag{4.2.10}$$

$$\mathbf{q}'^* = \mathbf{R}'\mathbf{q}'\mathbf{R}'^T = \mathbf{q}', \quad \mathbf{b}'^* = \mathbf{R}'\mathbf{b}'\mathbf{R}'^T = -\mathbf{b}', \tag{4.2.11}$$

and it can be shown that

$$V\left(\mathbf{q}^*, \mathbf{b}^*, \mathbf{q}'^*, \mathbf{b}'^*\right) = V\left(\mathbf{q}, \mathbf{b}, \mathbf{q}', \mathbf{b}'\right), \tag{4.2.12}$$

where the dependence of the function V on its arguments is just that given in Eq. (4.2.1). Thus, the special model $\gamma = 0, \xi = 1$ can be characterized by this symmetry, which we can interpret as a D_{4h} symmetry. In the next section we will explore the consequences of this pairwise potential symmetry over the order parameters manifold.

4.3. Symmetries

In this section we consider the parameterization of the potential in terms of the two tensors $(\mathbf{q}, \mathbf{b})$ introduced in Eq. (4.2.1) and specialize the general mean field approximation to the simplified model (4.2.1). In this approximation, the pair potential is replaced by the pseudo-potential (see Chapter 2)

$$\Omega\left(\varphi, \vartheta, \psi\right) = -U_0 \Psi, \tag{4.3.1}$$

where

$$\Psi = \sum_{jk=1}^{4} d_{jk} \left\langle s_j \right\rangle s_k = \mathbf{q} \cdot \mathbf{Q} + \lambda \mathbf{b} \cdot \mathbf{B}, \tag{4.3.2}$$

and the matrix $\mathbf{d}$ is diagonal and represented by

$$[\mathbf{d}] = \begin{pmatrix} \frac{2}{3} & 0 & 0 & 0 \\ 0 & \frac{4}{3} & 0 & 0 \\ 0 & 0 & 4\lambda & 0 \\ 0 & 0 & 0 & 8\lambda \end{pmatrix}. \tag{4.3.3}$$

The Boltzmann distribution function in this approximation is

$$f = \frac{1}{Z}\exp\left(\beta\Psi\right), \quad Z = \int_{\mathbb{T}} \exp\left(\beta\Psi\right) d\omega, \tag{4.3.4}$$

where $\beta = \frac{U_0}{k_B t}$, k_B is the Boltzmann constant and t the absolute temperature. Z is the partition function with $\mathbb{T}$ denoting the torus manifold parameterized by the Euler angles $\omega = (\varphi, \vartheta, \psi)$ and $d\omega := \sin\vartheta d\vartheta d\varphi d\psi$ the area measure on it. Accordingly, the mean-field free energy is

$$\begin{aligned} \mathcal{F}\left(S, T, S', T'; \beta, \lambda\right) &= U_0 \left\{ \frac{1}{3}S^2 + T^2 + \frac{1}{3}\lambda S'^2 + \lambda T'^2 - \frac{1}{\beta}\ln\left(\frac{Z}{8\pi^2}\right) \right\} \\ &= U_0 \left\{ \frac{1}{2}\sum_{jk=1}^{4} d_{jk}\left\langle s_j\right\rangle\left\langle s_k\right\rangle - \frac{1}{\beta}\ln\left(\frac{Z}{8\pi^2}\right) \right\}. \end{aligned} \tag{4.3.5}$$

As a consequence, four consistency conditions arise for the order parameters (S, T, S', T')

$$S = \frac{1}{Z}\int_{\mathbb{T}} s_1 \exp\left(\beta\Psi\right) d\omega, \tag{4.3.6}$$

$$T = \sqrt{\frac{2}{3}}\frac{1}{Z}\int_{\mathbb{T}} s_2 \exp\left(\beta\Psi\right) d\omega, \tag{4.3.7}$$

$$S' = \frac{\sqrt{6}}{Z}\int_{\mathbb{T}} s_3 \exp\left(\beta\Psi\right) d\omega, \tag{4.3.8}$$

$$T' = \frac{2}{Z}\int_{\mathbb{T}} s_4 \exp\left(\beta\Psi\right) d\omega, \tag{4.3.9}$$

which entail the extremum conditions of the free energy (4.3.5). This macroscopic potential enjoys the general symmetry properties illustrated in Chapter 2, that is

$$\begin{aligned} &(S, T, S', T') \mapsto (S, -T, S', -T'), \\ &(S, T, S', T') \mapsto \left(\tfrac{\pm 3T - S}{2}, \tfrac{T \pm S}{2}, \tfrac{\pm 3T' - S'}{2}, \tfrac{T' \pm S'}{2}\right), \end{aligned} \tag{4.3.10}$$

These transformations leave invariant $\mathcal{F}$. Moreover, the D_{4h} symmetry of the microscopic potential V for this special case $\xi = 1,\ \gamma = 0$, implies the further symmetry transformation on the order parameters

$$(\mathbf{q}, \mathbf{b}) \mapsto (\mathbf{q}, -\mathbf{b}) \Rightarrow (\mathbf{Q}, \mathbf{B}) \mapsto (\mathbf{Q}, -\mathbf{B}), \tag{4.3.11}$$

since the pseudo–potential Ω and the distribution function f inherit the pairwise potential invariance. In terms of the order parameters (S, T, S', T'), this transformation becomes

$$\left(S, T, S', T'\right) \mapsto \left(S, T, -S', -T'\right), \tag{4.3.12}$$

and, by composition with the first one of (4.3.10), the following invariance mapping holds

$$\left(S, T, S', T'\right) \mapsto \left(S, -T, -S', T'\right). \tag{4.3.13}$$

As for (4.3.10), (4.3.12) and (4.3.13) leave invariant $\mathcal{F}$. All these symmetry transformations for the order parameters have profound consequences on the bifurcation analysis of the mean-field theory. Finally, we can make explicit the D_{4h} symmetry in terms of the relative Euler angles $\hat{\omega}$. By construction, the pairwise potential is $D_{2h}-$invariant and so it is a combination of the invariant functions $\{s_k(\hat{\omega})\}$ (see Eq. (2.3.48)). This means that V is invariant under the transformations

$$\left(\hat{\varphi}, \hat{\vartheta}, \hat{\psi}\right) \mapsto \left(\hat{\varphi} + \pi, \hat{\vartheta}, \hat{\psi}\right),$$

$$\left(\hat{\varphi}, \hat{\vartheta}, \hat{\psi}\right) \mapsto \left(\hat{\varphi}, \hat{\vartheta}, \hat{\psi} + \pi\right),$$

$$\left(\hat{\varphi}, \hat{\vartheta}, \hat{\psi}\right) \mapsto \left(\hat{\varphi} - \pi, \pi - \hat{\vartheta}, -\hat{\psi}\right).$$

The additional symmetry arising in the model potential with $\gamma = 0$ is

$$\left(\hat{\varphi}, \hat{\vartheta}, \hat{\psi}\right) \mapsto \left(\hat{\varphi} + \frac{\pi}{2}, \hat{\vartheta}, \hat{\psi} + \frac{\pi}{2}\right). \tag{4.3.14}$$

Actually, under (4.3.14), $s_2(\hat{\omega}) \mapsto -s_2(\hat{\omega})$ and $s_3(\hat{\omega}) \mapsto -s_3(\hat{\omega})$, the potential V remaining invariant since $\gamma = 0$.

Finally, the symmetry transformation (4.3.13) is a direct consequence of the D_{4h} symmetry of the intermolecular potential. More precisely, we observe that, in order to preserve the mean field equations, when we apply the transformation (4.3.14), we are forced to reverse simultaneously the sign of S' and T. On the other hand, by construction, our mean field should take into account the microscopic symmetry properties and should be constructed accordingly, so since under (4.3.14) $s_2(\omega) \mapsto -s_2(\omega)$ and $s_3(\omega) \mapsto -s_3(\omega)$, we must impose $\langle s_2 \rangle \mapsto -\langle s_2 \rangle$ and $\langle s_3 \rangle \mapsto -\langle s_3 \rangle$, i.e., $S' \mapsto -S'$ and $T \mapsto -T$ in (4.3.2).

4.4. Equivariance

In general, the system of compatibility equations (2.4.36) can be written in the form

$$F_1(S,T,S',T';\beta,\xi,\lambda,\gamma) := S - G_1(S,T,S',T';\beta,\xi,\lambda,\gamma) = 0, \tag{4.4.1}$$

$$F_2(S,T,S',T';\beta,\xi,\lambda,\gamma) := T - G_2(S,T,S',T';\beta,\xi,\lambda,\gamma) = 0, \tag{4.4.2}$$

$$F_3(S,T,S',T';\beta,\xi,\lambda,\gamma) := S' - G_3(S,T,S',T';\beta,\xi,\lambda,\gamma) = 0, \tag{4.4.3}$$

$$F_4(S,T,S',T';\beta,\xi,\lambda,\gamma) := T' - G_4(S,T,S',T';\beta,\xi,\lambda,\gamma) = 0. \tag{4.4.4}$$

It can be shown that the l. h. s. functions satisfy equivariance relations with respect to a group of transformations. More precisely, if we denote by $\mathbf{x} \in \mathbb{R}^4$ the state vector $(S,T,S',T')^T$, by $\mathbf{G}$ and $\mathbf{F}$ the vector valued functions $(G_1,G_2,G_3,G_4)^T$ and $(F_1,F_2,F_3,F_4)^T$, the equivariance property takes the form

$$\mathbf{F}(\hat{S}\mathbf{x};\beta,\xi,\lambda,\gamma) = \hat{S}\mathbf{F}(\mathbf{x};\beta,\xi,\lambda,\gamma) \Leftrightarrow \mathbf{G}(\hat{S}\mathbf{x};\beta,\xi,\lambda,\gamma) = \hat{S}\mathbf{G}(\mathbf{x};\beta,\xi,\lambda,\gamma),$$

for all $\hat{S} \in \mathcal{S}$, with $\mathcal{S}$ a subgroup of $gl(4)$ of nonsingular 4×4 matrices, which can be represented as a collection $\mathcal{S} = \left\{\hat{I}, \hat{S}_1, \hat{S}_2, \hat{S}_3, \hat{S}_1\hat{S}_3, \hat{S}_2\hat{S}_3\right\}$ of 3 involution operators, the identity operator and their mutual matrix compositions. The three operators $\hat{S}_i$ are such that $\hat{S}_i \neq \hat{I}, \quad \hat{S}_i = \hat{S}_i^{-1} \quad i = 1,2,3$. More explicitly the involution operators are

$$\left[\hat{S}_{1,2}\right] = \begin{pmatrix} -\frac{1}{2} & \pm\frac{3}{2} & 0 & 0 \\ \pm\frac{1}{2} & \frac{1}{2} & 0 & 0 \\ 0 & 0 & -\frac{1}{2} & \pm\frac{3}{2} \\ 0 & 0 & \pm\frac{1}{2} & \frac{1}{2} \end{pmatrix}, \quad \left[\hat{S}_3\right] = \begin{pmatrix} 1 & 0 & 0 & 0 \\ 0 & -1 & 0 & 0 \\ 0 & 0 & 1 & 0 \\ 0 & 0 & 0 & -1 \end{pmatrix}$$

These operators realize the so-called $\mathbb{Z}_2$-equivariance of the system (4.4.1-4.4.4).

Moreover the model $\gamma = 0, \xi = 1$ enjoys an additional symmetry and the corresponding involution operator $\hat{S}_4$ is represented by

$$\left[\hat{S}_4\right] = \begin{pmatrix} 1 & 0 & 0 & 0 \\ 0 & -1 & 0 & 0 \\ 0 & 0 & -1 & 0 \\ 0 & 0 & 0 & 1 \end{pmatrix}, \tag{4.4.5}$$

thus for this model the full equivariance group $\mathcal{S}$ is larger (it is of order 12) and it is generated by the collection $\left\{I, \hat{S}_1, \hat{S}_2, \hat{S}_3, \hat{S}_4\right\}$ and their mutual matrix products. In particular the symmetry (4.4.5) is a direct consequence of the D_{4h} symmetry of the intermolecular potential. More precisely, we observe that, in order to preserve the mean field equations, when we make transformations (4.3.11) act, we are forced to reverse sign simultaneously to S' and T, leading to the equivariance operator $\hat{S}_4$.

Finally, the full equivariance group must leave invariant any macroscopic potential expressed in terms of the order parameters (S, T, S', T') and in particular the free energy.

4.4.1. Symmetry-breaking bifurcation points. For each $i = 1, 2, 3, 4$ the matrix $\hat{S}_i$ induces a unique decomposition of $\mathbb{R}^4$ into symmetric and antisymmetric subspaces

$$\mathbb{R}^4 = \mathbb{R}^4_{s,i} \oplus \mathbb{R}^4_{a,i},$$

where

$$\mathbb{R}^4_{s,i} = \left\{\mathbf{x} \in \mathbb{R}^4 : \hat{S}_i \mathbf{x} = \mathbf{x}\right\},$$

and

$$\mathbb{R}^4_{a,i} = \left\{\mathbf{x} \in \mathbb{R}^4 : \hat{S}_i \mathbf{x} = -\mathbf{x}\right\}.$$

In general, symmetry matters only in points where it is broken. At a symmetry-breaking bifurcation point $(\mathbf{x}_c, \beta_c, \lambda_c)$ the following conditions hold

$$\mathbf{x}_c \in \mathbb{R}^4_{s,i},$$

$$Ker\left(J_{\mathbf{F}}\left(\mathbf{x}_c, \beta_c, \lambda_c\right)\right) = Span\left\{\mathbf{a}\right\}, \quad \mathbf{a} \in \mathbb{R}^4_{a,i}, \mathbf{a} \neq \mathbf{0},$$

$$Im\left(J_{\mathbf{F}}\left(\mathbf{x}_c, \beta_c, \lambda_c\right)\right) = \left\{\mathbf{y} \in \mathbb{R}^4 : \mathbf{z}^T \mathbf{y} = 0\right\}, \quad \mathbf{z} \in \mathbb{R}^4, \mathbf{z} \neq \mathbf{0},$$

where $J_{\mathbf{F}}\left(\mathbf{x}, \beta, \lambda\right)$ represents the Jacobian matrix of $\mathbf{F}$ with respect to $\mathbf{x}$ for $\gamma = 0$ and $\xi = 1$.

As a consequence, the symmetry-breaking bifurcation points are computed as regular solutions of the extended system (see Refs. **[63]**, **[64]**)

$$\mathbf{E}\left(\mathbf{v}; \beta\right) = \begin{pmatrix} \mathbf{F}\left(\mathbf{x}, \beta, 1, \lambda, 0\right) \\ J_{\mathbf{F}}\left(\mathbf{x}, \beta, \lambda\right) \mathbf{a} \\ \mathbf{a}^T \mathbf{a} - 1 \end{pmatrix} = \mathbf{0}, \tag{4.4.6}$$

in the unknown vector

$$\mathbf{v}^T = \left(\mathbf{x}^T, \mathbf{a}^T, \lambda\right), \quad \mathbf{v} \in \mathbb{R}^4_{s,i} \times \mathbb{R}^4_{a,i} \times \mathbb{R},$$

$$\mathbf{E} : \mathbb{R}^4_{s,i} \times \mathbb{R}^4_{a,i} \times \mathbb{R} \to \mathbb{R}^4_{s,i} \times \mathbb{R}^4_{a,i} \times \mathbb{R}.$$

4.4.1.1. *Bifurcation points.*

Operators $\hat{S}_3$ and $\hat{S}_4$. A symmetry-breaking bifurcation point occurs with respect to the operator $\hat{S}_3$ from an equilibrium branch lying in the symmetric space of $\hat{S}_3$, i.e., $(S, 0, S', 0)$, giving rise to a branch in the antisymmetric space. But the symmetric branch lies itself in the antisymmetric space of the operator $\hat{S}_4$, i.e., $(S, 0, S', 0)$, bifurcating from the symmetric branch $(S_0, 0, 0, 0)$, which is the Maier-Saupe curve (see Sec. 3.4.2 in Chapter 3). So we can characterize this branch (stemming from the classical Maier-Saupe theory) as the symmetric curve with respect to $\hat{S}_3$ and $\hat{S}_4$. Thus we can state that, by virtue of the symmetry $\hat{S}_4$, the classical Maier-Saupe curve for the uniaxial nematic phase always remains a solution of the model. In turn, this state arises as a consequence of the breaking of the $O(3)$ symmetry group (the invariance group of the sphere), whose symmetric state is the isotropic phase $(0, 0, 0, 0)$, which takes into account the fact that in the isotropic state the orientations of the molecules are uniformly distributed. As a consequence, the system (4.4.6) includes the symmetry-breaking bifurcation point of the Maier-Saupe theory, which occurs at $\beta = \frac{15}{2}$, and the Maier-Saupe model solution $(S_0(\beta), 0, 0, 0)$, satisfying the trascendental equation

$$\frac{2}{3}S = -\frac{1}{3} - \frac{1}{2S} + \frac{\exp(S\beta)}{\sqrt{\pi S\beta}Erfi(\sqrt{S\beta})}, \tag{4.4.7}$$

to which the full compatibility system reduces setting $\lambda = 0$ too. Now we analyse in more detail these symmetric states and the operators $\hat{S}_3$, $\hat{S}_4$. In general, the one-dimensional space $(S, 0, 0, 0)$ is symmetric with respect to the subgroup $\left\{I, \hat{S}_3, \hat{S}_4, \hat{S}_3\hat{S}_4\right\}$. The operator $\hat{S}_3$ induces the following decomposition of the states manifold

$$\mathbb{R}^4_{s,3} = \left\{\mathbf{x} \in \mathbb{R}^4 : \hat{S}_3\mathbf{x} = \mathbf{x}\right\} = Span\left\{(1,0,0,0)^T, (0,0,1,0)^T\right\},$$

$$\mathbb{R}^4_{a,3} = \left\{\mathbf{x} \in \mathbb{R}^4 : \hat{S}_3\mathbf{x} = -\mathbf{x}\right\} = Span\left\{(0,1,0,0)^T, (0,0,0,1)^T\right\},$$

$$\mathbb{R}^4 = \mathbb{R}^4_{s,3} \oplus \mathbb{R}^4_{a,3}.$$

By solving the extended system (4.4.6) the following bifurcation line is found

$$\lambda_3(S_0(\beta), \beta) = \frac{24}{2(5 + 7S_0(\beta))\beta - 3}, \tag{4.4.8}$$

and the antisymmetric bifurcating branch lies in $Span\left\{(0,0,0,1)^T\right\}$, i.e., it has $T = S' = 0$. This bifurcating branch represents a biaxial state and we can conclude that the biaxial phase for this model is a consequence of the $\mathbb{Z}_2$ symmetry-breaking. On the other hand the operator $\hat{S}_4$ induces the decomposition

$$\mathbb{R}^4_{s,4} = \left\{\mathbf{x} \in \mathbb{R}^4 : \hat{S}_4\mathbf{x} = \mathbf{x}\right\} = Span\left\{(1,0,0,0)^T, (0,0,0,1)^T\right\},$$

$$\mathbb{R}^4_{a,4} = \left\{\mathbf{x} \in \mathbb{R}^4 : \hat{S}_4\mathbf{x} = -\mathbf{x}\right\} = Span\left\{(0,1,0,0)^T, (0,0,1,0)^T\right\},$$

$$\mathbb{R}^4 = \mathbb{R}^4_{s,4} \oplus \mathbb{R}^4_{a,4},$$

and the corresponding symmetry-breaking line is

$$\lambda_4\left(S_0(\beta), \beta\right) = \frac{4}{2\left(1 - S_0(\beta)\right)\beta - 3}. \tag{4.4.9}$$

The antisymmetric branch lies in $Span\left\{(0,0,1,0)^T\right\}$, i.e., it is characterized by having $T = T' = 0$. This means that this branch represents a negative-ordered (it bifurcates with a branch having $S < 0$) uniaxial solution. It is a consequence of the $\hat{S}_4$ symmetry-breaking of the model $\gamma = 0, \xi = 1$, and, in turn, it is due to the D_{4h} intermolecular potential symmetry.

Another symmetry arises from the product of the two above: $\hat{S}_3\hat{S}_4$

$$\left[\hat{S}_3\hat{S}_4\right] = \begin{pmatrix} 1 & 0 & 0 & 0 \\ 0 & 1 & 0 & 0 \\ 0 & 0 & -1 & 0 \\ 0 & 0 & 0 & -1 \end{pmatrix},$$

which decomposes the states manifold into

$$\mathbb{R}^4_{s,34} = \left\{\mathbf{x} \in \mathbb{R}^4 : \hat{S}_3\hat{S}_4\mathbf{x} = \mathbf{x}\right\} = Span\left\{(1,0,0,0)^T, (0,1,0,0)^T\right\},$$

$$\mathbb{R}^4_{a,34} = \left\{\mathbf{x} \in \mathbb{R}^4 : \hat{S}_3\hat{S}_4\mathbf{x} = -\mathbf{x}\right\} = Span\left\{(0,0,1,0)^T, (0,0,0,1)^T\right\}.$$

The extended system implies that the symmetry-breaking occurs for $S = 0$, i.e., from the isotropic state and the line is

$$\lambda_{3,4}\left(\beta\right) = \frac{5}{2\beta}. \tag{4.4.10}$$

The antisymmetric branches point in the space $\mathbb{R}^4_{a,34}$, one in $Span\left\{(0,0,1,0)^T\right\}$, and the other in $Span\left\{(0,0,0,1)^T\right\}$. As mentioned above, this is not the only bifurcation point arising from the isotropic state. Another solution of (4.4.6) occurs at $\beta = \frac{15}{2}$, which is independent of λ, and it coincides with the line (4.4.10) for $\lambda = \frac{1}{3}$. Until now, we have analyzed special bifurcation points, i.e., symmetry-breaking points. Other noticeable bifurcation points are the so-called *limit points* or *quadratic turning points*, which, in particular, could be limits of stability for the free energy. These points are characterized by the fact that $J_{\mathbf{F}}\left(\mathbf{x}, \beta, \lambda\right)$ is singular with rank defect 1, and are regular

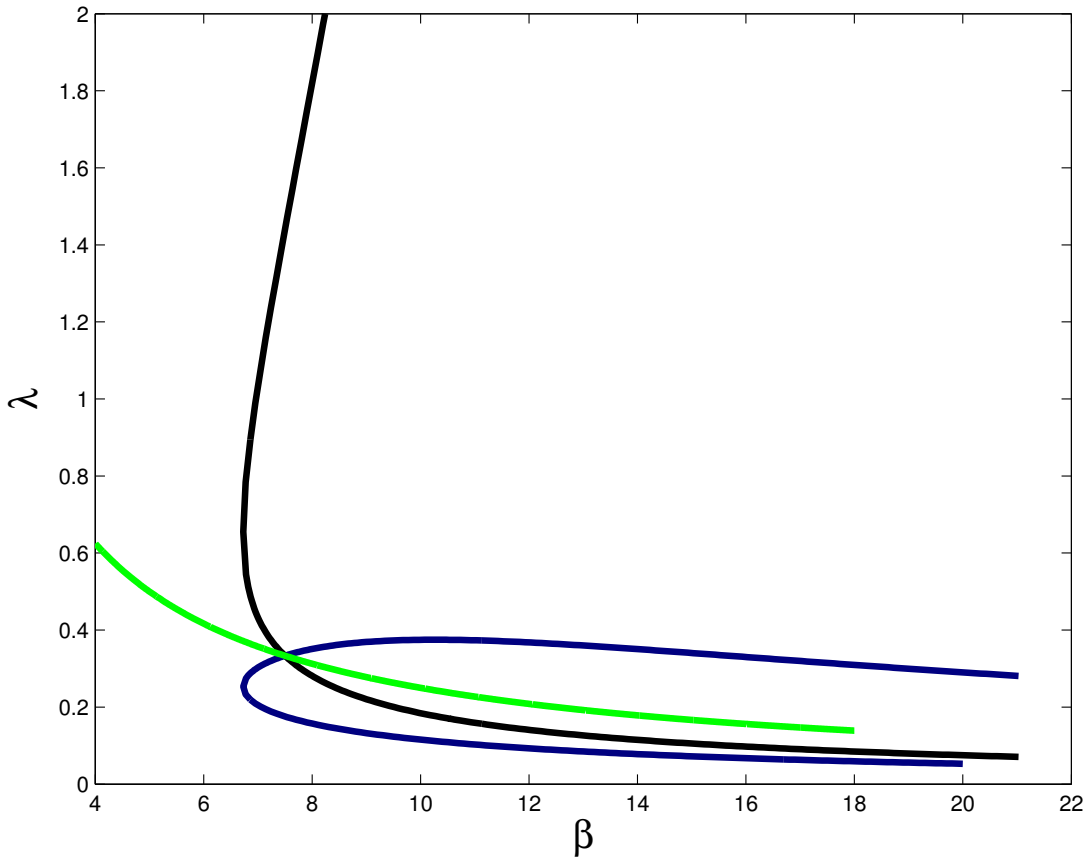

FIGURE 4.4.1. Bifurcation diagram: λ as function of β along the bifurcation lines: the blue curve represents the symmetry-breaking bifurcation points (4.4.8), the black curve represents the symmetry-breaking bifurcation points (4.4.9), the green curve the symmetry-breaking bifurcation points (4.4.10).

solutions of the Moore-Spence extended system

$$\mathbf{L}(\mathbf{z};\beta) = \begin{pmatrix} \mathbf{F}(\mathbf{x},\beta,1,\lambda,0) \\ J_{\mathbf{F}}(\mathbf{x},\beta,\lambda)\,\mathbf{w} \\ \mathbf{w}^T\mathbf{w}-1 \end{pmatrix} = \mathbf{0} \tag{4.4.11}$$

in the unknown generic vector $\mathbf{z}^T = \left(\mathbf{x}^T, \mathbf{w}^T, \lambda\right) \in \mathbb{R}^4 \times \mathbb{R}^4 \times \mathbb{R}$, (see **[65]**, **[66]** and **[64]**). As explained above, the biaxial solutions are given by the states $(S,0,0,T')$ which are symmetric branches with respect to $\hat{S}_4$, therefore the limit points on them are characterized by having $\mathbf{w},\mathbf{x} \in \mathbb{R}^4_{s,4}$, i.e. lying in the symmetric component of $\hat{S}_4$. The uniaxial states $(S,0,S',0)$ are symmetric with respect to $\hat{S}_3$ and the turning bifurcation points on them are characterized by $\mathbf{w},\mathbf{x} \in \mathbb{R}^4_{s,3}$.

Operators $\hat{S}_{1,2}$. We now analyze the role of the other two $\mathbb{Z}_2-$operators. First of all we find the induced decomposition of the states manifold. It can be shown that

$$\mathbb{R}^4_{s,1} = \left\{\mathbf{x} \in \mathbb{R}^4 : \hat{S}_1\mathbf{x} = \mathbf{x}\right\} = Span\left\{\frac{\sqrt{2}}{2}(1,1,0,0)^T, \frac{\sqrt{2}}{2}(0,0,1,1)^T\right\},$$

$$\mathbb{R}^4_{a,1} = \left\{ \mathbf{x} \in \mathbb{R}^4 : \hat{S}_1 \mathbf{x} = -\mathbf{x} \right\} = Span \left\{ \frac{1}{2} (-3,1,0,0)^T , \frac{1}{2} (0,0,-3,1)^T \right\},$$

and

$$\mathbb{R}^4_{s,2} = \left\{ \mathbf{x} \in \mathbb{R}^4 : \hat{S}_2 \mathbf{x} = \mathbf{x} \right\} = Span \left\{ \frac{\sqrt{2}}{2} (1,-1,0,0)^T , \frac{\sqrt{2}}{2} (0,0,1,-1)^T \right\},$$

$$\mathbb{R}^4_{a,2} = \left\{ \mathbf{x} \in \mathbb{R}^4 : \hat{S}_2 \mathbf{x} = -\mathbf{x} \right\} = Span \left\{ \frac{1}{2} (3,1,0,0)^T , \frac{1}{2} (0,0,3,1)^T \right\}.$$

A rather interesting observation is that

$$\hat{S}_1 \mathbf{s}_2 \in \mathbb{R}^4_{s,3}, \quad \forall \mathbf{s}_2 \in \mathbb{R}^4_{s,2}, \qquad \hat{S}_2 \mathbf{s}_1 \in \mathbb{R}^4_{s,3}, \quad \forall \mathbf{s}_1 \in \mathbb{R}^4_{s,1}, \tag{4.4.12}$$

$$\hat{S}_1 \mathbf{a}_2 \in \mathbb{R}^4_{a,3}, \quad \forall \mathbf{a}_2 \in \mathbb{R}^4_{a,2}, \qquad \hat{S}_2 \mathbf{a}_1 \in \mathbb{R}^4_{a,3}, \quad \forall \mathbf{a}_1 \in \mathbb{R}^4_{a,1}. \tag{4.4.13}$$

In terms of the state variables (S, T, S', T'), the duality relations (4.4.12) mean that uniaxial states $(S, 0, S', 0)$, are conjugated by $\hat{S}_2$ to uniaxial states (S, S, S', S'), and by $\hat{S}_1$ to uniaxial states $(S, -S, S', -S')$.

On the other hand, (4.4.13) means that biaxial states bifurcating from uniaxial states $(S, 0, S', 0)$ with branches pointing in the antisymmetric space $\mathbb{R}^4_{a,3}$ are conjugated by $\hat{S}_2$ to biaxial states bifurcating in directions lying in $\mathbb{R}^4_{a,1}$, and by $\hat{S}_1$ in directions lying in $\mathbb{R}^4_{a,2}$. In other words the operators $\hat{S}_2$ and $\hat{S}_1$ realize only a reparameterization of the states, as illustrated in Chapter 2, Sec. 2.4.

4.5. Numerical computations

We can distinguish two regimes: $\lambda \leq \frac{1}{3}$ and $\lambda \geq \frac{1}{3}$, the critical value $\lambda = \frac{1}{3}$ being the intersection point of the three bifurcation lines (see Fig. 4.4.1).

For $\lambda < \frac{1}{3}$, numerical computations show first a splitting off the Maier-Saupe curve effect and then a wrapping of the two bifurcating branches around it (Fig. 4.5.1). The primary bifurcating branches, i.e. occurring for a smaller value of β, correspond to the symmetry-breaking branches in the T' order parameter with $T = S' = 0$ (Figs. 4.5.1 and 4.5.2), bifurcating from the points (4.4.8). They give rise to a stable biaxial phase described macroscopically by the tensors

$$\begin{aligned} \mathbf{Q} &= S \left(\boldsymbol{e}_z \otimes \boldsymbol{e}_z - \tfrac{1}{3}\mathbf{I} \right), \\ \mathbf{B} &= T' \left(\boldsymbol{e}_x \otimes \boldsymbol{e}_x - \boldsymbol{e}_y \otimes \boldsymbol{e}_y \right). \end{aligned} \tag{4.5.1}$$

The secondary branches bifurcate from the points on the line (4.4.9) and correspond to symmetry-breaking branches in the S' order parameter with $T = T' = 0$ (Figs. 4.5.1 and 4.5.3). In principle they would represent uniaxial states since $T = T' = 0$, and, by using the transformation operators $\hat{S}_{1,2}$,

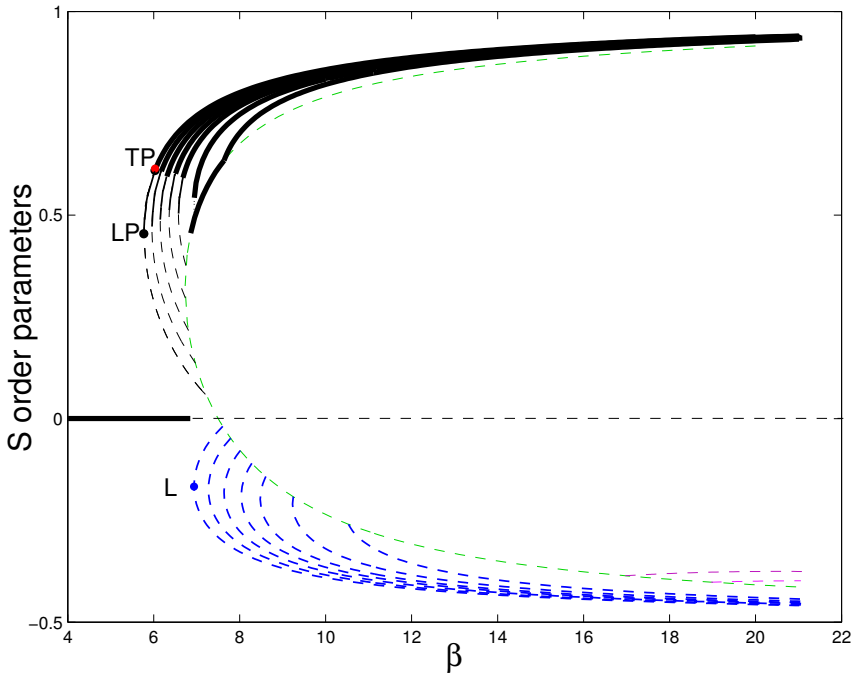

FIGURE 4.5.1. Order parameters S versus β for different values of λ in the range $[0, 1/3]$, showing the wrapping effect of Maier-Saupe's model solution. The dominant solutions correspond to the branches bifurcating from the upper part of the curve, it corresponds to positive values of the Maier-Saupe curve $S_0(\beta)$ and solutions with dominant order parameters S and T' depicted in Figure 4.5.2. The blue branches below correspond to solutions with order parameters S and $S'$and the other ones null. The point TP is the transition point, while the point LP marks the limit of stability. L marks the turning point on the unstable solution $(S, 0, S', 0)$. Such a notation must be extended for all values of λ.

they can be conjugated to macroscopic order tensors

$$\begin{aligned} \mathbf{Q} &= S\left(\boldsymbol{e}_y \otimes \boldsymbol{e}_y - \tfrac{1}{3}\mathbf{I}\right), \\ \mathbf{B} &= S'\left(\boldsymbol{e}_y \otimes \boldsymbol{e}_y - \tfrac{1}{3}\mathbf{I}\right), \end{aligned} \tag{4.5.2}$$

or to states with order tensors

$$\begin{aligned} \mathbf{Q} &= S\left(\boldsymbol{e}_x \otimes \boldsymbol{e}_x - \tfrac{1}{3}\mathbf{I}\right), \\ \mathbf{B} &= S'\left(\boldsymbol{e}_x \otimes \boldsymbol{e}_x - \tfrac{1}{3}\mathbf{I}\right). \end{aligned} \tag{4.5.3}$$

On the other hand, the stability analysis shows that they are unstable solutions and precisely they are unstable against perturbations in T'. They are represented by the dashed blue lines in Figs. (4.5.1, 4.5.2 and 4.5.3), where L marks a turning point (see Eq. 4.4.11). In the same Figures, the black heavy solid portions of the bifurcating branches represent the effective phases, while the dashed portions are unstable up to the turning points LP (limit of stability in this case) where the branches become stable and then, after the transition point TP, the branches have a value of free–energy $\mathcal{F}$ less than that assumed on the isotropic state. Thus the direct isotropic-to-biaxial or isotropic-to-uniaxial-to-biaxial

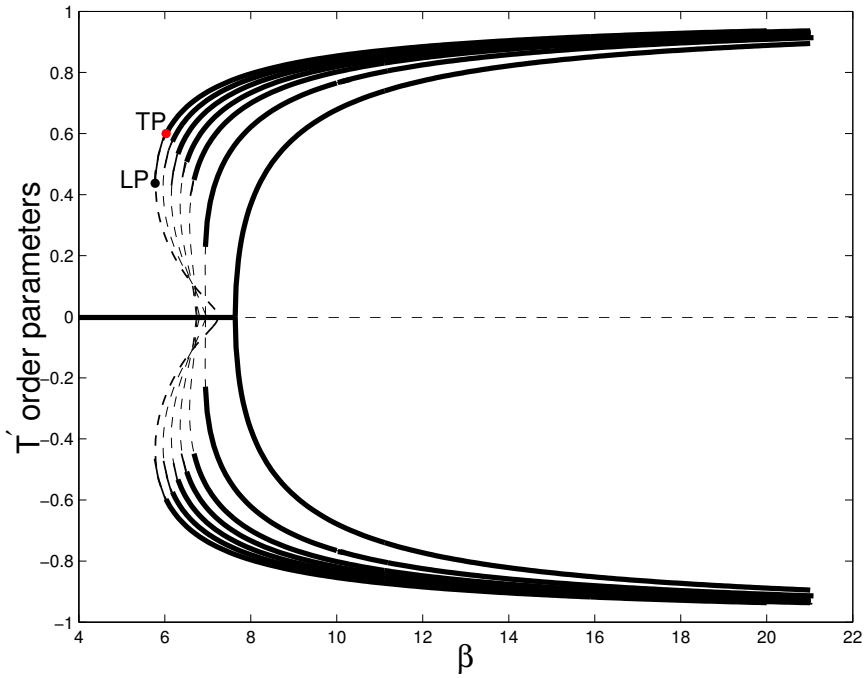

FIGURE 4.5.2. Order parameters T' versus β for different values of λ in the range $[0, 1/3]$. They correspond to the dominant solutions bifurcating from the upper side of the $S_0(\beta)$ curve in Figure 4.5.1. TP marks the transition point, where the transition takes place, while LP marks the limit of stability of the biaxial phase.

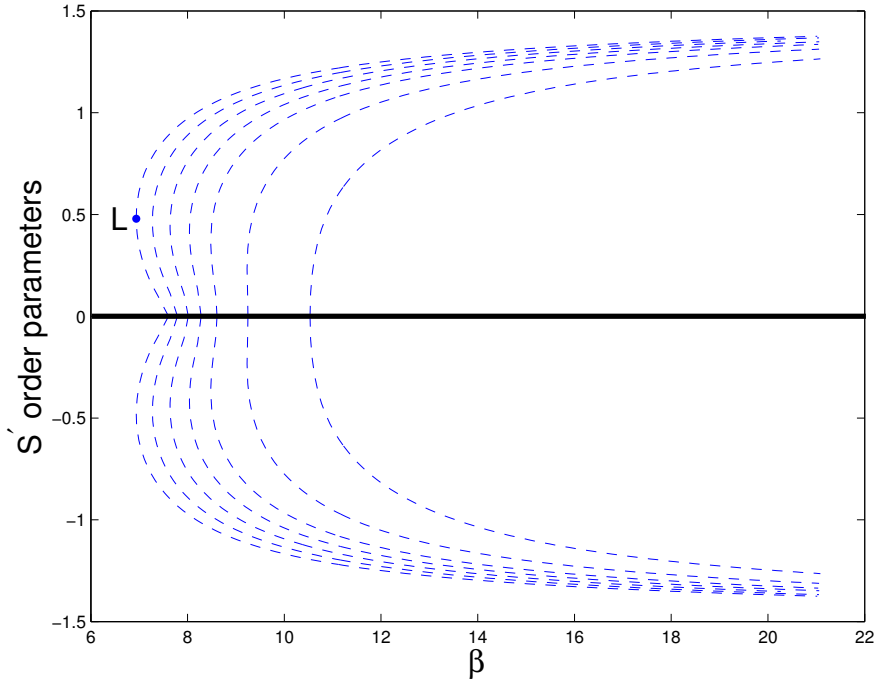

FIGURE 4.5.3. Order parameters S' versus β for different values of λ in the range $[0, 1/3]$. They correspond to the unstable solutions bifurcating from the lower side of the $S_0(\beta)$ curve in Figure 4.5.1. L marks the bifurcation turning point.

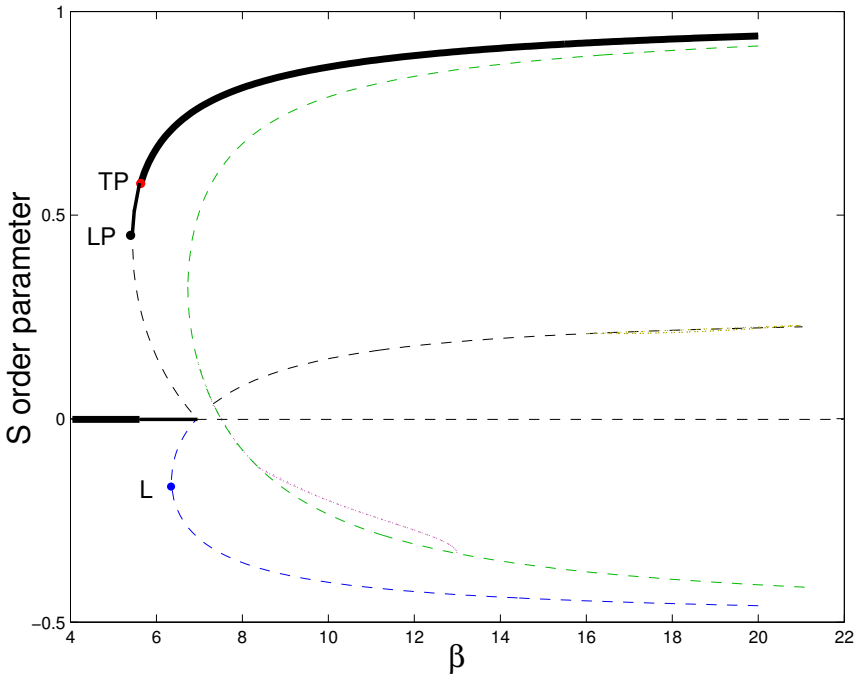

FIGURE 4.5.4. Order parameter S versus inverse temperature β for $\lambda = 0.36$.

transition takes place. By increasing λ, the primary bifurcation point moves and the biaxial branch wraps the Maier–Saupe curve (green curve in Fig. 4.5.1): the limit bifurcation point on it occurs for smaller values of β than that on the Maier–Saupe curve, and a direct isotropic-to-biaxial first-order phase transition takes place in the liquid crystal.

In general, for an assigned value of λ, the transition point from the isotropic to a condensed (biaxial or uniaxial) phase is computed by requiring that the free–energy (4.3.5) of the condensed phase is equal to the value at the isotropic phase which is zero, so we have to solve the compatibility equations coupled with the scalar equation

$$\mathcal{F}\left(S, T, S', T'; \beta, \lambda\right) = 0, \tag{4.5.4}$$

and the transition line on the $(\lambda, 1/\beta)$-phase diagram is the continuation in λ of the solutions of this extended system. On the other hand, for the uniaxial-to-biaxial transition line, we have to add the scalar condition

$$\mathcal{F}\left(S, T, S', T'; \beta, \lambda\right) = \mathcal{F}\left(S, 0, S', 0; \beta, \lambda\right). \tag{4.5.5}$$

When we set λ to have values greater than $1/3$, the bifurcations (4.4.8) and (4.4.9) become secondary, and the line (4.4.10) becomes primary. This is a bifurcation from the isotropic state and it always exists together with the other two in Figs. (4.5.1, 4.5.2 and 4.5.3).

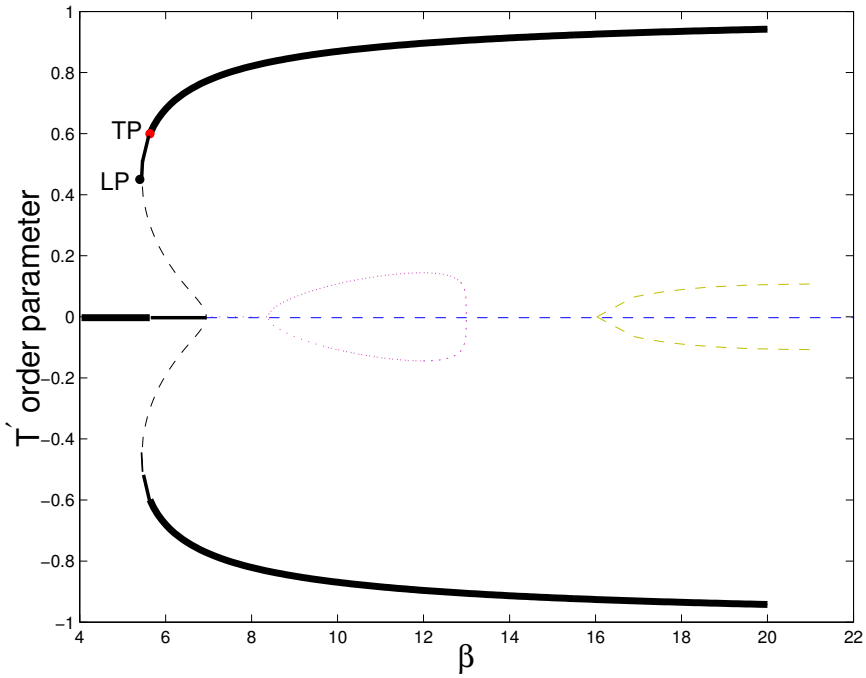

FIGURE 4.5.5. Order parameter T' versus inverse temperature β for $\lambda = 0.36$.

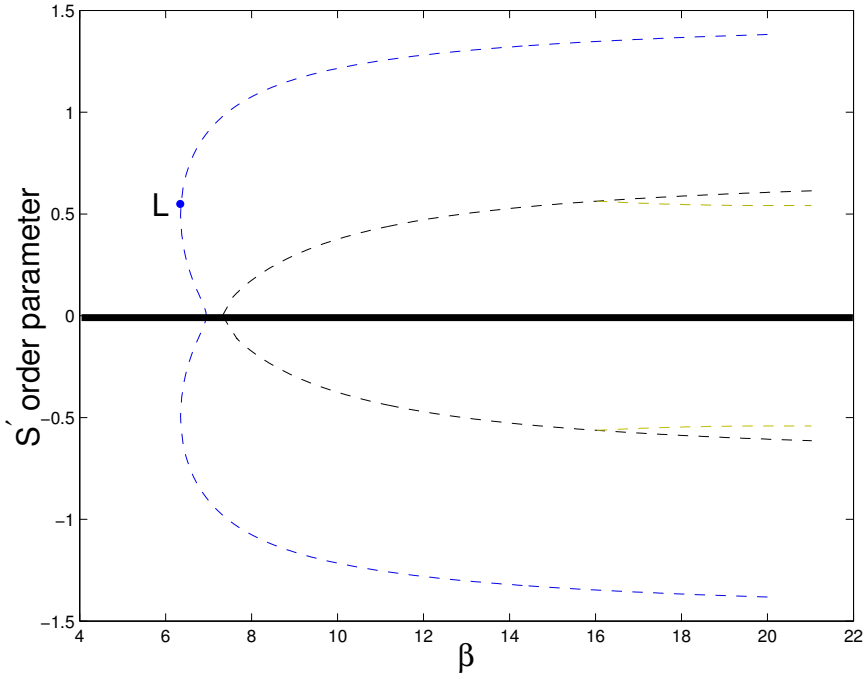

FIGURE 4.5.6. Order parameter S' versus inverse temperature β for $\lambda = 0.36$.

A stable biaxial branch and a unstable uniaxial one germinate from it, the solutions scenario evolving as depicted in Figs. 4.5.4, 4.5.5 and 4.5.6. The graphs for T are not reproduced here because T can be set equal to zero at all primary bifurcations. In Fig. 4.5.4 the order parameter S is plotted. It is apparent that the classical Maier–Saupe model solution (green curve) is completely hidden by the primary bifurcating branches splitting off the isotropic state at $\beta = 5/2\lambda_{3,4}$. The biaxial branch

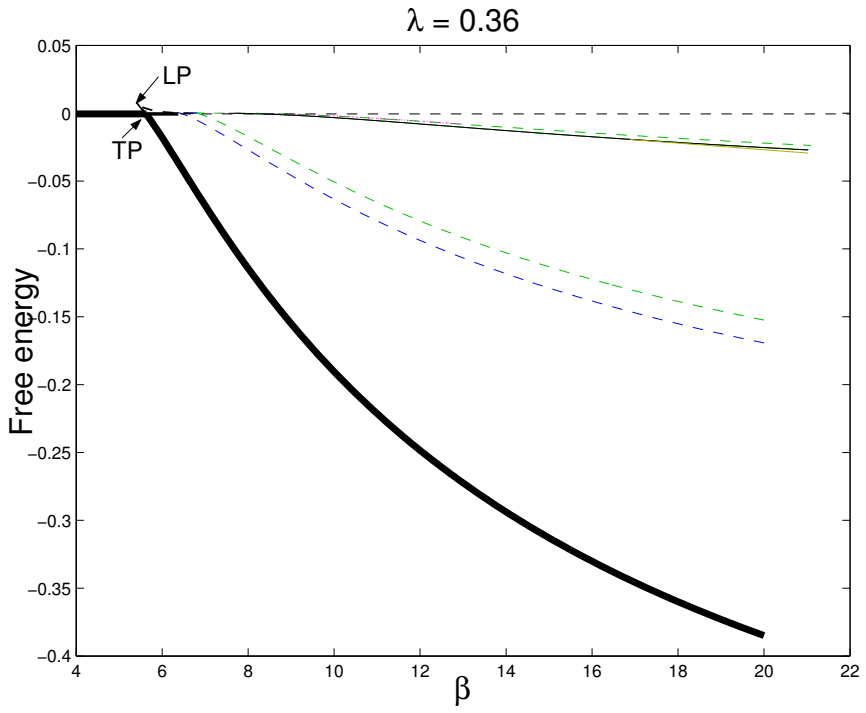

FIGURE 4.5.7. Free-energy $\mathcal{F}$ versus inverse temperature β for $\lambda = 0.36$.

$(S, 0, 0, T')$ gives to an intrinsic biaxial phase (heavy solid portion in Figs. 4.5.4, 4.5.5 and 4.5.6), while the blue dashed branch corresponds to the unstable uniaxial state $(S, 0, S', 0)$ with $S < 0$ that can be put in the tensorial forms (4.5.2) or (4.5.3). The L point on it marks the turning bifurcation point (see again Eq. 4.4.11). As a consequence, an isotropic-to-biaxial first-order phase transition continues to take place in the liquid crystal.

Moreover in Fig. (4.5.7) the free-energy $\mathcal{F}$ is plotted as a function of β for all the bifurcating branches. The heavy solid black function corresponds to the effective biaxial phase. In Figs. 4.5.4, 4.5.5 and 4.5.6, all the other secondary branches bifurcating from S_0 are depicted and, in cascade, other possible bifurcations from them: they were found with the continuation method employed here (the pseudo–arclength continuation **[67]**). They all emanate from solutions that are either unstable or with higher free energy. For example, the yellow branches bifurcating at $\beta \approx 16$ from the uniaxial curve $(S, 0, S', 0)$ breaks the symmetry $\hat{S}_3$ and, in fact, the bifurcating branch points in the T' direction of the order parameter space.

It is apparent from the temperature evolution of the two dominant order parameters S and T' that the transition from the isotropic to biaxial phase is first-order for $\lambda = 0.36$, but by exploring their $\lambda-$continuation we observe that after a critical value $\lambda_t = 17/21$, the transition becomes second-order and continues to remain of that order for $\lambda \geq \lambda_t$, as predicted in chapter 3 and in **[47]**.

Choosing, for example $\lambda = 0.92$, we plot in Figs. 4.5.8 and 4.5.9, the order parameters S and T' which continue to be dominant with the other two order parameters $T = S' = 0$. In Fig. 4.5.10, we

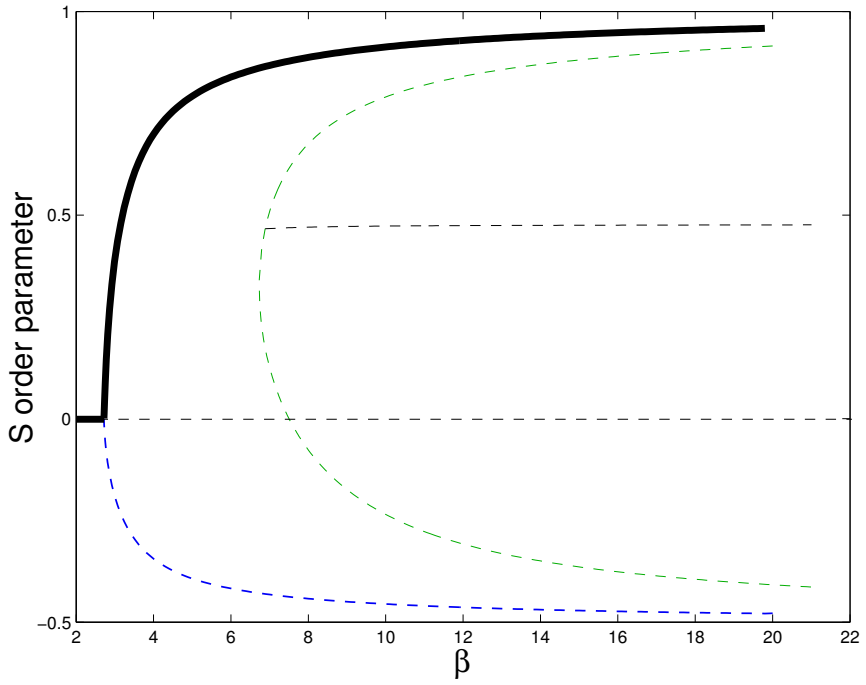

FIGURE 4.5.8. Order parameter S versus the inverse temperature β for $\lambda = 0.92$.

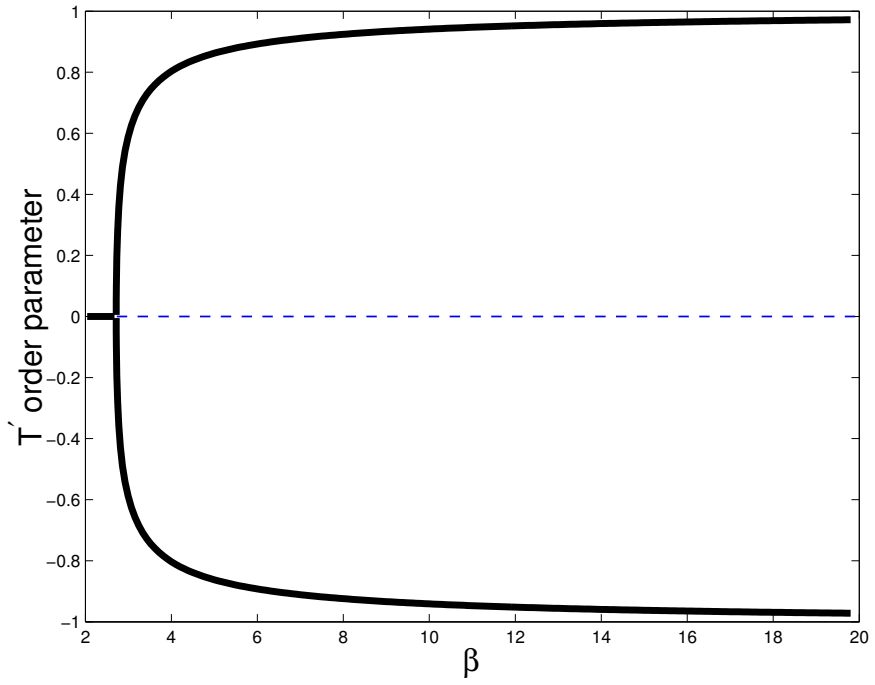

FIGURE 4.5.9. Order parameter T' versus the inverse temperature β for $\lambda = 0.92$.

represent the parameter S' which pertains to a secondary (unstable) solution characterized by having a negative value of S and the other two order parameters T and T' equal to 0.

In Fig. 4.5.11 the free–energy is plotted as a function of β and the biaxial curve (heavy solid) exhibits a second-order behaviour since it does not present a discontinuity in the derivative with respect to β at the transition to the isotropic state.

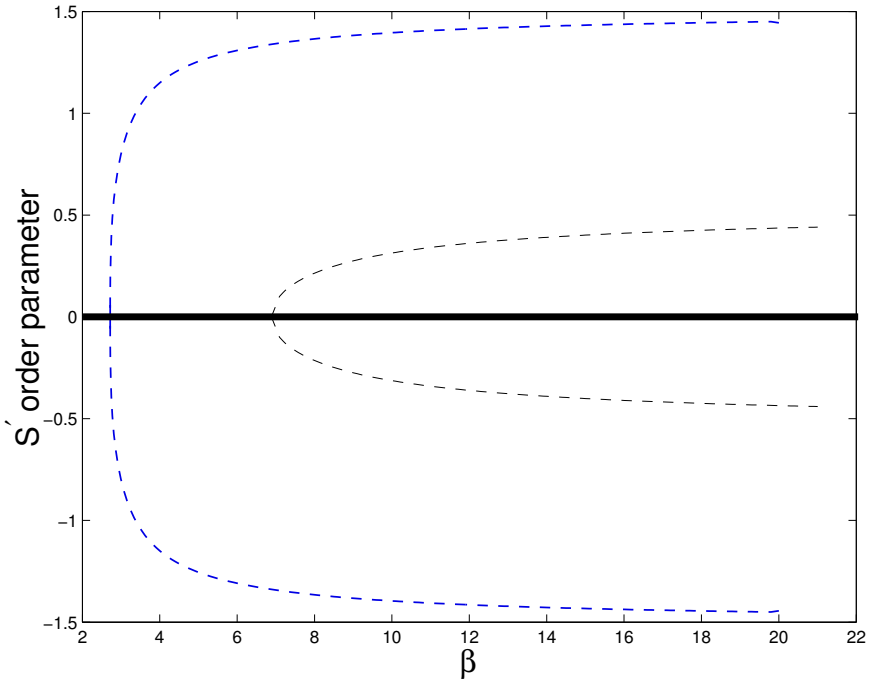

FIGURE 4.5.10. Order parameter S' versus the inverse temperature β for $\lambda = 0.92$.

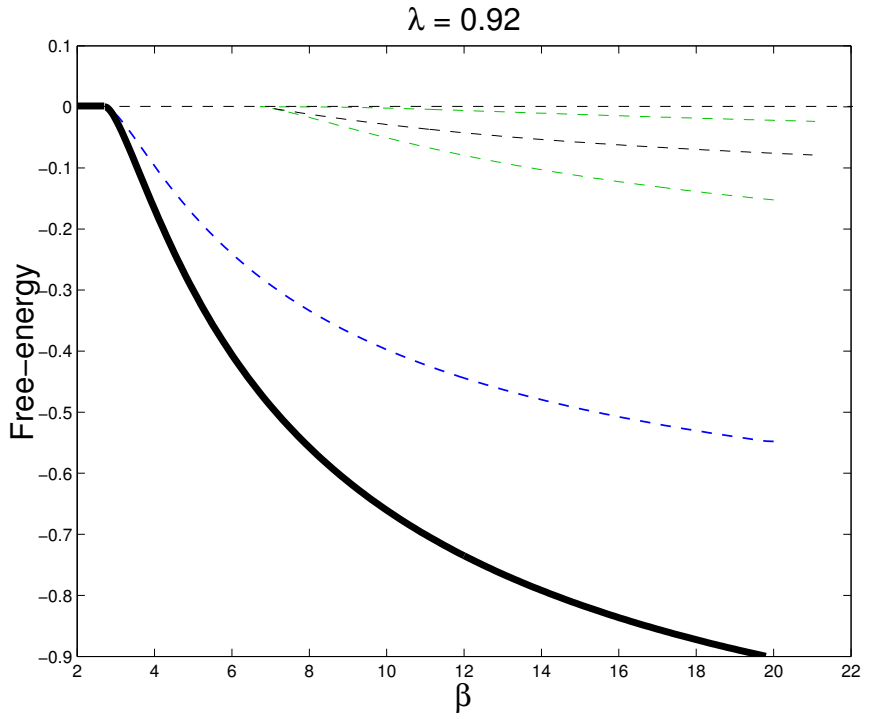

FIGURE 4.5.11. Free-energy $\mathcal{F}$ versus the inverse temperature β for $\lambda = 0.92$.

As a conclusion, the model predicts that two order parameters, S and T', prevail over the others: the one pertains to **Q** and the other to **B**.

The numerical continuation ([**67**] and [**64**]) analysis allows us to build the phase diagram of the model in the $(\lambda, 1/\beta)$ −plane and it is represented in Fig. 4.5.12. In this figure the three symmetry-breaking bifurcation lines (4.4.8, 4.4.9 and 4.4.10) are represented by the light dashed lines meeting in M. The red heavy dashed line starting from $(0,0)$ and finishing in the tricritical point C_1 is the second-order uniaxial-to-biaxial transition portion of the line (4.4.9). The red heavy dashed line starting from the second tricritical point $C_2\left(\frac{17}{21}, \frac{34}{105}\right)$ and going to infinity is the second-order isotropic-to-biaxial transition line; while the red heavy solid lines represent the first-order transition lines. It is the continuation in λ of the extended system made up of the compatibility equations and the scalar condition (4.5.4) for the isotropic-to-biaxial phase transition. For the sake of completeness, we represent the fold point (limit of stability) line (black heavy solid line) which is the continuation in λ of the limit of stability point on the biaxial branches $(S, 0, 0, T')$; it is tangent in C_1 to the symmetry-breaking line (4.4.9) and in C_2 to the symmetry-breaking line (4.4.10). Thus, in particular, they are cusp points for the compatibility equations. The turning points (blue solid line) obtained by continuing in λ the points marked with L in Figs. 4.5.1, 4.5.3, 4.5.4 and 4.5.6, are plotted as well. This line is tangent to the symmetry-breaking line (4.4.8) at the cusp point K. Moreover the tricritical point on the isotropic-to-biaxial phase transition line can be characterized as a symmetry-breaking (with respect to the operator $\hat{S}_4$) bifurcation point on the line of fold points (quadratic turning points) lying in the symmetric space of $\hat{S}_4$, i.e., on $(S, 0, 0, T')$. Otherwise, it can be characterized as a symmetry-breaking (with respect to the operator $\hat{S}_3$) bifurcation point on the line of fold points (quadratic turning points) lying in the symmetric space of $\hat{S}_3$, i.e., on $(S, 0, S', 0)$. In both cases, it is apparent that there is a common symmetry-breaking bifurcation point with respect to $\hat{S}_3$ and $\hat{S}_4$ or equivalently to their product in the symmetric space $(S, 0, 0, 0)$, which occurs at the point $(S = 0, 0, 0, 0)$, i.e., from the isotropic state. This bifurcation line in the (λ, β) −space is represented by

$$\lambda_{3,4}(\beta) = \frac{5}{2\beta}.$$

Thus, at the points $(0, 0, 0, 0, \beta, \lambda_{3,4}(\beta))$, the Jacobian matrix $J_{\mathbf{F}}(\mathbf{x}, \beta, \lambda)$ has rank 2 or rank defect 2.

As a conclusion, the phase diagram exhibits two *tricritical points*, where the type of transition is reverted from second to first–order.

4.5.1. A local analysis for the tricriticality. The two tricritical points have been predicted analytically in Chapter 3 and in [**47**], under the assumption of two prevailing order parameters S and T', which promotes biaxiality. In the previous section, they have been found numerically by means of the bifurcation analysis.

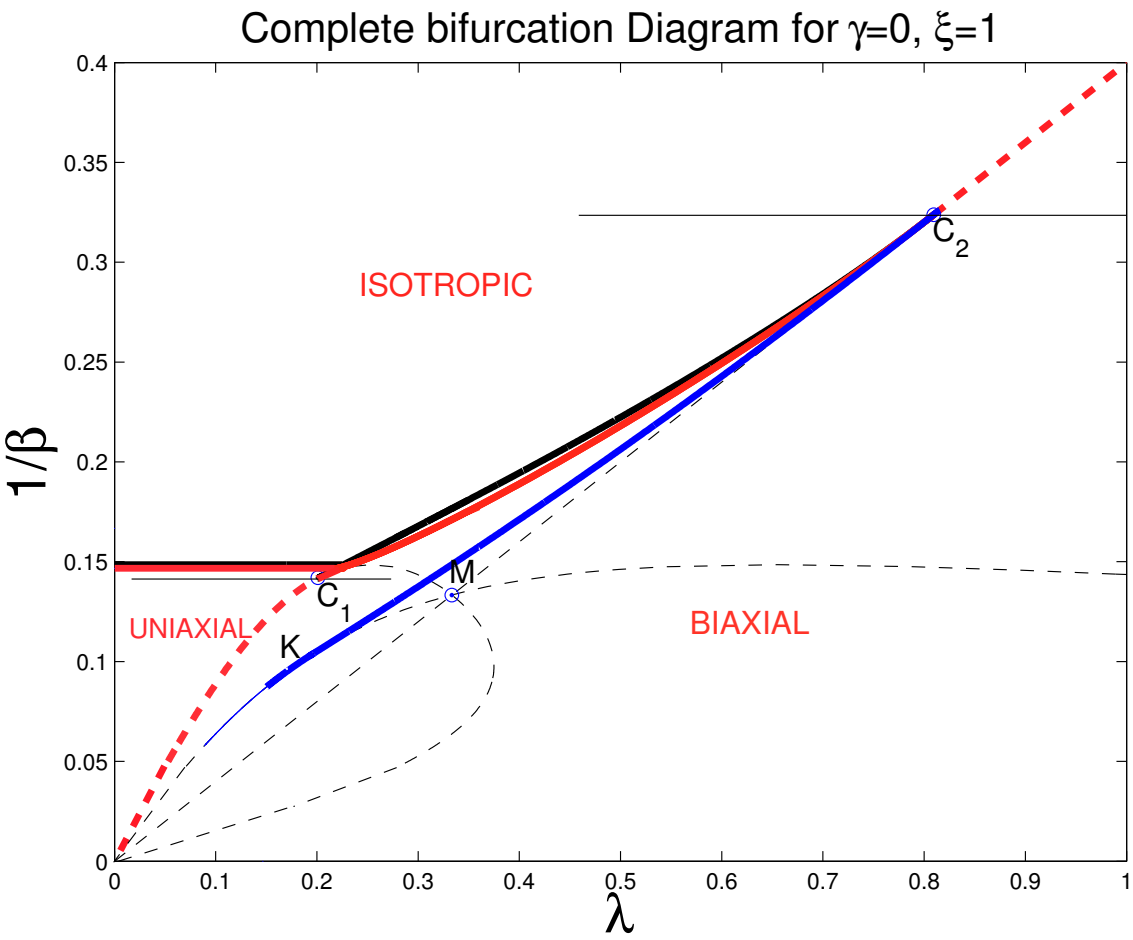

FIGURE 4.5.12. Phase diagram (heavy red lines) and stability diagram (heavy black lines) showing the reduced temperature $1/\beta$ versus the interaction parameter λ. The heavy solid red lines mark all first-order phase transitions; the dashed red lines mark the second-order transitions. C_1 and C_2 are the two tricritical points. M is the meeting point of the three symmetry-breaking lines (4.4.8,4.4.9 and 4.4.10). K is the cusp point on the turning points path (solid blue line) of the unstable uniaxial solution $(S, 0, S', 0)$.

As this analysis predicts, it is apparent that the isotropic-to biaxial phase transition is characterized by having **two** order parameters and, more precisely, S and T'. This is a consequence of the symmetry-breaking corresponding to the operators $\hat{S}_3$ and $\hat{S}_4$ and their exclusion action, as seen above. Thus, from an effective point of view, our theory is characterized by two order parameters, being the free energy stable against all perturbations in the remaining order parameters S' and T as observed numerically. We can reduce our analysis to the $(S, T')-$section of the state manifold and apply the two-order parameters tricriticality criterion. The symmetry-breaking system (4.4.6) is equivalent to the spinodal or critical line equation

$$\frac{\partial^2 \mathcal{F}}{\partial T'^2}\left(S_0(\beta), 0, 0, 0\right) = 0 \Leftrightarrow \lambda = \begin{cases} \lambda_3\left(S_0(\beta), \beta\right) & \lambda \leq \frac{1}{3} \\ \lambda_{3,4}\left(\beta\right) & \lambda \geq \frac{1}{3} \end{cases}, \tag{4.5.6}$$

since the primary bifurcation point lies on the symmetric curve (classical Maier-Saupe's) with respect to $\hat{S}_3$ for $\lambda \leq \frac{1}{3}$, approaching the isotropic state for $\lambda \geq \frac{1}{3}$. The spinodal line of $\mathcal{F}$ hosts a tricritical point whenever

$$\frac{\partial^4 \mathcal{F}}{\partial T'^4}(S_0(\beta),0,0,0)\frac{\partial^2 \mathcal{F}}{\partial S^2}(S_0(\beta),0,0,0) = 3\left(\frac{\partial^3 \mathcal{F}}{\partial T'^2 \partial S}(S_0(\beta),0,0,0)\right)^2. \tag{4.5.7}$$

By means of the equations (4.5.6, 4.5.7) we are able to locate in the $\left(\lambda, \frac{1}{\beta}\right)$ −plane, the first tricritical point at $(0.201, 0.142)$, as found in **[30]** and a second tricritical point at $\left(\frac{17}{21}, \frac{34}{105}\right)$ (see **[47]**). As a consequence, the isotropic-to-biaxial transition line becomes second-order and continues to be of this type for all $\lambda \geq \frac{17}{21}$. Finally, in the phase diagram a reentrant behaviour is revealed, the two tricritical points being the re-entrance points. Moreover, it should be noticed that the coordinates of C_2 are also solutions of the system involving the order parameters S and S' relative to the unstable uniaxial solution

$$\frac{\partial^2 \mathcal{F}}{\partial S'^2}(S_0(\beta),0,0,0) = 0 \Leftrightarrow \lambda = \begin{cases} \lambda_4(S_0(\beta),\beta) & \lambda \leq \frac{1}{3} \\ \lambda_{3,4}(\beta) & \lambda \geq \frac{1}{3} \end{cases}, \tag{4.5.8}$$

and

$$\frac{\partial^4 \mathcal{F}}{\partial S'^4}(S_0(\beta),0,0,0)\frac{\partial^2 \mathcal{F}}{\partial S^2}(S_0(\beta),0,0,0) = 3\left(\frac{\partial^3 \mathcal{F}}{\partial S'^2 \partial S}(S_0(\beta),0,0,0)\right)^2. \tag{4.5.9}$$

This is a general result and it means that all the branches bifurcating from the isotropic state undergo the tricritical behaviour.

Actually, a more detailed study can be done. It consists of expanding the compatibility equations about the isotropic phase and making a local stability analysis for the location of the second tricritical point. At the lowest approximation these equations reduce to the following linear system

$$\begin{pmatrix} 2F_4 & F_{13} & F_3 \\ 2F_{13} & 4F_{21} & 2F_{26}+p \\ 2F_3 & 2F_{26}+p & 4F_2 \end{pmatrix}\begin{pmatrix} S \\ S'^2 \\ T'^2 \end{pmatrix} = \begin{pmatrix} 0 \\ -2F_{10} \\ -2F_1 \end{pmatrix}, \tag{4.5.10}$$

where $p = -\frac{F_{19}^2}{2F_9}$, and all the symbols F_j are the coefficients of the Taylor expansion (up to the fourth order) of the free energy $\mathcal{F}$ around $(0,0,0,0)$ and depend on (β,λ) (see the Appendix), while $T^2 = -\frac{F_{19}^2}{4F_9^2}T'^2S'^2 + o(T'^2S'^2)$ is negligible up to the lowest order, this means that we are considering solutions with $T = 0$, avoiding to consider the conjugated ones by the symmetry operators $\hat{S}_1$ and $\hat{S}_2$. It can be shown that the matrix of the linear system (4.5.10) has rank 2 or rank defect 1 and this property does not depend on the choice of (β,λ), but it is a consequence of the symmetry properties: this implies that there exists a leading order parameter, but in general this is not the case. By virtue

of this fact, we can reduce the system to the two independent equations

$$d\left(S'^2 - 3T'^2\right) = -gS, \tag{4.5.11}$$

$$c_1 S'^2 + mT'^2 = -2F_{10}, \tag{4.5.12}$$

where

$$d(\beta,\lambda) = F_{13}(\beta,\lambda) = \frac{8\beta^2\lambda^2}{315}, \qquad g(\beta,\lambda) = 2F_4(\beta) = \frac{2}{45}(15-2\beta),$$
$$c_1(\beta,\lambda) = 4F_{21}(\beta,\lambda) - \frac{F_{13}^2(\beta,\lambda)}{F_4(\beta)} = \frac{16\beta^3(34\beta-105)\lambda^4}{11025(2\beta-15)}, \quad m(\beta,\lambda) = 3c_1(\beta,\lambda),$$
$$F_{10}(\beta,\lambda) = \frac{\lambda}{15}(5-2\beta\lambda).$$

Notice that both S'^2 and T'^2 are close to zero, provided that $F_{10}(\beta,\lambda)$ is close to zero, which means that we are close to the bifurcation line $\lambda_{3,4}(\beta)$, this implies that we are in the regime $\lambda > \frac{1}{3}$, which, in turn, implies that $F_4(\beta) = \frac{1}{2}\frac{\partial^2\mathcal{F}}{\partial S^2}(0,0,0,0) > 0$ and $F_9(\beta) = \frac{1}{2}\frac{\partial^2\mathcal{F}}{\partial T^2}(0,0,0,0) > 0$, i.e., stability against all perturbations in S and T.

A natural admissibility condition emerges from the second equation (4.5.12)

$$S'^2 > 0, \quad T'^2 > 0 \Leftrightarrow c_1 F_{10} < 0, \tag{4.5.13}$$

which is closely connected to the $\mathbb{Z}_2-$equivariance property of the compatibility equations. In the $\left(T'^2, S'^2\right)-$plane (4.5.12) represents the admissible orbit $\mathcal{O}$ (a segment) of states, while (4.5.11) represents a sheaf of parallel straight lines parameterized by S. The solutions of the system (4.5.11+4.5.12) lie on the segment $\mathcal{O}$ and the corresponding values of S are given by (4.5.11); notice that this orbit is invariant under $\hat{S}_3$ and $\hat{S}_4$, but not under $\hat{S}_{1,2}$, since $T = 0$. They represent the bifurcating branches from the isotropic state. We can analyze the stability of these branches from the Hessian form H on $\mathcal{O}$ associated with the free energy $\mathcal{F}$

$$[H_{\mathcal{O}}] = \begin{pmatrix} 2F_4 & 0 & -\frac{1}{3}F_{19}S' & F_{19}T' \\ 0 & 6F_4 & F_{19}T' & F_{19}S' \\ -\frac{1}{3}F_{19}S' & F_{19}T' & a & 0 \\ F_{19}T' & F_{19}S' & 0 & b \end{pmatrix},$$

where

$$a = -6T'^2 c_1 - \frac{16}{9}\frac{F_2 F_{10}}{c_1}, \quad b = 18c_1 T'^2 - \frac{F_{19}^2 F_{10}}{3c_1 F_4}.$$

By direct computation, it can be shown that the solutions within the orbit $\mathcal{O}$ are stable (minima for $\mathcal{F}$) if and only if $c_1(\beta,\lambda) > 0$ and $F_{10}(\beta,\lambda) < 0$, while they are unstable (saddle points for $\mathcal{F}$) if

$c_1(\beta,\lambda) < 0$ and $F_{10}(\beta,\lambda) > 0$. While, on the two solutions $(S,0,0,T')$ and $(S,0,S',0)$, which are the end points of $\mathcal{O}$

$$\det H = 0, \tag{4.5.14}$$

which means that these two points are bifurcation points on $\mathcal{O}$ or, equivalently, that from these two branches the orbit $\mathcal{O}$ bifurcates connecting them. It can be shown numerically that on the two branches such bifurcation points connecting them do not exist, but their virtual existence and the presence of the orbit is a consequence of the intrinsic degeneracy of the model $\gamma = 0$ around the isotropic state. Nevertheless, the study of the orbit allows to identify the tricriticality. Actually, the free energy variation with respect to the isotropic state of this orbit of solutions can be estimated at this lowest approximation, obtaining

$$(\Delta\mathcal{F})_{\mathcal{O}} = -2\frac{F_{10}^2}{c_1} + o\left(T'^2\right),$$

which gives the sign of the variation for the germinating sheaf of branches. Thus we can conclude that

$$c_1(\beta,\lambda) > 0, \quad F_{10}(\beta,\lambda) < 0 \Rightarrow \forall s \in \mathcal{O},\ s\ stable,\ (\Delta\mathcal{F})_{\mathcal{O}} < 0,$$

$$c_1(\beta,\lambda) < 0, \quad F_{10}(\beta,\lambda) > 0 \Rightarrow \forall s \in \mathcal{O},\ s\ unstable,\ (\Delta\mathcal{F})_{\mathcal{O}} > 0.$$

This means that the points in the $(\beta,\lambda)-$plane that are solutions of

$$\begin{cases} c_1(\beta,\lambda) = 0 \\ F_{10}(\beta,\lambda) = 0 \end{cases} \tag{4.5.15}$$

are tricritical points for the system. In correspondence of these solutions, the matrix of the linear system (4.5.10) has rank 1, i.e., its rank defect increases. The unique solution of (4.5.15) is $\left(\frac{17}{21}, \frac{34}{105}\right)$, which coincides with the value found above, so the isotropic-to-biaxial phase transition becomes second order for $\lambda > \frac{17}{21}$. On the other hand the equation $F_{10}(\beta,\lambda) = 0$ is nothing but the equation for the critical line (4.5.6), while the equation $c_1(\beta,\lambda) = 0$ is equivalent to the equation (4.5.7), both computed at $S_0 = 0$ since we are exploring the isotropic-to-biaxial transition line. Notice that the tricritical behaviour leaves out of consideration the particular solution on the orbit, whether it is a biaxial solution $(S,0,0,T')$ or a uniaxial one $(S,0,S',0)$. Both these solutions reveal a tricritical property, together with the solutions conjugated to them by all the symmetry operators. But the biaxial one is stable and the energetically most favorable (this can be observed by computing the free energy and the branches numerically), while the uniaxial one is unstable and a biaxial phase takes place.

4.6. Monte Carlo simulations

In addition to the above "global" mean field treatment, for assigned values of the potential parameter λ, one can numerically solve the consistency equations and minimize the mean field free energy over a fine temperature grid, and thus calculate the temperature dependence for the resulting thermodynamic and structural properties (this analysis has been performed by Prof. Silvano Romano in Ref. **[62]**). We consider a 3−dimensional simple-cubic lattice $\mathbf{Z}^3$ whose axes define the orthonormal basis $\{\boldsymbol{e}_x, \boldsymbol{e}_y, \boldsymbol{e}_z\}$. At each site we associate the center of mass of a single molecule whose coordinate vector we denote by $\boldsymbol{x}_\mu$. The interaction potential V is restricted to nearest neighbours, involving molecules or sites labelled by μ and ν, respectively. The orientation of each molecule is specified via the orthonormal triplet of 3−component vectors, say $\{\boldsymbol{e}_\mu, \boldsymbol{e}_{\perp\mu}, \boldsymbol{m}_\mu\}$ for the molecule on the site μ and $\{\boldsymbol{e}_\nu, \boldsymbol{e}_{\perp\nu}, \boldsymbol{m}_\nu\}$ for the molecule sited in ν. The interaction potential is

$$V = \epsilon \left\{ -P_2 \left(\boldsymbol{m}_\mu \cdot \boldsymbol{m}_\nu \right) - \lambda \left[2P_2 \left(\boldsymbol{e}_{\perp\mu} \cdot \boldsymbol{e}_{\perp\nu} \right) + 2P_2 \left(\boldsymbol{e}_\mu \cdot \boldsymbol{e}_\nu \right) - P_2 \left(\boldsymbol{m}_\mu \cdot \boldsymbol{m}_\nu \right) \right] \right\}, \tag{4.6.1}$$

where $\epsilon = \frac{2}{3} U_0$.

Allowing for a lattice situation, the mean-field formalism changes as follows. The pseudo-potential (4.3.1) felt by a molecule must be modified in order to take into account the interaction energy between molecules in the lattice. Since each molecule interacts with its 6 nearest neighbours, the pseudo-potential (4.3.1) is replaced by the following

$$\widetilde{\Omega} = 2\rho\Omega = -2\rho U_0 \Psi, \tag{4.6.2}$$

where $\rho = 3$ is one half of the coordination number for a cubic lattice. The global factor 2ρ takes account of the interaction energy in the basic cluster of the lattice, which is formed of $2\rho = 6$ pairs of molecules. Accordingly, the free energy is

$$\widetilde{\mathcal{F}} = U_0 \left\{ \rho \sum_{jk=1}^{4} d_{jk} \left\langle s_j \right\rangle \left\langle s_k \right\rangle - \frac{1}{\beta} \ln \left(\frac{\widetilde{Z}}{8\pi^2} \right) \right\}, \qquad \widetilde{Z} = \int_{\mathbb{T}} \exp \left(2\rho\beta\Psi \right) d\omega. \tag{4.6.3}$$

As a consequence, we employ a different temperature scale T^* which differs from $\frac{1}{\beta}$ by a factor 9 due to the coordination number used for MC simulations and to a different energy scale for the microscopic potential which differs from that used in the preceding sections by a factor $\frac{3}{2}$ (chosen so as to enforce a better compatibility with Lebwohl-Lasher model). More precisely the following mapping exists between the temperature scales

$$T^* = \frac{k_B t}{\epsilon} = 9 \left(\frac{1}{\beta} \right). \tag{4.6.4}$$

Simulations were carried out for $\lambda = 1$ (where mean-field predicts a direct second-order isotropic-to-biaxial phase transition) on a periodically repeated cubic sample, consisting of $N = l^3$ particles, $l = 10, 20, 30$; calculations were run in cascade, in order of increasing temperature; each cycle (or sweep) consisted of $2N$ MC steps, including a sub-lattice sweep **[68]**; the finest temperature step used was $\Delta T^* = 0.005$, in the transition region.

Equilibration runs took between 25 000 and 100 000 cycles, and production runs took between 200 000 and 800 000; macrostep averages for evaluating statistical errors were taken over 1 000 cycles. Calculated thermodynamic quantities include mean potential energy per site U^* and configurational specific heat per particle C^*.

Simulation estimates of the order parameters $\langle s_k \rangle$ **[69, 70, 71]** were calculated by analyzing a configuration every cycle, and according to methodologies discussed in detail by other Authors **[25, 29, 70, 69]**; the four order parameters $\langle s_k \rangle$ are all different from zero in a biaxial phase (although $\langle s_3 \rangle$ and $\langle s_2 \rangle$ may be rather small), while both $\langle s_2 \rangle$ and $\langle s_4 \rangle$ vanish in a uniaxial phase **[69, 70, 71]**. MC estimates of the fourth-rank order parameter $\langle P_4 \rangle$ were determined as well **[69, 70, 71, 73, 74]**.

We also evaluated the so-called short-range order parameters **[69, 70]**

$$\sigma_{L,1} = \langle P_L(\boldsymbol{e}_\mu \cdot \boldsymbol{e}_\nu) \rangle, \ \sigma_{L,2} = \langle P_L(\boldsymbol{e}_{\perp\mu} \cdot \boldsymbol{e}_{\perp\nu}) \rangle, \ \sigma_{L,3} = \langle P_L(\boldsymbol{m}_\mu \cdot \boldsymbol{m}_\nu) \rangle, \quad L = 2, 4 \tag{4.6.5}$$

measuring correlations between corresponding pairs of unit vectors $\boldsymbol{e}_\mu$, $\boldsymbol{e}_{\perp\mu}$, $\boldsymbol{m}_\mu$ and $\boldsymbol{e}_\nu$, $\boldsymbol{e}_{\perp\nu}$, $\boldsymbol{m}_\nu$, associated with nearest-neighbour molecules; the functional form of the interaction entails that the potential energy U^* is a linear combination of quantities $\sigma_{2,1}$, $\sigma_{2,2}$ and $\sigma_{2,3}$; moreover, the condition $\gamma = 0$ entails $\sigma_{L,1} = \sigma_{L,2}$.

The mean-field transition temperature was found to be $\Theta_{MF} = \frac{18}{5}$, which in the $\frac{1}{\beta}$ scale corresponds to the value $\frac{2}{5}$; here potential energy and order parameters vanish continuously, whereas C^*_{MF} exhibits a discontinuous jump to 0; in the present case, mean field predicts both $\langle s_3 \rangle$ and $\langle s_2 \rangle$ to be practically zero even in the biaxial phase, as found also in Ref. **[30]**.

Results for various observables are collected in the Figures 4.6.1, 4.6.2, 4.6.3, 4.6.4, 4.6.5, 4.6.6.

MC results for U^* (not shown here) exhibit a gradual and monotonic change with temperature, and a very weak sample-size dependency. Results for C^* (Fig. 4.6.1) exhibit a more recognizable sample-size dependency, and show a peak at $T^* \approx 2.9$. The order parameters (S, T, S', T') are obtained by averaging the 4 symmetry adapted functions s_k

$$S = \langle s_1 \rangle, \quad T = \sqrt{\frac{2}{3}} \langle s_2 \rangle, \quad S' = \sqrt{6} \langle s_3 \rangle, \quad T' = 2 \langle s_4 \rangle. \tag{4.6.6}$$

Results for the order parameters are shown in Figs 4.6.2 to 4.6.6; S, T' and $\langle P_4 \rangle$ (Figures 4.6.2, 4.6.3 and 4.6.4) appear to decrease monotonically with temperature, whereas the other two order parameters

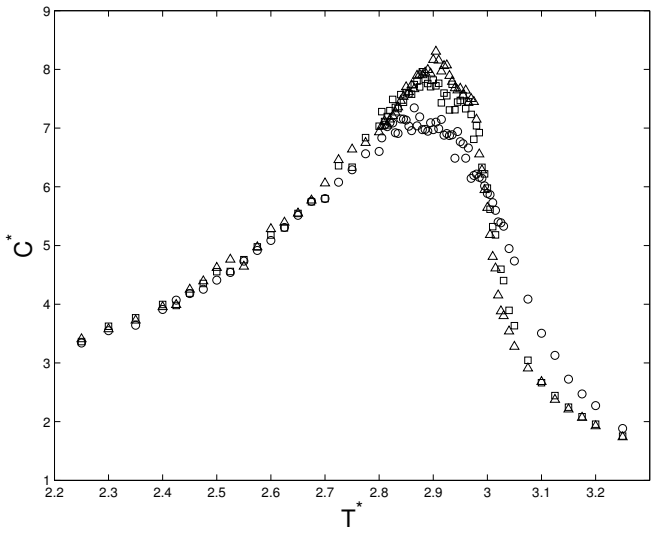

FIGURE 4.6.1. Simulation results for the configurational heat capacity; discrete symbols have been used for results, obtained with different sample sizes, and have the following meanings: circles: $l = 10$; squares: $l = 20$; triangles: $l = 30$; here the associated statistical errors, not shown, range between 1 and 5 %.

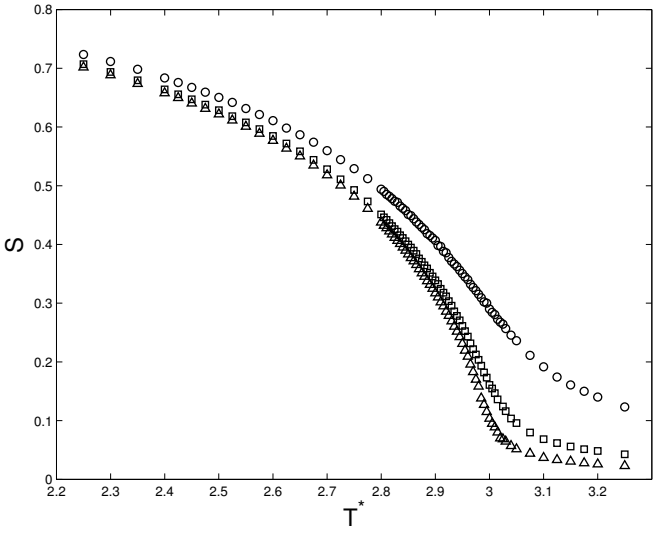

FIGURE 4.6.2. Simulation results for the order parameters $\langle P_2 \rangle = \langle s_1 \rangle$, obtained with different sample sizes; same meaning of symbols as in Fig. 4.6.1; here and in the following Figures, the associated statistical errors fall within symbol sizes.

T and S' (Figs. 4.6.5 and 4.6.6) increase up to a maximum at $T^* \approx 2.85$ and then decrease; all the order parameters appear to evolve with temperature in a gradual and continuous way, and, for $T^* \gtrsim 2.9$, all of them exhibit a pronounced decrease with increasing sample sizes.

Simulation results for the quantities $\sigma_{L,1}$, $\sigma_{L,2}$, $\sigma_{L,3}$, not shown here, exhibit a gradual and monotonic decrease with temperature, and a very weak sample-size dependency.

Based on the above results, we propose a direct biaxial to isotropic continuous transition, and the value $\Theta_{MC} = 2.91 \pm 0.01$ for the transition temperature; the estimated uncertainty is based on the temperature step used in the investigated range, and the ratio $\frac{\Theta_{MC}}{\Theta_{MF}}$ is 0.808. As before we can

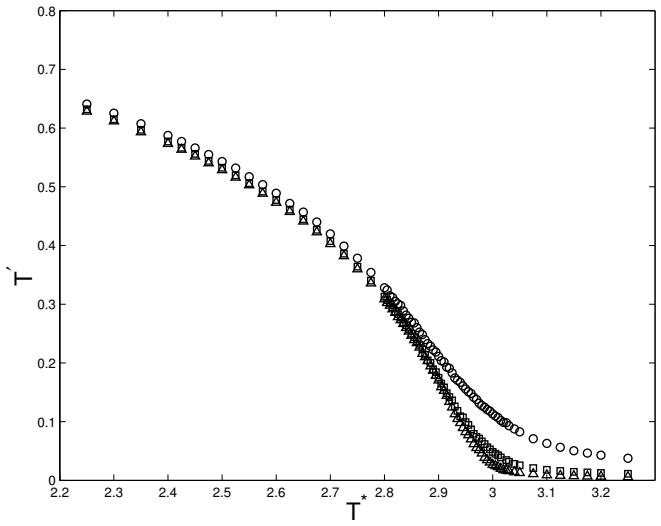

FIGURE 4.6.3. Simulation results for the order parameter $T' = \langle s_4 \rangle$, obtained with different sample sizes: same meaning of symbols as in Fig. 4.6.1.

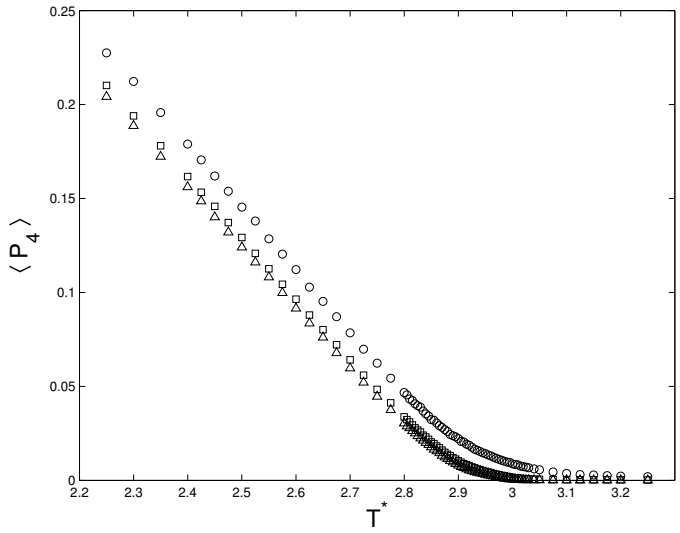

FIGURE 4.6.4. Simulation results for the fourth-rank order parameter $\langle P_4 \rangle$, obtained with different sample sizes; same meaning of symbols as in Fig. 4.6.1.

represents this MC prediction for the second-order transition temperature on the $\frac{1}{\beta}$ scale in the phase diagram in Fig. 4.5.12 obtaining

$$\lambda = 1, \qquad \frac{1}{\beta_{MC}} = 0.323 \pm 0.001. \tag{4.6.7}$$

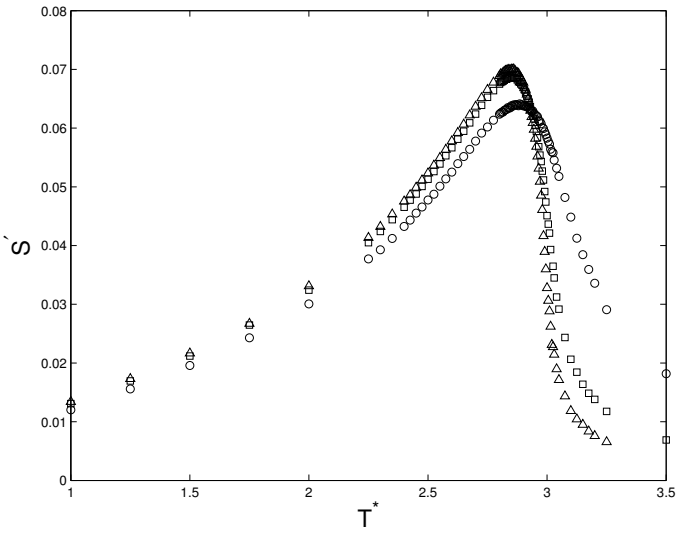

FIGURE 4.6.5. Simulation results for the order parameter S', obtained with different sample sizes: same meaning of discrete symbols as in Fig. 4.6.1.

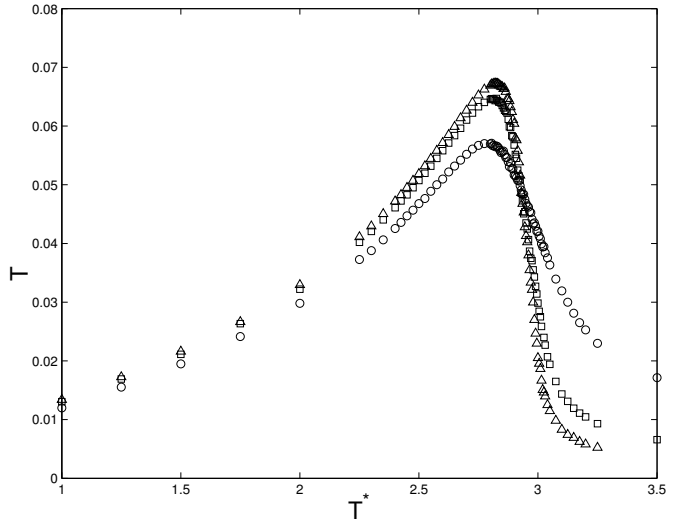

FIGURE 4.6.6. Simulation results for the order parameter T, obtained with different sample sizes: same meaning of discrete symbols as in Fig. 4.6.1.

Appendix

In this Appendix we list the coefficients entering the expressions in Sec. 4.5.1 and the relations among them because of the symmetry

$$F_1(\lambda,\beta) = \frac{1}{2}\frac{\partial^2 \mathcal{F}}{\partial T'^2}(0,0,0,0) = \lambda - \frac{2\beta\lambda^2}{5},$$

$$F_2(\lambda,\beta) = \frac{1}{4!}\frac{\partial^4 \mathcal{F}}{\partial T'^4}(0,0,0,0) = \frac{4\beta^3\lambda^4}{175},$$

$$F_3(\lambda,\beta) = \frac{1}{2}\frac{\partial^3 \mathcal{F}}{\partial T'^2 \partial S}(0,0,0,0) = -\frac{8\beta^2\lambda^2}{105},$$

$$F_4(\beta) = \frac{1}{2}\frac{\partial^2 \mathcal{F}}{\partial S^2}(0,0,0,0) = \frac{1}{45}(15-2\beta),$$

$$F_9(\beta) = \frac{1}{2}\frac{\partial^2 \mathcal{F}}{\partial T^2}(0,0,0,0) = 1 - \frac{2\beta}{15} = 3F_4(\beta),$$

$$F_{10}(\lambda,\beta) = \frac{1}{2}\frac{\partial^2 \mathcal{F}}{\partial S'^2}(0,0,0,0) = \frac{\lambda}{15}(5-2\beta\lambda) = \frac{1}{3}F_1(\lambda,\beta),$$

$$F_{13}(\lambda,\beta) = \frac{1}{2}\frac{\partial^3 \mathcal{F}}{\partial S'^2 \partial S}(0,0,0,0) = \frac{8\beta^2\lambda^2}{315} = -\frac{1}{3}F_3(\lambda,\beta),$$

$$F_{19}(\lambda,\beta) = \frac{\partial^3 \mathcal{F}}{\partial T' \partial S' \partial T}(0,0,0,0) = -\frac{16\beta^2\lambda^2}{105} = -6F_{13}(\lambda,\beta),$$

$$F_{21}(\lambda,\beta) = \frac{1}{4!}\frac{\partial^3 \mathcal{F}}{\partial S'^4}(0,0,0,0) = \frac{4\beta^3\lambda^4}{1575} = \frac{1}{9}F_2(\lambda,\beta),$$

$$F_{26}(\lambda,\beta) = \frac{1}{4}\frac{\partial^4 \mathcal{F}}{\partial T'^2 \partial S'^2}(0,0,0,0) = \frac{8\beta^3\lambda^4}{525}.$$

CHAPTER 5

Conjugacy

This Chapter is devoted to the problem of conjugacy of the general pairwise quadrupolar interaction energy V in Eq. (2.3.1) and to the relationship between this property and the general problem of diagonalizing the bilinear form V. Moreover, we prolong the conjugacy property to the macroscopic tensors and to the equilibrium equations of the mean–field model put forward in Chapter 2. We then apply the conjugacy relationships to the construction of the corresponding phase diagrams.

5.1. Potential symmetries and conjugacy relations

5.1.1. Conjugacy chart. We consider the pair potential in the general form (2.3.1)

$$V = -U_0 \left\{ \xi \mathbf{q} \cdot \mathbf{q}' + \gamma \left(\mathbf{q} \cdot \mathbf{b}' + \mathbf{b} \cdot \mathbf{q}' \right) + \lambda \mathbf{b} \cdot \mathbf{b}' \right\}. \tag{5.1.1}$$

In Chapter 2 we have shown, by referring to an electrostatic model, how it is possible to transform the model parameters ξ, γ, λ and, simultaneously the molecular vectors $\boldsymbol{e}, \boldsymbol{e}_\perp, \boldsymbol{m}$ leaving V unchanged. These transformations induce three basic mappings in the model parameters space, one for each of the swapping operators τ_1, τ_2, τ_3 introduced in Chapter 2

$$\begin{aligned} \xi_1' &= \frac{1}{4} \left(\xi + 6\gamma + 9\lambda \right), \\ \gamma_1' &= \frac{1}{4} \left(2\gamma - 3\lambda + \xi \right), \\ \lambda_1' &= \frac{1}{4} \left(\xi - 2\gamma + \lambda \right), \end{aligned} \tag{5.1.2}$$

and

$$\begin{aligned} \xi_2' &= \xi, \\ \gamma_2' &= -\gamma, \\ \lambda_2' &= \lambda, \end{aligned} \tag{5.1.3}$$

$$\begin{aligned} \xi_3' &= \frac{1}{4} \left(\xi - 6\gamma + 9\lambda \right), \\ \gamma_3' &= \frac{1}{4} \left(2\gamma + 3\lambda - \xi \right), \\ \lambda_3' &= \frac{1}{4} \left(\xi + 2\gamma + \lambda \right). \end{aligned} \tag{5.1.4}$$

Now, we simplify these transformations, by setting $\xi = 1$ and by rescaling the energy constant U_0. More precisely, we have the following transformations for τ_1

$$\begin{aligned} \lambda_1' &= \frac{1+\lambda-2\gamma}{1+6\gamma+9\lambda}, \\ \gamma_1' &= \frac{2\gamma-3\lambda+1}{1+6\gamma+9\lambda}, \end{aligned} \tag{5.1.5}$$

while for τ_2

$$\lambda_2' = \lambda, \quad \gamma_2' = -\gamma, \tag{5.1.6}$$

and for τ_3

$$\begin{aligned} \lambda_3' &= \frac{1+\lambda+2\gamma}{1-6\gamma+9\lambda}, \\ \gamma_3' &= \frac{2\gamma+3\lambda-1}{1-6\gamma+9\lambda}. \end{aligned} \tag{5.1.7}$$

In Chapter 2 we have presented the stability analysis of the ground state represented by the complete alignment of two interacting molecules. This analysis has singled out a fan–shaped region depicted in Fig. 2.3.1. Now, we make further considerations on these results in connection with the equivalence transformations (5.1.5, 5.1.6, 5.1.7).

Rescaling U_0 is equivalent to rescale the temperature, taking in mind that we have defined $\beta = \frac{U_0}{k_B t}$ in solving the model in the mean–field framework. Hence, if we consider the τ_3 swapping operator, then the corresponding transformations are accompanied by the following

$$\beta_3' = \frac{\beta}{4}\left(1-6\gamma+9\lambda\right), \tag{5.1.8}$$

which implies, or better, requires the further restriction on the fan–shaped region of stability, which we represent here in Fig. 5.1.1

$$1-6\gamma+9\lambda > 0; \tag{5.1.9}$$

the equation $1-6\gamma+9\lambda = 0$ represents the tangent straight line to the parabola curve $\lambda = \gamma^2$ at the point $\left(\frac{1}{3}, \frac{1}{9}\right)$. This constraint allows us to extend the transformations including the temperature in the transformed variables. Another restriction comes from the τ_1 swapping operator which leads to the

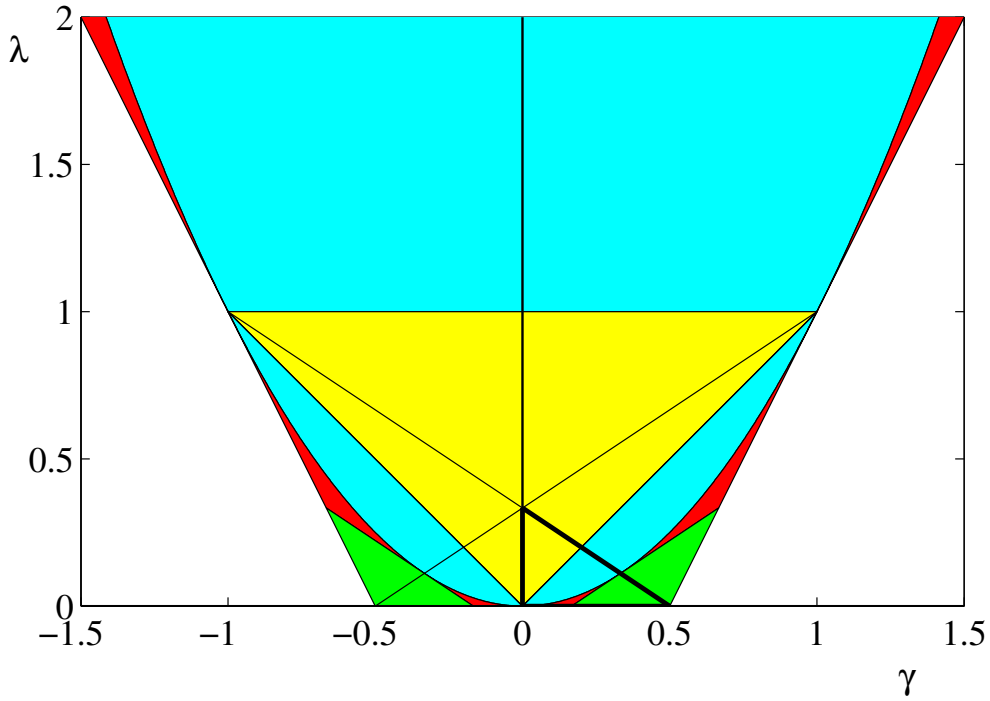

FIGURE 5.1.1. Conjugacy chart. The regions with the same colour are equivalent in the sense of the transformations (5.1.5), (5.1.6) and (5.1.7).

scale transformation

$$\beta_1' = \frac{\beta}{4}\,(1 + 6\gamma + 9\lambda)\,, \tag{5.1.10}$$

provided that $1+6\gamma+9\lambda > 0$, where the straight line $1+6\gamma+9\lambda = 0$ is tangent to the parabola $\lambda = \gamma^2$ for $\gamma = -\frac{1}{3}$ and it is conjugated to the other by reversing the sign of γ, or equivalently, by applying the τ_2 swap operator. Thus, requiring a thermodynamic equivalence of different sectors of the fan–shaped stability region, we are automatically forced to exclude from the consideration the regions where the restriction (5.1.9) and the dual one cease to be valid. In Fig. 5.1.1 these regions are identified by the two green coloured symmetric triangles. By applying the transformations (5.1.5, 5.1.6, 5.1.7), we can identify equivalent sectors within the fan–shaped region and thus, we can reduce the analysis to the triangle bordered by black solid heavy lines which represents all the other sectors. As a conclusion, the equivalence relations induced by τ_1, τ_2, τ_3 constitute a reduction criterion which confines the analysis to the reference triangle in Fig. 5.1.3. On the other hand, the green regions are excluded from this thermodynamic equivalence only apparently. Actually, we can recover such an equivalence by rescaling

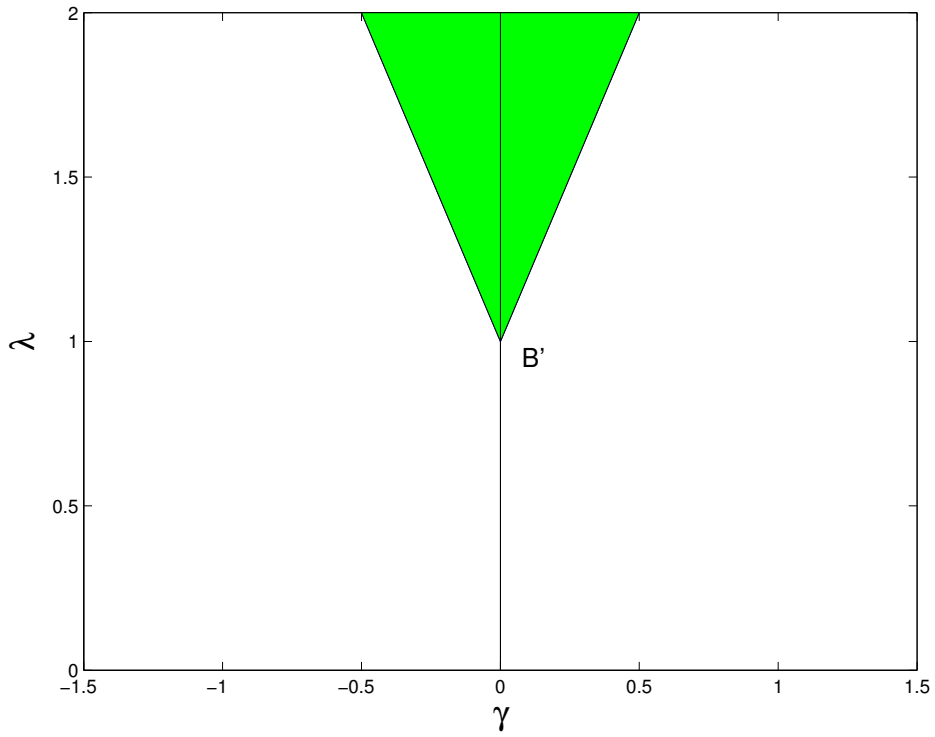

FIGURE 5.1.2. This region on the plane $\xi = -1$ is conjugated to the green regions inside the stability region for $\xi = 1$ represented in Fig. 5.1.1.

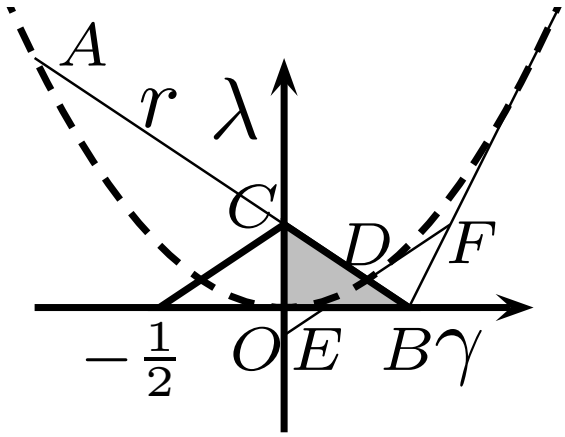

FIGURE 5.1.3. Reference triangle with vertices $O(0,0)$, $C\left(0,\frac{1}{3}\right)$ and $B\left(\frac{1}{2},0\right)$. The segments $\overline{BE}$ (with $E\left(\frac{1}{6},0\right)$) and $\overline{BF}$ (with $F\left(\frac{2}{3},\frac{1}{3}\right)$) are conjugated to the straight lines $\lambda + 2\gamma - 1 = 0$ with $\xi = -1$ and $\lambda - 2\gamma - 1 = 0$ with $\xi = -1$, while the point $B\left(\frac{1}{2},0\right)$ corresponds to $B'(0,1)$ with $\xi = -1$ (see Fig.5.1.2).

β as follows

$$\beta_3' = \frac{\beta}{4}\left|1 - 6\gamma + 9\lambda\right|, \tag{5.1.11}$$

which, inside the green region, means

$$\beta_3' = \frac{\beta}{4}\left(6\gamma - 9\lambda - 1\right). \tag{5.1.12}$$

This is equivalent to transform the potential under τ_3 and changing the parameters in such a way that

$$\begin{aligned}\xi_3' &= \frac{1}{4}\left(6\gamma - 9\lambda - 1\right),\\ \gamma_3' &= \frac{1}{4}\left(2\gamma + 3\lambda - 1\right),\\ \lambda_3' &= \frac{1}{4}\left(1 + 2\gamma + \lambda\right),\end{aligned}$$

or, by rescaling β via (5.1.12), transforming λ and γ as follows

$$\begin{aligned}\lambda_3' &= \frac{1+\lambda+2\gamma}{6\gamma - 9\lambda - 1},\\ \gamma_3' &= \frac{2\gamma+3\lambda-1}{6\gamma - 9\lambda - 1},\end{aligned} \tag{5.1.13}$$

and setting $\xi_3' = -1$. Thus, the green regions turn out to be conjugated to an *antinematic* model potential (meaning that the uniaxial term is antinematic or repulsive) and precisely to the unbounded V–shaped region partially depicted in Fig. 5.1.2 on the plane $\xi = -1$, starting from $B'(0,1)$ and extending to infinity. The point B' is conjugated to the point $B\left(\frac{1}{2},0\right)$ on the plane $\xi = 1$ in Fig. 5.1.3. The semi-line $\lambda \geq 1$ on the plane $\xi = -1$ is mapped onto the segment $\overline{DB}$ on the plane $\xi = 1$, while the semi-lines $\lambda - 2\gamma - 1 = 0$ and $\lambda + 2\gamma - 1 = 0$ are conjugated to the segments $\overline{BF}$ and $\overline{BE}$ respectively. The V–shaped region is the region of stability for the model $\xi = -1$ as illustrated in Chapter 2 and represented in Fig. 2.3.2, which corresponds to the stability region for the complete alignment ground state.

5.1.2. Symmetries of the pairwise potential: self-dual planes. In this section, we focus our attention to special relationships involving the model parameters. The transformations (5.1.2, 5.1.3, 5.1.4) allow us to single out three self-dual planes which remain invariant under their action. With respect to (5.1.2), such a plane is represented by the equation

$$2\gamma + 3\lambda - \xi = 0, \tag{5.1.14}$$

while for (5.1.4) is the plane

$$3\lambda - 2\gamma - \xi = 0, \tag{5.1.15}$$

and $\gamma = 0$ is the self-dual plane with respect to (5.1.3). Now, we investigate their meaning in more detail. We study the symmetry properties of (5.1.1), more precisely we are interested in finding special models of the two parameters potentials family (5.1.1) enjoying an invariance property. This procedure does not solve the general symmetry problem of V, since it avoids considering general

transformations. We restrict attention to a class of linear transformations acting simultaneously over the pairs of interacting molecules and leaving unchanged the potential V. We consider the set of orthogonal involution operators

$$\tau \in O(3), \quad \tau^2 = \mathbf{I},$$

and in particular the three operators τ_1, τ_2, τ_3, represented by

$$[\tau_1] = \begin{pmatrix} 1 & 0 & 0 \\ 0 & 0 & 1 \\ 0 & 1 & 0 \end{pmatrix}, \qquad [\tau_2] = \begin{pmatrix} 0 & 1 & 0 \\ 1 & 0 & 0 \\ 0 & 0 & 1 \end{pmatrix}, \qquad [\tau_3] = \begin{pmatrix} 0 & 0 & 1 \\ 0 & 1 & 0 \\ 1 & 0 & 0 \end{pmatrix}.$$

In terms of the molecular arms $\{\boldsymbol{e}, \boldsymbol{e}_\perp, \boldsymbol{m}\}$ and $\{\boldsymbol{e}', \boldsymbol{e}'_\perp, \boldsymbol{m}'\}$, the potential takes the form

$$V = -U_0 \left\{ (\xi - \lambda) \left(\boldsymbol{m} \cdot \boldsymbol{m}'\right)^2 + 2(\lambda - \gamma) \left(\boldsymbol{e} \cdot \boldsymbol{e}'\right)^2 + 2(\lambda + \gamma) \left(\boldsymbol{e}_\perp \cdot \boldsymbol{e}'_\perp\right)^2 - \left(\lambda + \frac{\xi}{3}\right) \right\}.$$

We are interested in determining the conditions on the model parameters (ξ, λ, γ) under which the potential remains invariant. More precisely, consider the action of τ_1

$$\tau_1 \boldsymbol{m} = \boldsymbol{e}_\perp, \ \tau_1 \boldsymbol{e}_\perp = \boldsymbol{m}, \ \tau_1 \boldsymbol{e} = \boldsymbol{e}$$

$$\Updownarrow$$

$$\mathbf{q} \mapsto \tau_1 \mathbf{q} \tau_1^t = -\frac{1}{2}(\mathbf{q} + \mathbf{b}), \quad \mathbf{b} \mapsto \tau_1 \mathbf{b} \tau_1^t = \frac{1}{2}(\mathbf{b} - 3\mathbf{q})$$

and similar transformations for the primed molecule. These transformations act simultaneously and independently over the two molecules and the invariance requirement becomes a specification of the molecular structure via the interaction potential. The transformed potential is

$$V^* = -U_0 \left\{ (\xi - \lambda) \left(\tau_1 \boldsymbol{m} \cdot \tau_1 \boldsymbol{m}'\right)^2 + 2(\lambda - \gamma) \left(\tau_1 \boldsymbol{e} \cdot \tau_1 \boldsymbol{e}'\right)^2 + 2(\lambda + \gamma) \left(\tau_1 \boldsymbol{e}_\perp \cdot \tau_1 \boldsymbol{e}'_\perp\right)^2 - \left(\lambda + \frac{\xi}{3}\right) \right\} =$$

$$= -U_0 \left\{ (\xi - \lambda) \left(\boldsymbol{e}_\perp \cdot \boldsymbol{e}'_\perp\right)^2 + 2(\lambda - \gamma) \left(\boldsymbol{e} \cdot \boldsymbol{e}'\right)^2 + 2(\lambda + \gamma) \left(\boldsymbol{m} \cdot \boldsymbol{m}'\right)^2 - \left(\lambda + \frac{\xi}{3}\right) \right\},$$

the invariance condition implies

$$V = V^* \Leftrightarrow (3\lambda + 2\gamma - \xi) \left[\left(\boldsymbol{e}_\perp \cdot \boldsymbol{e}'_\perp\right)^2 - \left(\boldsymbol{m} \cdot \boldsymbol{m}'\right)^2 \right] = 0 \quad \forall \left(\{\boldsymbol{e}, \boldsymbol{e}_\perp, \boldsymbol{m}\}, \{\boldsymbol{e}', \boldsymbol{e}'_\perp, \boldsymbol{m}'\} \right),$$

that is for all the molecular pairs, this is possible if and only if

$$3\lambda + 2\gamma - \xi = 0. \tag{5.1.16}$$

This condition represents the self–dual plane of τ_1 and selects a class of potential models corresponding to a special symmetry, in particular the potentials of this class are

$$V = -U_0 \left\{ (\xi - \lambda) \left[\left(\boldsymbol{m} \cdot \boldsymbol{m}' \right)^2 + \left(\boldsymbol{e}_\perp \cdot \boldsymbol{e}'_\perp \right)^2 \right] + (5\lambda - \xi) \left(\boldsymbol{e} \cdot \boldsymbol{e}' \right)^2 - \left(\lambda + \frac{\xi}{3} \right) \right\},$$

which are invariant under $\boldsymbol{m} \leftrightarrow \boldsymbol{e}_\perp$ which is the D_{4h} symmetry respect to $\boldsymbol{e}$. Similar considerations for τ_2 lead to the following transformations

$$\tau_2 \boldsymbol{m} = \boldsymbol{m},\ \tau_2 \boldsymbol{e}_\perp = \boldsymbol{e},\ \tau_2 \boldsymbol{e} = \boldsymbol{e}_\perp$$

$$\Updownarrow$$

$$\mathbf{q} \mapsto \tau_2 \mathbf{q} \tau_2^t = \mathbf{q}, \quad \mathbf{b} \mapsto \tau_2 \mathbf{b} \tau_2^t = -\mathbf{b}.$$

In this case the invariance condition yields

$$V^* = -U_0 \left\{ (\xi - \lambda) \left(\boldsymbol{m} \cdot \boldsymbol{m}' \right)^2 + 2 (\lambda - \gamma) \left(\boldsymbol{e}_\perp \cdot \boldsymbol{e}'_\perp \right)^2 + 2 (\lambda + \gamma) \left(\boldsymbol{e} \cdot \boldsymbol{e}' \right)^2 - \left(\lambda + \frac{\xi}{3} \right) \right\} = V$$

if and only if

$$\gamma \left[\left(\boldsymbol{e}_\perp \cdot \boldsymbol{e}'_\perp \right)^2 - \left(\boldsymbol{e} \cdot \boldsymbol{e}^\perp \right)^2 \right] = 0 \quad \forall \left(\{ \boldsymbol{e}, \boldsymbol{e}_\perp, \boldsymbol{m} \}, \{ \boldsymbol{e}', \boldsymbol{e}'_\perp, \boldsymbol{m}' \} \right),$$

that is

$$\gamma = 0. \tag{5.1.17}$$

which represents the self–dual plane with respect to (5.1.6).

The third symmetry operator leads to the transformations

$$\tau_3 \boldsymbol{m} = \boldsymbol{e},\ \tau_3 \boldsymbol{e}_\perp = \boldsymbol{e}_\perp,\ \tau_3 \boldsymbol{e} = \boldsymbol{m}$$

$$\Updownarrow$$

$$\mathbf{q} \mapsto \tau_3 \mathbf{q} \tau_3^t = \frac{1}{2} (\mathbf{b} - \mathbf{q}), \quad \mathbf{b} \mapsto \tau_3 \mathbf{b} \tau_3^t = \frac{1}{2} (3\mathbf{q} + \mathbf{b}),$$

and the invariance condition gives

$$V = V^* \Leftrightarrow (\xi - 3\lambda + 2\gamma) \left[\left(\boldsymbol{e} \cdot \boldsymbol{e}' \right)^2 - \left(\boldsymbol{m} \cdot \boldsymbol{m}' \right)^2 \right] = 0 \quad \forall \left(\{ \boldsymbol{e}, \boldsymbol{e}_\perp, \boldsymbol{m} \}, \{ \boldsymbol{e}', \boldsymbol{e}'_\perp, \boldsymbol{m}' \} \right),$$

which means

$$\xi - 3\lambda + 2\gamma = 0. \tag{5.1.18}$$

All these symmetry properties generalize that of Chapter 4 for the case $\gamma = 0$ and $\xi = 1$. The three self–dual planes (5.1.16), (5.1.17), (5.1.18) meet on the straight line $\gamma = 0, \xi = 3\lambda$, which represents the place of the highest symmetry.

5.1.3. Symmetries of the free energy and equivariance of the equilibrium equations. On the macroscopic side, we are considering the tensor variables employed in the mean–field equations

$$\mathbf{Q} = S\left(\mathbf{e}_z \otimes \mathbf{e}_z - \frac{1}{3}\mathbf{I}\right) + T\left(\mathbf{e}_x \otimes \mathbf{e}_x - \mathbf{e}_y \otimes \mathbf{e}_y\right),$$

$$\mathbf{B} = S'\left(\mathbf{e}_z \otimes \mathbf{e}_z - \frac{1}{3}\mathbf{I}\right) + T'\left(\mathbf{e}_x \otimes \mathbf{e}_x - \mathbf{e}_y \otimes \mathbf{e}_y\right),$$

and accordingly, the free energy

$$\mathcal{F}\left(\mathbf{Q}, \mathbf{B}, \beta, \xi, \lambda, \gamma\right) = U_0 \left\{ \frac{1}{2}\left(\xi \mathbf{Q}\cdot\mathbf{Q} + \lambda \mathbf{B}\cdot\mathbf{B} + 2\gamma \mathbf{Q}\cdot\mathbf{B}\right) - \frac{1}{\beta} Z\left(\mathbf{Q}, \mathbf{B}, \beta, \xi, \lambda, \gamma\right) \right\},$$

$$Z\left(\mathbf{Q}, \mathbf{B}, \beta, \xi, \lambda, \gamma\right) = \int_{\mathcal{N}} \exp\left(\beta\left(\xi \mathbf{q}\cdot\mathbf{Q} + \lambda \mathbf{b}\cdot\mathbf{B} + \gamma\left(\mathbf{q}\cdot\mathbf{B} + \mathbf{Q}\cdot\mathbf{b}\right)\right)\right) d\mathcal{N},$$

where $\beta = \frac{U_0}{k_B t}$ and $d\mathcal{N}$ is the area measure of the manifold $\mathcal{N}$ defined in Chapter 2. The integration is over all the traceless and symmetric microscopic tensors $(\mathbf{q}, \mathbf{b})$ on the manifold

$$\mathcal{N} = \left\{ (\mathbf{q}, \mathbf{b}) : \det \mathbf{b} = 0, \operatorname{tr}\left(\mathbf{b}^2\right) = 2, \mathbf{q}\cdot\mathbf{b} = 0, \operatorname{tr}\left(\mathbf{q}^2\right) = \frac{2}{3}, [\mathbf{q}, \mathbf{b}] = \mathbf{0} \right\}, \tag{5.1.19}$$

which remains invariant under the transformations τ_1, τ_2, τ_3. On the other hand the pseudo–potential Ω, entering the expression for the partition function Z

$$\Omega = -U_0 \left\{ \xi \mathbf{q}\cdot\mathbf{Q} + \gamma\left(\mathbf{q}\cdot\mathbf{B} + \mathbf{b}\cdot\mathbf{Q}\right) + \lambda \mathbf{b}\cdot\mathbf{B} \right\}, \tag{5.1.20}$$

enjoys the same symmetry properties of the microscopic potential, since it mimicks its action via a mean–field, thus we have to consider the transformations induced by the swap operators τ_i as acting simultaneously and independently on the single molecule $(\mathbf{q}, \mathbf{b})$ and on the mean–field $(\mathbf{Q}, \mathbf{B})$ created by all the other molecules. It follows that the single particle distribution function f and, as a consequence, the free energy, turn out to be invariant under the transformations

$$\mathbf{Q} \to \tau_1 \mathbf{Q} \tau_1^t = -\frac{1}{2}\left(\mathbf{Q} + \mathbf{B}\right) \qquad \mathbf{B} \to \tau_1 \mathbf{B} \tau_1^t = \frac{1}{2}\left(\mathbf{B} - 3\mathbf{Q}\right), \qquad 3\lambda + 2\gamma - \xi = 0, \tag{5.1.21}$$

$$\mathbf{Q} \to \tau_2 \mathbf{Q} \tau_2^t = \mathbf{Q} \qquad \mathbf{B} \to \tau_2 \mathbf{B} \tau_2^t = -\mathbf{B}, \qquad \gamma = 0, \tag{5.1.22}$$

$$\mathbf{Q} \to \tau_3 \mathbf{Q} \tau_3^t = \frac{1}{2}\left(\mathbf{B} - \mathbf{Q}\right) \qquad \mathbf{B} \to \tau_3 \mathbf{B} \tau_3^t = \frac{1}{2}\left(3\mathbf{Q} + \mathbf{B}\right), \qquad \xi - 3\lambda + 2\gamma = 0. \tag{5.1.23}$$

accompanied by the corresponding transformations on the microscopic tensors.

More precisely the transformations (5.1.21) in terms of the order parameters are

$$\begin{aligned} S &\rightarrow -\tfrac{(S+S')}{2}, \\ T &\rightarrow -\tfrac{(T+T')}{2}, \\ S' &\rightarrow \tfrac{S'-3S}{2}, \\ T' &\rightarrow \tfrac{T'-3T}{2}, \end{aligned}$$

while for (5.1.22)

$$\begin{aligned} S &\rightarrow S, \\ T &\rightarrow T, \\ S' &\rightarrow -S', \\ T' &\rightarrow -T', \end{aligned}$$

and, finally, for (5.1.23)

$$\begin{aligned} S &\rightarrow \tfrac{(S'-S)}{2}, \\ T &\rightarrow \tfrac{(T'-T)}{2}, \\ S' &\rightarrow \tfrac{S'+3S}{2}, \\ T' &\rightarrow \tfrac{T'+3T}{2}. \end{aligned}$$

The compatibility equations, which entail the extremum conditions for $\mathcal{F}$, take the form

$$\mathbf{Q} = \langle \mathbf{q} \rangle_f ,$$

$$\mathbf{B} = \langle \mathbf{b} \rangle_f ,$$

$$f = \frac{\exp\left(\beta\left(\xi \mathbf{q}\cdot\mathbf{Q} + \lambda \mathbf{b}\cdot\mathbf{B} + \gamma\left(\mathbf{q}\cdot\mathbf{B} + \mathbf{Q}\cdot\mathbf{b}\right)\right)\right)}{Z\left(\mathbf{Q},\mathbf{B},\beta,\xi,\lambda,\gamma\right)}.$$

and they turn out to be equivariant with respect to the transformations (5.1.21), (5.1.22) and (5.1.23), which are a generalization of the equivariance transformations for the model $\gamma = 0$ and $\xi = 1$ studied in Chapter 4.

5.2. Diagonalization of the potential quadratic form: connection with self–duality

Now, we rewrite the potential in a diagonal form [**75**]. It can be written as a bilinear form

$$V = -U_0 \left\{ \begin{bmatrix} \mathbf{q} & \mathbf{b} \end{bmatrix} \begin{bmatrix} \xi & \gamma \\ \gamma & \lambda \end{bmatrix} \begin{bmatrix} \mathbf{q}' \\ \mathbf{b}' \end{bmatrix} \right\}. \tag{5.2.1}$$

The matrix associated with this form,

$$[\mathbf{C}] = \begin{bmatrix} \xi & \gamma \\ \gamma & \lambda \end{bmatrix}$$

is real symmetric and so it can be diagonalized by an orthogonal matrix. Before going on with the diagonalization, we slightly depart from our normalization of the molecular tensors $\mathbf{q}, \mathbf{b}$ (see the definition of $\mathcal{N}$ in (5.1.19)), and we change the basis of these tensors, by defining

$$\mathbf{s} := \sqrt{\frac{3}{2}}\mathbf{q}, \quad \mathbf{p} := \frac{1}{\sqrt{2}}\mathbf{b}, \tag{5.2.2}$$

so that

$$\mathbf{s}\cdot\mathbf{s} = \mathbf{p}\cdot\mathbf{p} = 1, \quad \mathbf{s}\cdot\mathbf{p} = 0. \tag{5.2.3}$$

Thus, the bilinear form defined by the pair potential V in this variables becomes

$$V = -U_0 \left\{ \begin{bmatrix} \mathbf{s} & \mathbf{p} \end{bmatrix} \begin{bmatrix} \frac{2}{3}\xi & \frac{2}{\sqrt{3}}\gamma \\ \frac{2}{\sqrt{3}}\gamma & 2\lambda \end{bmatrix} \begin{bmatrix} \mathbf{s}' \\ \mathbf{p}' \end{bmatrix} \right\}, \tag{5.2.4}$$

and the matrix associated with this form is

$$[\mathbf{C}'] = \begin{bmatrix} \frac{2}{3}\xi & \frac{2}{\sqrt{3}}\gamma \\ \frac{2}{\sqrt{3}}\gamma & 2\lambda \end{bmatrix}.$$

This matrix can be diagonalized by an orthogonal matrix

$$\mathbf{R} = \mathbf{Y}\mathbf{C}'\mathbf{Y}^T, \quad [\mathbf{R}] = \begin{bmatrix} r_1 & 0 \\ 0 & r_2 \end{bmatrix}, \quad [\mathbf{Y}] = \begin{bmatrix} y_{11} & y_{12} \\ y_{21} & y_{22} \end{bmatrix}, \tag{5.2.5}$$

where r_1, r_2 are real eigenvalues

$$r_{1,2} = \left(\lambda + \frac{\xi}{3}\right) \pm \sqrt{\left(\lambda - \frac{\xi}{3}\right)^2 + \frac{4}{3}\gamma^2}. \tag{5.2.6}$$

Hence, letting the diagonalizing transformation act, the bilinear function V can be written in a diagonal form

$$V = -U_0 \left\{ r_1 \hat{\mathbf{s}}\cdot\hat{\mathbf{s}}' + r_2 \hat{\mathbf{p}}\cdot\hat{\mathbf{p}}' \right\}, \tag{5.2.7}$$

with

$$\hat{\mathbf{s}} := y_{11}\mathbf{s} + y_{12}\mathbf{p} \quad \hat{\mathbf{s}}' := y_{11}\mathbf{s}' + y_{12}\mathbf{p}'$$

$$\hat{\mathbf{p}} := y_{21}\mathbf{s} + y_{22}\mathbf{p} \quad \hat{\mathbf{p}}' := y_{21}\mathbf{s}' + y_{22}\mathbf{p}',$$

which, in general, are not fully uniaxial or biaxial, but a superposition of both these components.

The orthonormalization conditions (5.2.3) are preserved thanks to the orthogonality of $\mathbf{Y}$. Since the molecular tensors belong to $\mathcal{N}$, then the singularity condition over $\mathbf{b}$ becomes

$$\det \hat{\mathbf{p}} = \det \hat{\mathbf{p}}' = 0 \Leftrightarrow -\sqrt{\frac{2}{3}} y_{21} \left(\frac{y_{22}^2}{2} - \frac{y_{21}^2}{6} \right) = 0, \tag{5.2.8}$$

which is satisfied whenever $y_{21} = 0$ or $y_{22}^2 = \frac{y_{21}^2}{3}$. We now consider the diagonalization with the constraint (5.2.8). The inverse transformations linking the tensors $\mathbf{s}, \mathbf{p}$ and $\hat{\mathbf{s}}, \hat{\mathbf{p}}$ are

$$\begin{aligned} \mathbf{s} &:= y_{11}\hat{\mathbf{s}} + y_{21}\hat{\mathbf{p}} \quad \mathbf{s}' := y_{11}\hat{\mathbf{s}}' + y_{21}\hat{\mathbf{p}}' \\ \mathbf{p} &:= y_{12}\hat{\mathbf{s}} + y_{22}\hat{\mathbf{p}} \quad \mathbf{p}' := y_{12}\hat{\mathbf{s}}' + y_{22}\hat{\mathbf{p}}', \end{aligned}$$

and, by inserting them into the bilinear form, we get

$$\begin{aligned} V \;=\; & -U_0 \left\{ \left(\frac{2}{3}\xi y_{11}^2 + \frac{4}{\sqrt{3}}\gamma y_{11}y_{12} + 2\lambda y_{12}^2 \right) \hat{\mathbf{s}} \cdot \hat{\mathbf{s}}' + \left(\frac{2}{3}\xi y_{21}^2 + \frac{4}{\sqrt{3}}\gamma y_{21}y_{22} + 2\lambda y_{22}^2 \right) \hat{\mathbf{p}} \cdot \hat{\mathbf{p}}' \right. \\ & \left. + \left(\hat{\mathbf{p}} \cdot \hat{\mathbf{s}}' + \hat{\mathbf{s}} \cdot \hat{\mathbf{p}}' \right) \left(\frac{2}{3}\xi y_{11}y_{21} + \frac{2}{\sqrt{3}}\gamma y_{11}y_{22} + \frac{2}{\sqrt{3}}\gamma y_{12}y_{21} + 2\lambda y_{12}y_{22} \right) \right\}. \end{aligned} \tag{5.2.9}$$

Thus, the bilinear form is diagonal if and only if the crossing term vanishes, leading to the following general condition

$$\xi y_{11}y_{21} + \sqrt{3}\gamma y_{11}y_{22} + \sqrt{3}\gamma y_{12}y_{21} + 3\lambda y_{12}y_{22} = 0, \tag{5.2.10}$$

and by taking into account that the diagonalizing transformation is orthogonal and that the constraint (5.2.8) holds, we arrive at the following relationships between the model parameters ξ, γ, λ

$$\mp\xi + 2\gamma \pm 3\lambda = 0, \quad \text{or} \quad \gamma = 0, \tag{5.2.11}$$

which are exactly the self-dual planes with respect to the transformations (5.1.2, 5.1.3, 5.1.4).

In general, if we consider a general orthogonal transformation preserving the constraint (5.2.8), but without diagonalizing V, then the potential takes the form

(5.2.12)

$$V = -U_0 \left\{ \frac{2}{3}\frac{1}{4}\left(\xi \mp 6\gamma + 9\lambda\right) \hat{\mathbf{s}} \cdot \hat{\mathbf{s}}' + \frac{2}{\sqrt{3}}\frac{1}{4}\left(\pm\xi - 2\gamma \mp 3\lambda\right) \left(\hat{\mathbf{p}} \cdot \hat{\mathbf{s}}' + \hat{\mathbf{s}} \cdot \hat{\mathbf{p}}' \right) + 2\frac{1}{4}\left(\xi \pm 2\gamma + \lambda\right) \hat{\mathbf{p}} \cdot \hat{\mathbf{p}}' \right\},$$

or

$$V = -U_0 \left\{ \frac{2}{3}\xi \hat{\mathbf{s}} \cdot \hat{\mathbf{s}}' \pm \frac{2}{\sqrt{3}}\gamma \left(\hat{\mathbf{p}} \cdot \hat{\mathbf{s}}' + \hat{\mathbf{s}} \cdot \hat{\mathbf{p}}' \right) + 2\lambda \hat{\mathbf{p}} \cdot \hat{\mathbf{p}}' \right\}. \tag{5.2.13}$$

In terms of the usual $\mathbf{q}, \mathbf{b}$ molecular tensors, (5.2.12) and (5.2.13) take the form

(5.2.14)
$$V = -U_0 \left\{ \frac{1}{4} \left(\xi \mp 6\gamma + 9\lambda \right) \hat{\mathbf{q}} \cdot \hat{\mathbf{q}}' + \frac{1}{4} \left(\pm\xi - 2\gamma \mp 3\lambda \right) \left(\hat{\mathbf{b}} \cdot \hat{\mathbf{q}}' + \hat{\mathbf{q}} \cdot \hat{\mathbf{b}}' \right) + \frac{1}{4} \left(\xi \pm 2\gamma + \lambda \right) \hat{\mathbf{b}} \cdot \hat{\mathbf{b}}' \right\},$$

and

(5.2.15)
$$V = -U_0 \left\{ \xi \hat{\mathbf{q}} \cdot \hat{\mathbf{q}}' \pm \gamma \left(\hat{\mathbf{b}} \cdot \hat{\mathbf{q}}' + \hat{\mathbf{q}} \cdot \hat{\mathbf{b}}' \right) + \lambda \hat{\mathbf{b}} \cdot \hat{\mathbf{b}}' \right\},$$

thus reflecting the general transformations (5.1.2, 5.1.3, 5.1.4). The corresponding transformations on the molecular tensors $\mathbf{q}, \mathbf{b}$ are those of the swapping operators τ_1, τ_2, τ_3, thus leading to pairs of tensors consisting of a fully uniaxial component and a fully biaxial one.

As a conclusion, it is always possible to write the interaction potential in a diagonal form (5.2.7), but the tensors are biaxial, the exceptions being the self-dual cases which are the unique cases in which the diagonalization can be done by means of fully uniaxial and fully biaxial tensors as in the case $\gamma = 0$.

Within this approach, another case deserves note, that is the dispersive approximation $\lambda\xi = \gamma^2$. In this case one of the eigenvalues of the bilinear form is zero and the potential can be put in the diagonal form as follows

(5.2.16)
$$V = -U_0 \frac{\xi + \lambda}{\gamma^2 + \lambda^2} \left(\gamma \mathbf{q} + \lambda \mathbf{b} \right) \left(\gamma \mathbf{q}' + \lambda \mathbf{b}' \right) = -U_0 \frac{1}{\xi} \left(\xi \mathbf{q} + \gamma \mathbf{b} \right) \cdot \left(\xi \mathbf{q}' + \gamma \mathbf{b}' \right).$$

In the nematic case $\xi = 1$, this potential reduces to the $\lambda = \gamma^2-$model and this model intersects the self-dual straight lines $\gamma = 0$, $2\gamma - 3\lambda + 1 = 0$ and $2\gamma + 3\lambda - 1 = 0$ at special points (see Fig. 5.1.3). Since, by means of the reduction criterion we can confine our analysis to the reference triangle with vertices $O\,(0,0)$, $C\left(0, \frac{1}{3}\right)$ and $B\left(\frac{1}{2}, 0\right)$, we can consider only the intersections occurring within it. In particular the three self–dual lines meet at the point C, while $D\left(\frac{1}{3}, \frac{1}{9}\right)$ is the point where the parabola meets the line $2\gamma + 3\lambda - 1 = 0$. Finally, the origin O is the meeting point between the parabola and the line $\gamma = 0$. The D point, in particular deserves notice; it corresponds to the so-called **bi–critical point** or **Landau critical point** extensively studied by both mean–field theory (see Refs. **[15]**-**[22]**) and by simulation (see Refs. **[25]**, **[26]**, **[76]**). In Alben's terminology **[15]**, at the point D an accidental second-order phase transition takes place. This is the singular point where the second–order lines separating the biaxial phase from the prolate and oblate uniaxial phases, respectively, meet the first–order line, separating both uniaxial phases from the isotropic one: the meeting point in the phase diagram is a sharp cusp point where a direct transition from isotropic to biaxial phase occurs. This model is

equivalent, via the conjugacy relations, to the purely biaxial model

$$V = -\frac{4U_0}{9}\mathbf{b}^* \cdot \hat{\mathbf{b}}^{*\prime}, \tag{5.2.17}$$

where $\mathbf{b}^* = \boldsymbol{m} \otimes \boldsymbol{m} - \boldsymbol{e}_\perp \otimes \boldsymbol{e}_\perp$ is the transformed tensor under the action of τ_3. This model has been studied by simulation in [**77**], disclosing a second–order direct isotropic–to–biaxial phase transition at a temperature very close to that of the dispersive model corresponding to the point D. Now, we want to explore the behaviour of the liquid crystal around this special point and, firstly, we investigate the effect of conjugacy on the phase transitions and on the bifurcations diagrams.

5.3. Conjugated diagrams: bifurcation, stability and phase transitions diagram

We study the special model $2\gamma + 3\lambda - 1 = 0$, which corresponds to a self–dual line when $\xi = 1$. The model corresponding to this line is equivalent to the other two corresponding to the self–dual lines $\gamma = 0$, via the transformation τ_3, and to the self–dual line $2\gamma - 3\lambda + 1 = 0$ through τ_2. As a consequence, the potential for this special model takes the simplified form

$$V = -U_0 \left\{ \left(\frac{9\lambda - 1}{2} \right) \mathbf{q}^* \cdot \mathbf{q}^{*\prime} + \left(\frac{1 - \lambda}{2} \right) \mathbf{b}^* \cdot \mathbf{b}^{*\prime} \right\}, \tag{5.3.1}$$

where the molecular tensors $\mathbf{q}^*, \mathbf{b}^*$ are those obtained from $\mathbf{q}, \mathbf{b}$ by applying τ_3

$$\mathbf{q}^* := \boldsymbol{e} \otimes \boldsymbol{e} - \frac{1}{3}\mathbf{I}, \quad \mathbf{b}^* := \boldsymbol{m} \otimes \boldsymbol{m} - \boldsymbol{e}_\perp \otimes \boldsymbol{e}_\perp.$$

It is apparent that this model is equivalent to that with $\gamma = 0$ by transforming the model parameter λ and rescaling the inverse reduced temperature β as follows

$$V = -U_0 \left(\frac{9\lambda - 1}{2} \right) \left\{ \mathbf{q}^* \cdot \mathbf{q}^{*\prime} + \lambda^* \mathbf{b}^* \cdot \mathbf{b}^{*\prime} \right\}, \tag{5.3.2}$$

$$\lambda^* = \frac{1 - \lambda}{9\lambda - 1}, \quad \beta^* = \beta \left(\frac{9\lambda - 1}{2} \right). \tag{5.3.3}$$

By virtue of these transformations, we can map the semi-line $\lambda \geq 0, \gamma = 0$ onto the segment $\overline{AD}$ on the line $2\gamma + 3\lambda - 1 = 0$ in Fig. 5.1.3: the segment $\overline{AC}$ is mapped onto the segment $\overline{OC}$, the segment $\overline{CD}$ onto the semi-line $\lambda \geq \frac{1}{3}, \gamma = 0$. We can build directly the phase diagram corresponding to this model by mapping the phase diagram in Fig. 4.5.12, and precisely the red part of it, thus getting the phase diagram in Fig. 5.3.1. The two tricritical points C_1^* and C_2^* are conjugated to those for the model $\gamma = 0$ and their coordinates can be computed via (5.3.3): the tricritical point on the isotropic–to–biaxial transition line C_2^* occurs at $\lambda = \frac{19}{87}, \frac{1}{\beta} = \frac{119}{754}$, while C_1^* has coordinates $\lambda \approx 0.418, \frac{1}{\beta} \approx 0.196$. In particular the second–order line transition from isotropic to biaxial phase hosting the tricritical point

C_2^* has a simple expression like that of the $\gamma = 0-$model

$$\frac{1}{\beta} = \frac{1-\lambda}{5}, \quad 2\gamma + 3\lambda - 1 = 0,$$

which is conjugated to

$$\frac{1}{\beta} = \frac{2\lambda}{5}, \quad \gamma = 0.$$

In turn, the order tensors for this model can be computed from those for the model $\gamma = 0$, we can define

$$\mathbf{Q}^* := \langle \mathbf{q}^* \rangle, \quad \mathbf{B}^* := \langle \mathbf{b}^* \rangle,$$

and we can parameterize them as follows

$$\begin{aligned} \mathbf{Q}^* &= S^*(\boldsymbol{e}_z \otimes \boldsymbol{e}_z - \frac{1}{3}\mathbf{I}) + T^*(\boldsymbol{e}_x \otimes \boldsymbol{e}_x - \boldsymbol{e}_y \otimes \boldsymbol{e}_y), \\ \mathbf{B}^* &= S^{*\prime}(\boldsymbol{e}_z \otimes \boldsymbol{e}_z - \frac{1}{3}\mathbf{I}) + T^{*\prime}(\boldsymbol{e}_x \otimes \boldsymbol{e}_x - \boldsymbol{e}_y \otimes \boldsymbol{e}_y) \end{aligned}$$

with the following correspondence on the order parameters

$$\mathbf{Q}^* = \tau_3 \mathbf{Q} \tau_3^t = \frac{1}{2}(\mathbf{B} - \mathbf{Q}), \qquad \mathbf{B}^* = \tau_3 \mathbf{B} \tau_3^t = \frac{1}{2}(3\mathbf{Q} + \mathbf{B}), \tag{5.3.4}$$

or, by inverting

$$\begin{aligned} S &= \frac{S^{*\prime} - S^*}{2}, \quad T = \frac{T^{*\prime} - T^*}{2}, \\ S' &= \frac{S^{*\prime} + 3S^*}{2}, \quad T' = \frac{T^{*\prime} + 3T^*}{2}. \end{aligned}$$

We can conjugate the complete bifurcation analysis performed for the model with $\gamma = 0$. In particular, it is possible to build the diagram of the symmetry-breaking bifurcation lines and of the limit of stability points (and turning points). On the other hand, it is possible to start from the general equations for the computation of all bifurcations and perform the analysis. In the following we will pursue this objective, in order to illustrate how the general equations depart from those for the dispersive model $\lambda = \gamma^2$.

5.3.1. Uniaxial-to-Biaxial symmetry-breaking bifurcation lines. The model we are exploring is characterized by the symmetry transformations (5.1.21) on the order tensors. This symmetry implies the existence of an equivariance $\mathbb{Z}_2-$operator $\hat{S}_5$ acting on the order parameter space. It is

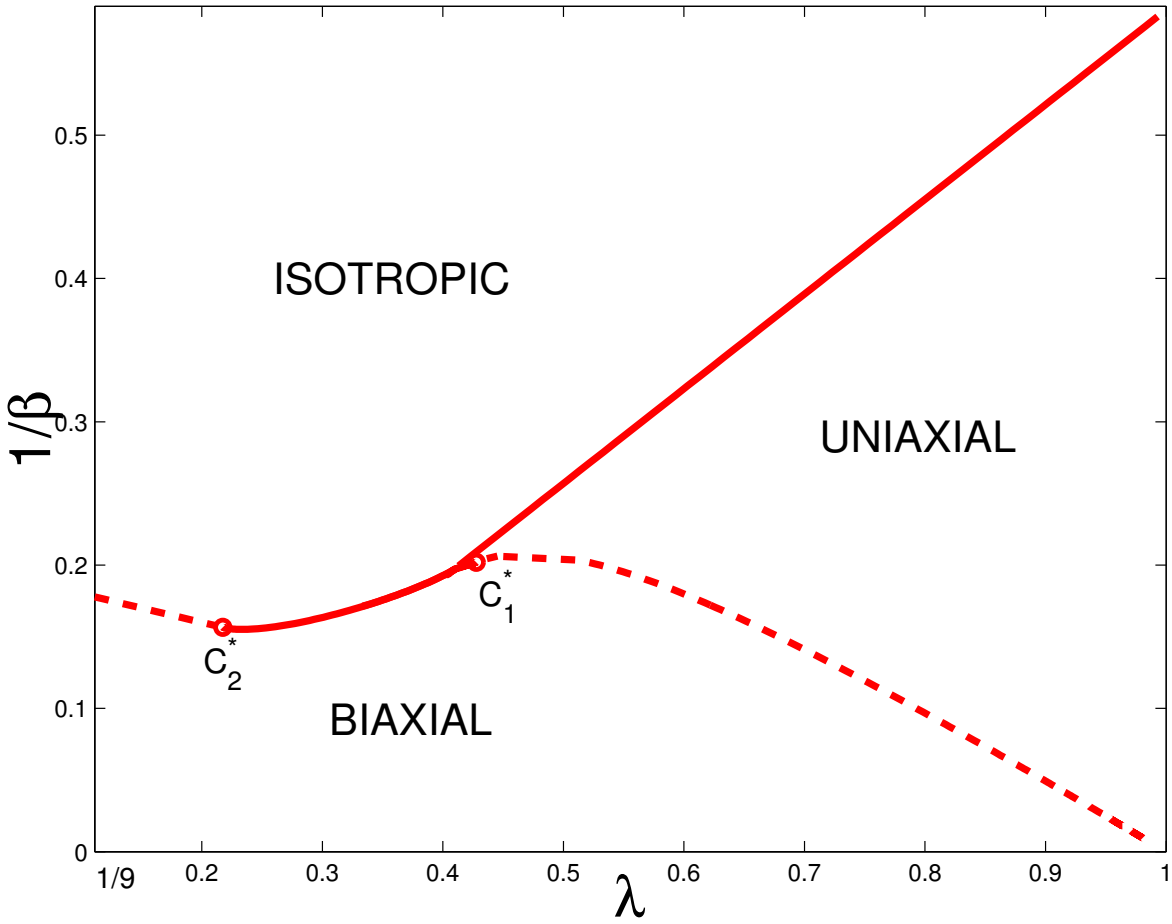

FIGURE 5.3.1. Phase diagram for the model $\gamma = \frac{(1-3\lambda)}{2}$ with $\lambda \in \left[\frac{1}{9}, 1\right]$. It represents the segment $\overline{AD}$ on the straight line r in Fig. 5.3.1. It is conjugated to that for the $\gamma = 0$ model in Fig. (4.5.12). It exhibits two tricritical points as expected C_1^* and C_2^*, on the uniaxial–to–biaxial transition line and on the isotropic–to–biaxial line respectively.

represented by the matrix

$$\left[\hat{S}_5\right] = \begin{pmatrix} -\frac{1}{2} & 0 & -\frac{1}{2} & 0 \\ 0 & -\frac{1}{2} & 0 & -\frac{1}{2} \\ -\frac{3}{2} & 0 & \frac{1}{2} & 0 \\ 0 & -\frac{3}{2} & 0 & \frac{1}{2} \end{pmatrix}, \tag{5.3.5}$$

and the mean–field equations for this model turn out to be equivariant with respect to it. This further symmetry corresponds to that of the $\gamma = 0-$model represented by the operator $\hat{S}_4$, or by the transformations (5.1.22). Thus, we can say that the model $2\gamma + 3\lambda - 1 = 0$ is a $\mathbb{Z}_2-$bifurcation problem equivariant with respect to the operators $\hat{S}_1, \hat{S}_2, \hat{S}_3$ defined in Chapter 4 and $\hat{S}_5$.

We consider the general equations for the symmetry-breaking bifurcations with respect to the symmetry operator $\hat{S}_3$. This is a $\mathbb{Z}_2-$equivariance operator for any triplet (ξ, γ, λ) of the potential model parameters. Here we specialize them for the attractive case $\xi = 1$, and then we use these

equations for the self–dual line $2\gamma + 3\lambda - 1 = 0$. These equations are

$$
\begin{aligned}
&4 - 4\beta\gamma\Delta_{TT'} - 2\beta\lambda\Delta_{T'T'} - 2\beta\Delta_{TT} + \beta^2\left(\lambda - \gamma^2\right)\left(\Delta_{TT}\Delta_{T'T'} - \Delta_{TT'}^2\right) = 0, \\
&S - \frac{1}{Z_{SS'}}\int_0^{\pi}\int_0^{2\pi} s_1(\vartheta)\exp\beta\left[\frac{2}{3}\left(S + \gamma S'\right)s_1(\vartheta) + \left(\gamma S + \lambda S'\right)s_2(\vartheta,\psi)\right]\sin\vartheta d\vartheta d\psi = 0, \\
&S' - \frac{\sqrt{6}}{Z_{SS'}}\int_0^{\pi}\int_0^{2\pi} s_2(\vartheta,\psi)\exp\beta\left[\frac{2}{3}\left(S + \gamma S'\right)s_1(\vartheta) + \left(\gamma S + \lambda S'\right)s_2(\vartheta,\psi)\right]\sin\vartheta d\vartheta d\psi = 0,
\end{aligned}
\tag{5.3.6}
$$

in the unknowns (S, S', β) at the bifurcation points and where s_j are the $D_{2h}-$symmetry adapted basis functions introduced in Chapter 2. The symbols in the equations are given by the following expressions

$$
\begin{aligned}
Z_{SS'} &:= \int_0^{\pi}\int_0^{2\pi}\exp\beta\left[\frac{2}{3}\left(S + \gamma S'\right)s_1(\vartheta) + \left(\gamma S + \lambda S'\right)s_2(\vartheta,\psi)\right]\sin\vartheta d\vartheta d\psi, \\
\Delta_{TT} &:= \frac{4}{3\pi Z_{SS'}}\int_0^{\pi}\int_0^{2\pi}\int_0^{2\pi} s_3^2(\varphi,\vartheta)\exp\beta\left[\frac{2}{3}\left(S + \gamma S'\right)s_1(\vartheta) + \left(\gamma S + \lambda S'\right)s_2(\vartheta,\psi)\right]d\omega, \\
\Delta_{TT'} &:= \frac{4\sqrt{6}}{3\pi Z_{SS'}}\int_0^{\pi}\int_0^{2\pi}\int_0^{2\pi} s_3(\vartheta,\psi)\,s_4(\omega)\exp\beta\left[\frac{2}{3}\left(S + \gamma S'\right)s_1(\vartheta) + \left(\gamma S + \lambda S'\right)s_2(\vartheta,\psi)\right]d\omega, \\
\Delta_{T'T'} &:= \frac{8}{\pi Z_{SS'}}\int_0^{\pi}\int_0^{2\pi}\int_0^{2\pi} s_4^2(\omega)\exp\beta\left[\frac{2}{3}\left(S + \gamma S'\right)s_1(\vartheta) + \left(\gamma S + \lambda S'\right)s_2(\vartheta,\psi)\right]d\omega,
\end{aligned}
$$

where $\omega = (\varphi, \vartheta, \psi)$ and $d\omega = \sin\vartheta d\vartheta d\varphi d\psi$. By means of these equations we can compute the bifurcation line conjugated to the line (4.4.8)

$$
\lambda_3\left(S_0(\beta), \beta\right) = \frac{24}{2\left(5 + 7S_0(\beta)\right)\beta - 3},
\tag{5.3.7}
$$

which is represented in Figs. 5.3.2 and 5.3.3 by the dashed line passing for M and the tricritical point C_1^*. The point M has coordinates $\left(\frac{1}{3}, \frac{15}{2}\right)$ as in Fig. 4.5.12 for the model $\gamma = 0$, it is a fixed point with respect to all the duality transformations.

5.3.2. Secondary bifurcations from the uniaxial states. Now, we analyze the branches bifurcating from the uniaxial states. With no loss of generality, we can consider the class of uniaxial states of the form $(S, 0, S', 0)$. Moreover the symmetry transformations in Eq. (5.1.23) reduce the uniaxial states to the form $S' = -3S$. The symmetry-breaking points are the solutions of the following non-linear system in the unknowns (S, β) at the bifurcation point

$$
\begin{aligned}
&\frac{4}{9} + \frac{4}{3}\gamma\beta\left(m_S m_{S'} - \delta_{SS'}\right) + \frac{2}{3}\beta\lambda\left(m_{S'}^2 - \delta_{S'S'}\right) + \frac{2}{3}\beta\left(m_S^2 - \delta_{SS}\right) + \\
&+\beta^2\left(\gamma^2 - \lambda\right)\left(m_S^2\delta_{S'S'} - 2m_S m_{S'}\delta_{SS'} + \delta_{SS}m_{S'}^2 - \delta_{SS}\delta_{S'S'} + \delta_{SS'}^2\right) = 0, \\
&S - \frac{1}{Z_S}\int_0^{\pi}\int_0^{2\pi} s_1(\vartheta)\exp\left[\beta S\left(1 - 3\gamma\right)\left(\frac{2}{3}s_1(\vartheta) + \sqrt{\frac{8}{3}}s_2(\vartheta,\psi)\right)\right]\sin\vartheta d\vartheta d\psi = 0,
\end{aligned}
\tag{5.3.8}
$$

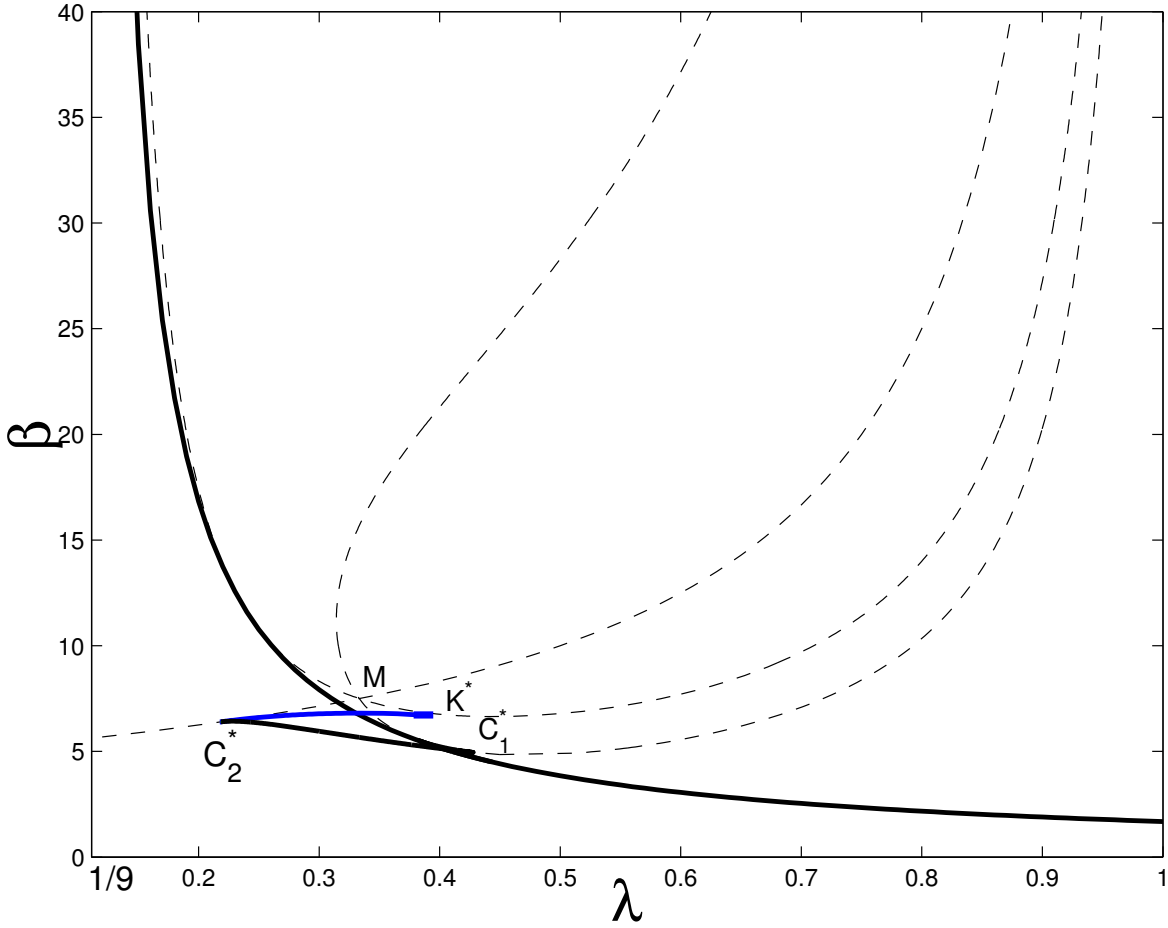

FIGURE 5.3.2. Bifurcation and Limit of stability diagram for the model $\gamma = \frac{(1-3\lambda)}{2}$. It is conjugated to that for the $\gamma = 0$ model in Fig. (4.5.12).

with the following meaning of the symbols

$$
\begin{aligned}
Z_S &:= \int_0^{\pi}\int_0^{2\pi} \exp\left[\beta S\left(1-3\gamma\right)\left(\frac{2}{3}s_1\left(\vartheta\right)+\sqrt{\frac{8}{3}}s_2\left(\vartheta,\psi\right)\right)\right]\sin\vartheta d\vartheta d\psi,\\
m_S &:= \frac{2}{3Z_S}\int_0^{\pi}\int_0^{2\pi} s_1\left(\vartheta\right)\exp\left[\beta S\left(1-3\gamma\right)\left(\frac{2}{3}s_1\left(\vartheta\right)+\sqrt{\frac{8}{3}}s_2\left(\vartheta,\psi\right)\right)\right]\sin\vartheta d\vartheta d\psi,\\
m_{S'} &:= \frac{\sqrt{8}}{\sqrt{3}Z_S}\int_0^{\pi}\int_0^{2\pi} s_2\left(\vartheta,\psi\right)\exp\left[\beta S\left(1-3\gamma\right)\left(\frac{2}{3}s_1\left(\vartheta\right)+\sqrt{\frac{8}{3}}s_2\left(\vartheta,\psi\right)\right)\right]\sin\vartheta d\vartheta d\psi,\\
\delta_{SS} &:= \frac{4}{9Z_S}\int_0^{\pi}\int_0^{2\pi} s_1^2\left(\vartheta\right)\exp\left[\beta S\left(1-3\gamma\right)\left(\frac{2}{3}s_1\left(\vartheta\right)+\sqrt{\frac{8}{3}}s_2\left(\vartheta,\psi\right)\right)\right]\sin\vartheta d\vartheta d\psi,\\
\delta_{SS'} &:= \frac{2\sqrt{8}}{3\sqrt{3}Z_S}\int_0^{\pi}\int_0^{2\pi} s_1\left(\vartheta\right)s_2\left(\vartheta,\psi\right)\exp\left[\beta S\left(1-3\gamma\right)\left(\frac{2}{3}s_1\left(\vartheta\right)+\sqrt{\frac{8}{3}}s_2\left(\vartheta,\psi\right)\right)\right]\sin\vartheta d\vartheta d\psi,\\
\delta_{S'S'} &:= \frac{8}{3Z_S}\int_0^{\pi}\int_0^{2\pi} s_2^2\left(\vartheta,\psi\right)\exp\left[\beta S\left(1-3\gamma\right)\left(\frac{2}{3}s_1\left(\vartheta\right)+\sqrt{\frac{8}{3}}s_2\left(\vartheta,\psi\right)\right)\right]\sin\vartheta d\vartheta d\psi.
\end{aligned}
$$

This bifurcation line breaks the symmetry of the uniaxial state $S' = -3S$, leading to uniaxial states antisymmetric with respect to the operator $\hat{S}_5$. In Figs. (5.3.3) and (5.3.2) this line is represented by the dashed line passing through the points M and K^*. It corresponds to the line (4.4.9) in Fig. (4.5.12) for the model $\gamma = 0$. The dashed line connecting the points M and C_2^* represents the symmetry–breaking bifurcation line from the isotropic phase, which has the simple analytical form

$$\frac{1}{\beta} = \frac{1-\lambda}{5}. \tag{5.3.9}$$

5.3.3. Limit of stability curves. In complete analogy with the case $\gamma = 0$, we can compute the limit of stability curves and in general the turning point curves. Both these lines are represented in Figs. (5.3.2) and (5.3.3) by the solid curves. The blue line is the turning point trajectory conjugated to the blue line in Fig. (4.5.12): this line can be computed by continuing in λ the solutions of the general Moore-Spence extended system in Eq. (4.4.11) relative to this specific model. In this case the state vector $\mathbf{x}$ and the tangent vector $\mathbf{w}$ lie both on the symmetric component of the state manifold with respect to the action of the operator $\hat{S}_3$. The black line joining C_1^* and C_2^* is the limit points trajectory of the biaxial phase and it can be computed by continuation of the solution to the Moore–Spence system in which the unknown variables $\mathbf{x}, \mathbf{w}$ belong to the component of the state manifold symmetric with respect to the operator $\hat{S}_5$. The other black line, with β going to infinity as λ goes to $\frac{1}{9}$, represents the limit of stability points corresponding to the uniaxial–to–isotropic phase transitions in the phase diagram (5.3.1). In particular it is conjugated to the horizontal solid black line in Fig. (4.5.12). The nature of the two tricritical points C_1^* and C_2^* is also conserved: they are cusp matching points between the symmetry–breaking bifurcation points line and the limit of stability points line.

Untill now, we have studied special models enjoying symmetry properties, lying on the edges of the essential triangular domain depicted in Figs.(5.1.1, 5.1.3). A further bifurcation analysis inside the essential triangular domain is needed in order to identify the general topology of the phase diagram and its convergence to the those pertaining to the models $\xi = 1, \gamma = 0, \lambda > 0$ and $\xi = 1, 2\gamma + 3\lambda - 1 = 0, \frac{1}{9} \leq \lambda \leq \frac{1}{3}$ analyzed in this thesis.

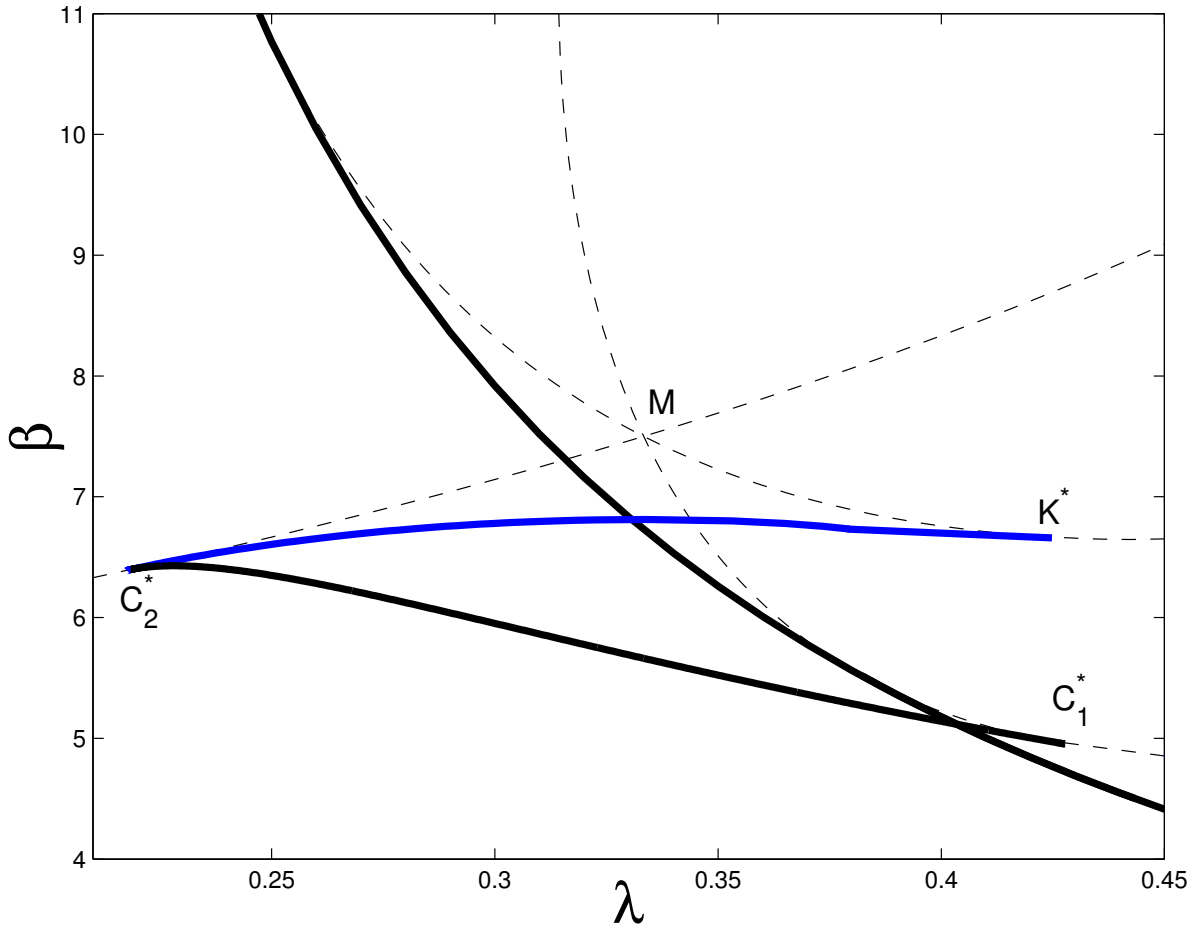

FIGURE 5.3.3. Tricritical region. The dashed lines represent the symmetry-breaking bifurcation lines meeting at the fixed point M. The black solid line connecting the points C_1^* and C_2^* represents the limits of stability line for the biaxial phase for the model $\gamma = \frac{(1-3\lambda)}{2}$. It corresponds to the black solid line in Fig. (4.5.12) bordered by the two tricritical points C_1 and C_2. The remaining black solid line corresponds to the limit of stability line separating the uniaxial from the isotropic phase. The blue solid line corresponds to the blue solid line in Fig. (4.5.12).

Perspectives

In the last chapter we have considered the problem of conjugacy of special models. We have seen that it is possible to reduce the analysis of the general Straley's quadrupolar interaction within the stability region of the complete microscopic alignment between two interacting molecules. This reduction allows us to focus the exploration to an essential triangular domain depicted in Fig. (5.1.1) and in Fig. (5.1.3). However, a triangular region (the green coloured one in Fig. (5.1.1)) is conjugated to an unbounded region in the antinematic plane $\xi = -1$. Nevertheless, this region preserves the stability of the biaxial ground state of complete alignment, even if it includes a uniaxially repulsive term due to the negative sign of ξ. A complete analysis of this mildly repulsive potential has to be done in order to characterize completely the general quadrupolar interaction energy [**79**].

On a macroscopic side, positing a complete theory for biaxial nematics requires writing the free–energy in terms of both tensors $\mathbf{Q}$ and $\mathbf{B}$ analogous to the Landau-deGennes theory for the uniaxial nematic liquid crystals in terms of $\mathbf{Q}$ only. An approximate expression for the Landau potential can be obtained by expanding in powers of β the free–energy of the mean field model [**30**]. For the model $\xi = 1, \gamma = 0$, this expansion takes the form

$$\begin{aligned} \mathcal{F}(\mathbf{Q},\mathbf{B}) &= U_0 \left\{ \frac{1}{15}\left[\left(\frac{15}{2}-\beta\right)\mathrm{tr}\mathbf{Q}^2 - \frac{4}{21}\beta^2\mathrm{tr}\mathbf{Q}^3 + \frac{1}{105}\beta^3\left(\mathrm{tr}\mathbf{Q}^2\right)^2\right] \right. \\ &+ \frac{1}{5}\lambda\beta\left(\frac{5}{2\beta}-\lambda\right)\mathrm{tr}\mathbf{B}^2 + \frac{4}{35}\lambda^2\beta^2\mathrm{tr}\mathbf{Q}\mathbf{B}^2 \\ &+ \left. \frac{1}{175}\lambda^2\beta^3\left[\frac{11}{3}\left(\mathrm{tr}\mathbf{Q}\mathbf{B}\right)^2 - 6\mathrm{tr}\mathbf{Q}^2\mathbf{B}^2 + \lambda^2\left(\mathrm{tr}\mathbf{B}^2\right)^2\right]\right\}. \end{aligned} \tag{5.3.10}$$

Setting $\lambda = 0$, we recover the expression obtained in Ref. [**83**] for Maier and Saupe's model. This is only an approximation as remarked in Ref. [**36**], where the Authors proposed an accurate approximation to the nonequilibrium free–energy $\mathcal{F}_{neq}$ in the vicinity of the equilibrium points correctly predicted by $\mathcal{F}$ in the mean–field model. Nevertheless, the expression in Eq. (5.3.10) shares some properties with $\mathcal{F}_{neq}$. First of all, for λ small enough, it attains its mimimum at the uniaxial phase $\mathbf{Q} \neq \mathbf{0}$ and $\mathbf{B} = \mathbf{0}$. Moreover, the terms $\mathrm{tr}\mathbf{Q}\mathbf{B}$, $\mathrm{tr}\mathbf{B}^3$, $\mathrm{tr}\mathbf{Q}^2\mathbf{B}$, $\mathrm{tr}\mathbf{Q}^3\mathbf{B}$ and $\mathrm{tr}\mathbf{Q}\mathbf{B}^3$, which are invariant under rotations, are missing because they are not invariant under the symmetry transformation $(\mathbf{q},\mathbf{b}) \mapsto (\mathbf{q},-\mathbf{b})$ and $(\mathbf{Q},\mathbf{B}) \mapsto (\mathbf{Q},-\mathbf{B})$. In the general case with all the model parameters ξ, γ, λ free to range, the number of invariants should be reduced by the general symmetry transformations found in Chapter 5 for all

the other self-duality relationships. In a phenomenological approach the coefficients of the expansion have to be determined, but they should preserve the same sign and depend on the temperature.

The theory outlined in Refs. [**84**], [**85**], once restricted to the fourth order in the tensors **Q** and **B**, employs only four invariants out of 14 possible ones [**86**].

All these considerations apply only to a single material point of the liquid crystal. Positing a continuum theory for biaxial nematics requires the addition of gradient terms to the bulk free–energy in (5.3.10). This leads to a proliferation of invariants in both the bulk contribution and in the elastic energy. All this pertains to future work.

Bibliography

[1] L. J. Yu, A. Saupe, Phys. Rev. Lett. **45** (1980) 1000 .

[2] S. M. Fan, I. D. Fletcher, B. Gündoğan, N. J. Heaton, G. Kothe, G. R. Luckhurst, K. Praefcke, Chem. Phys. Lett. **204** (1993) 517.

[3] G. R. Luckhurst, Thin Solid Films **393** (2001) 40.

[4] K. Praefcke, Mol. Cryst. Liq. Cryst. **364** (2001) 15.

[5] K. Praefcke, Braz. J. Phys. **32** (2002) 564.

[6] B. R. Acharya, A. Primak, S. Kumar, Liquid Crystals Today **13** (2004) 1.

[7] L. A. Madsen, T. J. Dingemans, M. Nakata, E. T. Samulski, Phys. Rev. Lett. **92** (2004) 145505.

[8] B. R. Acharya, A. Primak, S. Kumar, Phys. Rev. Lett. **92** (2004) 145506.

[9] K. Severing and K. Saalwächter Phys. Rev. Lett. **92**, 125501 (2004).

[10] K. Merkel, A. Kocot, J. K. Vij, R. Korlacki, G.H. Mehl, and T. Meyer, Phys. Rev. Lett. **93**, 237801 (2004).

[11] G. R. Luckhurst, Nature **430**, 22 July 2004.

[12] M. J. Freiser, Phys. Rev. Lett. **24** (1970) 1041.

[13] M. J. Freiser, Mol. Cryst. Liq. Cryst. **14** (1971) 165.

[14] W. Maier and A. Saupe, Z. Naturforsch. **14a**, 882 (1959)

[15] R. Alben, Phys. Rev. Lett. **30** (1973) 778.

[16] J. P. Straley, Phys. Rev. A **10**, 1881 (1974).

[17] G. R. Luckhurst, C. Zannoni, P. L. Nordio, U. Segre, Mol. Phys. **30** (1975) 1345.

[18] N. Boccara, R. Mejdani, L. De Seze, J. de Phys. (Paris) **38** (1976) 149.

[19] D. K. Remler, A. D. J. Haymet, J. Phys. Chem. **90** (1986) 5426.

[20] B. Bergersen, P. Palffy-Muhoray, D. A. Dunmur, Liq. Cryst. **3** (1988) 347.

[21] Zhang Zhi-Dong, Huang Xi-Min, Acta Phys. Sin. (Overseas edition) **6** (1997) 671.

[22] M. Hosino, H. Nakano, Mol. Cryst. Liq. Cryst. **348** (2000) 207.

[23] G. R. Luckhurst, S. Romano, Mol. Phys. **40** (1980) 129.

[24] C. D. Mukherjee, N. Chatterjee, Phys. Lett. A **189** (1994) 86.

[25] F. Biscarini, C. Chiccoli, P. Pasini, F. Semeria, C. Zannoni, Phys. Rev. Lett. **75** (1995) 1803.

[26] C. Chiccoli, P. Pasini, F. Semeria, C. Zannoni, Int. J. Mod. Phys. C **10** (1999) 469.

[27] P. Pasini, C. Chiccoli, C. Zannoni, Advances in the Computer Simulations of Liquid Crystals, ed. by P. Pasini and C. Zannoni, NATO Science Series, vol. C 545, Kluwer, Dordrecht, 2000 (Chapter 5).

[28] B. Mulder, Phys. Rev. A **39** (1989) 360.

[29] M. P. Allen, Liq. Cryst. **8** (1990) 499.

[30] A. M. Sonnet, E. G. Virga, G. E. Durand, Phys. Rev. E **67** (2003) 061701.

[31] G. Capriz, *Continua with microstructure*, New York, Heidelberg, and Berlin, Springer–Verlag

[32] E. G. Virga, *Variational Theories for Liquid Crystals*, London, Chapman & Hall, 1994

[33] Ericksen, J. L., *Liquid crystals with variable degree of orientation*, Arch. Rational Mech. Anal.,**113**,97-120,(1991).

[34] P. G. de Gennes and J. Prost, *The Physics of Liquid Crystals*, Clarendon Press, Oxford, Second edn, 1993.

[35] P. Palffy-Muhoray and G. L. Hoatson, Phys. Rev. A,**44**, 5052 (1991)

[36] J. Katriel, G. F. Kventsel, G. R. Luckhurst, and T. J. Sluckin, Liq. Cryst. **1**, 337 (1986).

[37] G. Kohring, R. E. Shrock, Nucl. Phys. **B 295** (1988) 36.

[38] S. Romano, Int. J. Mod. Phys. **B 8** (1994) 3389.

[39] H. G. Ballesteros, L. A. Fernández, V. Martín-Mayor, and A. Munõz-Sudupe, Phys. Lett. **B 378** (1996) 207; Nucl. Phys. B Proc. Suppl. **53** (1997) 686;Nucl. Phys. **B 483** (1997) 707.

[40] A. D. Buckingham, in Intermolecular Forces Adv. Chem. Phys. **12** (1967) 107, edited by J. O. Hirschfelder (Chapter 2); John Wiley, (London-New York).

[41] C. G. Gray, K. E. Gubbins, Theory of Molecular Fluids, volume 1: Fundamentals, Oxford University Press, Oxford, UK, 1984.

[42] S. Romano, Physica A **337** (2004) 505.

[43] D. M. Brink, G. R. Satchler, *Angular Momentum*, 2nd edition, Oxford University Press, Oxford, UK, 1968.

[44] D. A. Varshalovich, A. N. Moskalev, V. K. Khersonskii, *Quantum Theory of Angular Momentum*, World Scientific, Singapore, 1988.

[45] G. B. Arfken, H. J. Weber, *Mathematical Methods for Physicists*, 4th edition, Academic Press, San Diego, USA, 1995.

[46] R. L. Humphries, P. G. James and G. R. Luckhurst, J. Chem. Soc. Faraday Trans. 11, **68**, 1031.

[47] G. De Matteis and E. G. Virga, Physical Review E **71**, 061703 (2005).

[48] R. B. Griffiths and B. Widom, Phys. Rev. A **8**, 2173 (1973).

[49] W. L. McMillan, Phys. Rev. A **4**, 1238 (1971).

[50] R. B. Meyer and T. C. Lubensky, Phys. Rev. A **14**, 2307 (1976).

[51] J. Thoen, H. Marynissen, and W. Van Dael, Phys. Rev. Lett. **52**, 204 (1984).

[52] B. M. Ocko, R. J. Birgeneau, J. D. Litster, and M. E. Neubert, Phys. Rev. Lett. **52**, 208 (1984).

[53] R. B. Griffiths, Phys. Rev. B **7**, 545 (1973).

[54] E. G. D. Cohen, *Ed.*, *Fundamental Problems in Statistical Mechanics III* (Proceedings of the 1974 Wageningen Summer School, North Holland) 1975.

[55] I. D. Lawrie, and S. Sarbach, *Theory of tricritical points* in *Phase transitions and critical phenomena,* ed. by C. Domb and J.L. Lebowitz, vol. 9, Academic Press, 1984.

[56] R. B. Griffiths, , J. Chem. Phys., **60**, 195 (1974).

[57] J. R. Fox, J. Chem. Phys. **69**, 2231 (1978).

[58] J. T. Bartis, J. Chem. Phys. **59**, 5423 (1973).

[59] A. Kloczkowski and J. Stecki, Molec. Phys. **55**, 1223 (1985).

[60] L. Longa, J. Chem. Phys. **85**, 2974 (1986).

[61] L. Longa, Liq. Cryst. **5**, 443 (1989).

[62] G. De Matteis, S. Romano, and E. G. Virga, Physical Review E **72**, 041706 (2005).

[63] B. Werner and A. Spence, SIAM Journal of Numerical Analysis 21, 338 (1984).

[64] Willy J. F. Govaerts, *Numerical Methods for Bifurcations of Dynamical Equilibria*, SIAM, 2000.

[65] M. Golubitsky and D. G. Schaeffer, *Singularities and Groups in Bifurcation Theory*, Vol.I, Springer-Verlag, Berlin, New York, 1985.

[66] M. Golubitsky, I. Stewart, and D. G. Schaeffer, *Singularities and Groups in Bifurcation Theory*, Vol.II, Springer-Verlag, Berlin, New York, 1988.

[67] E.J. Doedel, R.C. Paffenroth, A.R. Champneys, T.F. Fairgrieve, Y.A. Kuznetsov, B.E. Oldeman, B. Sandstede, and X. Wang, Tech. Rep., Concordia University, Montreal, Canada (2002).
see also http://sourceforge.net/projects/auto2000

[68] R. Hashim, S. Romano, Int. J. Mod. Phys. B **13** (1999) 3879.

[69] C. Zannoni, *The Molecular Physics of Liquid Crystals*, ed. by G. R. Luckhurst and G. W. Gray, Academic Press, London, 1979 (Chapters 3 and 9).

[70] C. Zannoni, *Advances in the Computer Simulations of Liquid Crystals*, ed. by P. Pasini and C. Zannoni, NATO Science Series, vol. C 545, Kluwer, Dordrecht, 2000 (Chapter 2).

[71] G. R. Luckhurst, *Physical Properties of Liquid Crystals: Nematics*, ed by D. A. Dunmur, A. Fukuda, G. R. Luckhurst, INSPEC, London, UK, 2001 (Chapter 2.1).

[72] R. Alben, J. Chem. Phys. **59** (1973) 4299.

[73] U. Fabbri, C. Zannoni, Mol. Phys. **58** (1986) 763.

[74] C. Chiccoli, P. Pasini, F. Biscarini, C. Zannoni, Mol. Phys. **65** (1988) 1505.

[75] Prof. E. C. Gartland, private communication

[76] S. Romano, Physica A, in press.

[77] S. Romano, Phys. Lett. A,**333**, 110 (2004)

[78] R. Berardi and C. Zannoni, J. Chem Phys. **113**, 5971 (2000).

[79] F. Bisi, G. De Matteis, E. C. Gartland, G. E. Durand, E. G. Virga, Forthcoming (2005).

[80] E. F. Gramsberger, L. Longa and W. H. de Jeu, Phys. Rep. **135** (1986) 195.

[81] M. A. Bates, G. R. Luckhurst, Struct. Bonding (Berlin) **94** (1998) 65.

[82] A. Ferrarini, P. L. Nordio, E. Spolaore, G. R. Luckhurst, J. Chem. Soc. Faraday Trans. **91** (1995) 3177.

[83] P. Palffy–Muhoray and D. A. Dunmur, Phys. Lett. A **91**, 121 (1982)

[84] D. Allender and M. Lee, Mol. Cryst. Liquid Cryst.,**110**, 331 (1984)

[85] D. Allender, M. Lee and N. Hafiz, Mol. Cryst. Liquid Cryst.,**124**, 45 (1985)

[86] G. F. Smith, Arch. Rat. Mech. Anal., **18**, 282 (1965)